

# **Form factors in superconformal theories in four and three dimensions**

by

Ömer Can Gürdoğan

A thesis submitted to the University of London in partial fulfillment of the  
requirements of the degree of

Doctor of Philosophy

**Supervisor:** Prof. Gabriele Travaglini  
**Examiners:** Prof. Gregory Korchemsky  
Dr Nikolay Gromov

School of Physics and Astronomy  
Queen Mary University of London  
United Kingdom

May 2014

# Statement of Originality

I, Ömer Can Gürdoğan, confirm that the research included within this thesis is my own work or that where it has been carried out in collaboration with, or supported by others, that this is duly acknowledged below and my contribution indicated. Previously published material is also acknowledged below.

I attest that I have exercised reasonable care to ensure that the work is original, and does not to the best of my knowledge break any UK law, infringe any third party's copyright or other Intellectual Property Right, or contain any confidential material.

I accept that the College has the right to use plagiarism detection software to check the electronic version of the thesis.

I confirm that this thesis has not been previously submitted for the award of a degree by this or any other university.

The copyright of this thesis rests with the author and no quotation from it or information derived from it may be published without the prior written consent of the author.

Signature: 

Date: 12.05.2014

This thesis is based on the following publications in collaboration with Andreas Brandhuber, Dimitrios Korres, Robert Mooney, Gabriele Travaglini and Gang Yang:

- A. Brandhuber, O. Gurdogan, D.Korres, R.Mooney, G. Travaglini, *Two-loop Sudakov Form Factor in ABJM*, JHEP **1311** (2013) 022 [[arXiv:1305.2421 \[hep-th\]](https://arxiv.org/abs/1305.2421)] ,
- A. Brandhuber, O. Gurdogan, R. Mooney, G. Travaglini, G. Yang, *Harmony of super form factors*, JHEP **1110** (2011) 046 [[arXiv:1107.5067 \[hep-th\]](https://arxiv.org/abs/1107.5067)] .

The primary contribution of the author to the work on four dimensional form factors was the derivation of the solution for the split-helicity form factors. To the material related the three-dimensional form factors, the author has contributed with the derivation of the form factor integrands from unitarity cuts, evaluations thereof and the derivation of the non-planar scattering amplitude.

# Abstract

This thesis focuses on form factors in superconformal theories, in particular maximally supersymmetric Yang-Mills (MSYM) and ABJM. Scattering amplitudes in these theories have a wealth of special properties and significant amount of insight has been developed for these along with the modern techniques to calculate them. In this thesis, it is presented that form factors have very similar properties to scattering amplitudes and the techniques for scattering amplitudes can be successfully applied to form factors. After a review of the methods employed, the results for tree-level and multi-loop form factors of protected operators are derived.

In four dimensions, it is shown that the tree-level form factors can be computed using MHV diagrams BCFW relations by augmenting the set of vertices with elementary form factors. Tree and loop-level MHV and non-MHV form factors of protected operators in the stress-tensor multiplet of MSYM are computed as examples. A solution to the BCFW recursion relations for form factors is derived in terms of a diagrammatic representation. Supersymmetric multiplets of form factors of protected operators are constructed.

In three dimensions, Sudakov form factor of a protected biscalcar operator is computed in ABJM theory. This form factor captures the IR divergences of the scattering amplitudes. It is found that this form factor can be written in terms of a single, non-planar Feynman integral which is maximally transcendental. Additionally, the sub-leading colour corrections to the one-loop four-particle amplitude in ABJM is derived using unitarity cuts. Finally a basis of two-loop pure master integrals for the Sudakov form factor topology is constructed from a principle that relies on certain unitarity cuts.

# Table of Contents

<b>Statement of Originality</b>	<b>2</b>
<b>Abstract</b>	<b>3</b>
<b>1 Introduction</b>	<b>6</b>
1.1 MSYM . . . . .	9
1.1.1 MSYM Lagrangian and its symmetries . . . . .	11
1.1.2 Scattering in MSYM . . . . .	12
1.1.3 Hidden symmetries of scattering amplitudes in MSYM . . . . .	13
1.2 ABJM . . . . .	16
1.2.1 Comparison to MSYM . . . . .	17
1.3 Form factors . . . . .	18
<b>2 On-shell methods</b>	<b>21</b>
2.1 Supersymmetry multiplets of scattering amplitudes . . . . .	22
2.2 Colour ordering . . . . .	25
2.2.1 Colour structures in MSYM . . . . .	25
2.2.2 Colour structures in ABJM . . . . .	27
2.3 Tree-level recursion . . . . .	28
2.3.1 Recursion in four dimensions . . . . .	29
2.3.2 Recursion in three dimensions . . . . .	32
2.4 Unitarity . . . . .	33
2.4.1 Traditional Unitarity . . . . .	34
2.4.2 Generalised unitarity cuts of the integrand . . . . .	36
2.5 Some results for scattering amplitudes . . . . .	37
2.5.1 Tree-level $n$ -point MHV in four dimensions . . . . .	37
2.5.2 The colour-ordered one-loop MHV superamplitude in four MSYM	39
2.5.3 Tree-level amplitudes in ABJM . . . . .	43
2.5.4 The complete one-loop four-point amplitude in ABJM . . . . .	45
<b>3 Form factors in four dimensions</b>	<b>51</b>
3.1 MHV form factors of $\text{Tr } \phi_{12} \phi_{12}$ . . . . .	51
3.2 Tree-level bootstrap in four dimensions . . . . .	52
3.2.1 MHV diagrams . . . . .	52

---

3.2.2	Recursion relations . . . . .	55
3.3	Supersymmetric multiplets of form factors . . . . .	64
3.3.1	BPS Multiplets in MSYM . . . . .	64
3.3.2	Form factor of the chiral stress-tensor multiplet . . . . .	66
3.3.3	Examples . . . . .	70
3.3.4	Form factor of the complete stress-tensor multiplet . . . . .	73
3.3.5	Supersymmetric methods . . . . .	75
3.3.6	Supersymmetric recursion relations . . . . .	76
3.4	Vanishing of form factors at large $z$ . . . . .	77
3.4.1	Bosonic form factors . . . . .	77
3.4.2	Supersymmetric form factors . . . . .	78
3.5	Loop-level . . . . .	79
3.5.1	One-loop . . . . .	80
3.5.2	Two loops . . . . .	83
<b>4</b>	<b>Form factors in three dimensions</b>	<b>86</b>
4.1	BPS operators . . . . .	86
4.2	Sudakov form factor at loop level . . . . .	88
4.2.1	One-loop Sudakov form factor in ABJM . . . . .	89
4.2.2	Two-loop Sudakov form factor in ABJM . . . . .	90
4.3	Pure functions in three dimensions . . . . .	95
<b>5</b>	<b>Conclusion</b>	<b>100</b>
<b>A</b>	<b>Spinor/helicity in four dimensions</b>	<b>103</b>
<b>B</b>	<b>Spinor/helicity in three dimensions</b>	<b>106</b>
<b>C</b>	<b>Symmetry generators in MSYM</b>	<b>108</b>
<b>D</b>	<b>Non-MHV form factors</b>	<b>111</b>
<b>E</b>	<b>Feynman integrals</b>	<b>116</b>
<b>References</b>		<b>121</b>

# 1

# Introduction

Since it was first possible to access the subatomic world almost a century ago, scattering experiments have been the primary tool to probe its physics. In today's particle colliders such as the Large Hadron Collider, the physics of partons is probed by colliding two particles, such as protons, at high energies. Such processes are understood under the framework of the Standard Model of Particle Physics which includes the gauge theories *Quantum Chromodynamics* (QCD) and *Electroweak Theory* for the two main kinds of interactions that elementary particles go through in these processes. Our understanding of the laws of nature governing the interactions of the elementary particles is tested by confirming whether the Standard Model reproduces the data recorded by the detectors surrounding an interaction point.

The main ingredients for predicting scattering cross sections, that is roughly speaking the probability to produce some kind of particles due to the collision of two incoming particles, are the scattering amplitudes,  $M$ . In a quantum field theory, the existence of incoming and outgoing particles are represented by *multi-particle states* and scattering amplitudes are matrix elements corresponding to the inner product of an initial multi-particle state and a final one, which includes outgoing particles in the scattering process. In other words, the quantities which are schematically represented as

$$M = \langle \text{in} | S | \text{out} \rangle, \quad (1.1)$$

where  $S$  is the operator that evolves in time a multi-particle state  $\langle \text{in} |$ , need to be computed in order to make a prediction for a collider experiment.

Unfortunately, it is often impossible to perform exact computations in interacting quantum field theories and the gauge theories are not an exception. However, at energy scales where the coupling constants are small enough, it is possible to approximate the matrix elements in a perturbation series in the coupling constants. Although they are much easier than exact computations, apart from some very simple cases, perturbative computations in QFT are full of challenges and their computation is one of the major bottlenecks for making predictions for collider experiments.

The textbook-standard method for computing scattering amplitudes starts with the corresponding correlation function and then obtains the scattering amplitude using LSZ reduction and projecting it to the external polarisation data. To compute the correlation function perturbatively, one first draws all the Feynman diagrams relevant to the process of interest, which are limited by the desired number of their interaction vertices or the number of their loops. The edges and the vertices represent propagators and couplings, which have spacetime and colour dependence. One also has to integrate over the momenta that run in the loops, which can be a challenging task on its own.

The Feynman diagram method is highly straightforward and mechanical, in the sense that many of its steps can be automated on a computer. On the other hand, computations can become extremely heavy as the number of Feynman diagrams one can draw grows extremely rapidly. Even without any loops, for a  $n$ -particle process, one has to compute  $\mathcal{O}(n!)$  Feynman diagrams. To make such computations realistic, other methods need to be followed.

The computational load is not the only, and perhaps also not the main reason for expecting the existence of better methods to compute scattering amplitudes. Surprisingly simple results for scattering amplitudes have been known for decades, hinting that there should be methods other than Feynman diagrams, which are not only computationally more efficient, but also more transparent for understanding the results for the computed scattering amplitudes.

At tree level, the  $n$ -gluon colour-ordered<sup>1</sup> amplitude in QCD, which is valid for any four-dimensional Yang-Mills theory, has been conjectured in [1] to be

$$A = ig^{n-2} \frac{\langle ij \rangle^4}{\langle 12 \rangle \langle 23 \rangle \cdots \langle n1 \rangle}, \quad (1.2)$$

where two of the gluons, 1 and 2 in this case, are taken to have negative helicity while the rest have positive helicity. Here the quantities  $\langle ab \rangle$  are brackets of spinors associated with the momenta  $p_a$  and  $p_b$ , as defined in Appendix A.  $g$  is the Yang-Mills coupling constant. Apart from direct checks, this result can be proved using the factorisation properties of scattering amplitudes. A proof using recursion relations is provided in Chapter 2.

This result, and other scattering amplitudes that depend on the particle content of the theory one is interested in, can be derived without any reference to a Lagrangian, path integral and to Feynman diagrams. Starting with a simpler theory than QCD, namely

---

<sup>1</sup>Colour ordering is a procedure in which colour dependence is decoupled from kinematics dependence.

MSYM, several modern methods have been developed to construct these scattering amplitudes at tree level [2, 3] and also at loop level [4? ]. The common feature of these methods is that they rely on the factorisation properties of the scattering amplitudes. The idea of constructing scattering amplitudes from their factorisation properties is not new, but part of a long-lasting programme dating back to the 1960s, see for example [5].

Choosing the right variables to encode kinematical data is crucial for efficient and transparent computation of scattering amplitudes. The use of the spinor-helicity formalism provides considerable convenience even for Feynman diagram computations. Besides using spinors, dual momenta, twistors and other variables to encode kinematical data where appropriate, is crucial in obtaining simple and more transparent expressions for scattering amplitudes [6]. Conceptually, finding the correct variables to encode the kinematical data of scattering amplitudes is still an open problem [7, 8].

There is a very special quantum field theory, namely the maximally supersymmetric Yang-Mills (MSYM) theory, which is arguably the most symmetric gauge theory in four dimensions. As the name suggests, it has the maximal amount of supersymmetry (SUSY) a theory can have without introducing fields with spins higher than 1. In addition to supersymmetry, it is conformally invariant, meaning that the theory does not evolve with the energy scale and the coupling constant is actually a constant fixed at will.

The scattering amplitudes in MSYM theory are particularly simple and uncontaminated in a sense elaborated in the following Chapter, where explicit results for scattering amplitudes in this theory are presented. It is relatively easier to understand the mathematical properties of scattering amplitudes in the sterile environment of this theory.

Although simpler, MSYM is also considerably different than the physical theories that make up the Standard Model. The matter fields transform under the adjoint representation of the gauge group. *A priori*, there seems to be no reason to be interested in scattering amplitudes of the theory because there would be no experiments to compare the results with. However MSYM has been a perfect laboratory to develop technology for computing scattering amplitudes and many of the modern techniques have been developed in this theory. The automated computation of all QCD one-loop gauge theory amplitudes using unitarity techniques by the BlackHat collaboration [9] is a good example of how advances in MSYM have improved QCD computations.

## 1.1 MSYM

MSYM is the unique maximally supersymmetric Yang-Mills theory in four dimensions, up to the rank of the special unitary gauge group and the strength of a single, dimensionless coupling constant. The field content of this theory consists of an  $SU(N_c)$  gauge field and matter fields which are four Majorana fermions and six real scalar fields. The gauge fields and the matter fields are transformed into each other by supersymmetry transformations, thus they belong to the same adjoint representation of the gauge group  $SU(N_c)$ , more precisely they take values in its algebra  $\mathbf{su}(N_c)$

Historically, MSYM originates from string theory. It has first emerged as the effective model arising from string compactifications [10]. This model is the maximally supersymmetrised extension of a Yang-Mills theory. It has the unique particle content of a maximally supersymmetric theory in four dimensions.

Since its inception, it has been considered as a very special field theory, not only because of its unique maximal supersymmetry, but also due to the fact that it has a vanishing beta function in all orders in perturbation theory. This has been explicitly checked in perturbation theory up to three loops [11–13]. Alternatively, it can be proved using the proportionality between the beta function and the stress energy tensor and showing the vanishing of the latter using superconformal invariance [14, 15].

A commonly studied limit of MSYM is the planar limit where number of colour  $N_c$  is very large but  $g^2 N$  is kept fixed. In fact, every gauge theory is known to have simplifications in this limit, for example in general non-planar Feynman diagrams can be discarded as they contribute with subleading dependence on  $N_c$  [16]. The weak coupling regime is where  $g^2 N$  is taken to be small and perturbative quantities are defined in an expansion in the 't Hooft coupling constant

$$a = \frac{g^2 N_c}{16\pi^2 (4\pi)^{-\gamma_E}}, \quad (1.3)$$

where  $\gamma_E$  is the Euler-Mascheroni constant and  $\epsilon$  is the dimensional regularisation parameter in  $D = 4 - 2\epsilon$  dimensional computations.  $a$  is defined such that every order in the loop expansion comes with a nice coefficient of the form  $a^L$ , without the usual  $\gamma_E$  appearing in what multiplies it. In the entirety of this work, the planar MSYM and (ABJM) will be assumed and for brevity, the dependence on  $a$  will be dropped, which is implied from the number of loops considered.

In the strong coupling limit, where  $a$  is large, MSYM has a very nice interpretation in the framework of string theory. In the string theory picture, the MSYM theory with

a gauge group  $U(N_c)$  is the gauge theory living on the 3+1 dimensional world volume of a stack of  $N_c$  D3 branes. It has seen great interest after the late 90s when it was understood, by the seminal work of Maldacena [17], that in the planar strong coupling limit, the theory is dual to supergravity on an  $AdS_5 \times S^5$  manifold. As a consequence, it has become the the most prominent quantum field theory in which analytic strong coupling results can be obtained.

Although it is not within the focus of this thesis, a remarkable property of MSYM, that has to be mentioned, is integrability. Thanks to integrability, analytic results for many quantities in this theory can be obtained exactly. Integrability has been exploited to compute several quantities, such as correlation functions, anomalous dimensions, etc., see [18] and the references therein for a comprehensive review of integrability in MSYM. Recently, recursion relations between scattering amplitudes have been exploited to construct scattering amplitudes from the invariants of an infinite dimensional symmetry, namely the Yangian symmetry. These invariants can be obtained from integrability techniques such as the Bethe Ansatz [19–23].

As already a very interesting theory with the above-mentioned aspects, it is not surprising that MSYM has a very special perturbation theory. Firstly, in parallel with the vanishing beta function and conformal symmetry, scattering amplitudes and the correlation functions of protected operators do not have UV divergences. Furthermore, the simplicity of scattering amplitudes is not restricted to tree level, but also the loop corrections have a remarkable simplicity, in contrast to their counterparts in QCD. This is particularly the case for MHV amplitudes.

The unique properties of MSYM have allowed several breakthroughs in computations of scattering amplitudes to predate similar computations in QCD by several years. At the time of writing of this thesis, the state of the art computations include up to four-loop MHV scattering amplitudes of six gluons [24]<sup>2</sup>, while in QCD processes involving three or four particles and two or three loops are considered a challenge. Symmetries play a major role in this situation. For instance dual superconformal symmetry, which is discussed more in detail in Section 1.1.3, restricts the integral basis considerably such that generalised unitarity methods are applied more efficiently.

Inspired by the simple yet beautiful scattering amplitudes in MSYM, a natural questions arises: what are the the limits of the convenience that this theory provides are. To what extend can the lessons learned from advances in scattering amplitudes help us to perform computations in this theory and understand it better? How relevant are the

---

<sup>2</sup>The computation of the MHV amplitudes in MSYM rely one the duality with expectation values of Wilson loops, which are relatively easier to compute.

modern computational tools for other “observables” in this theory? It turns out that in many ways form factors in special theories like MSYM and ABJM are objects of a very similar nature to scattering amplitudes and their computation can be simplified drastically using similar methods.

### 1.1.1 MSYM Lagrangian and its symmetries

Although it has to be stressed that the knowledge of the Lagrangian is not necessary for computing scattering amplitudes or form factors, for definiteness, the Lagrangian of MSYM is presented in this Section. The Lagrangian of MSYM can be written as

$$\begin{aligned} \mathcal{L} = \text{Tr} \left[ -\frac{1}{2} F^2 + \frac{1}{2} D_\mu \phi_{AB} D^\mu \bar{\phi}^{AB} + \frac{1}{8} g^2 [\phi_{AB}, \phi_{CD}] [\bar{\phi}^{AB}, \bar{\phi}^{CD}] \right. \\ \left. + 2i \bar{\lambda}_{\dot{\alpha}, A} \sigma_\mu^{\dot{\alpha}\beta} D^\mu \lambda_\beta^A - \sqrt{2} g \lambda^{\alpha A} [\phi_{AB}, \lambda_\alpha^B] + \sqrt{2} g \bar{\lambda}_{\dot{\alpha}, A} [\bar{\phi}^{AB}, \bar{\lambda}_B^{\dot{\alpha}}] \right] \end{aligned} \quad (1.4)$$

Here  $F$ ,  $\lambda$ ,  $\bar{\lambda}$ ,  $\phi$  denote the gauge-field strength, Weyl fermions, their conjugates and scalar fields, respectively.  $\bar{\phi}$  is defined as follows:

$$\bar{\phi}_{AB} = (\phi^{AB})^* = \frac{1}{2} \epsilon_{ABCD} \phi^{CD}. \quad (1.5)$$

The index  $\mu$  is a space-time index.  $A, I$  are R-symmetry indices for the  $SU(4) \cong SO(6)$  R-symmetry index that run from 1 to 4 and 1 to 6, respectively. The gauge coupling  $g$  is a dimensionless free parameter.

All fields are in the adjoint representation of the algebra of the gauge group  $SU(N_c)$ :

$$X = X^a (T^a)_i^j, \quad X = A_\mu, \lambda_\alpha, \lambda^{\dot{\alpha}}, \phi_{AB} \quad (1.6)$$

Many of the symmetries of scattering amplitudes can be seen in the Lagrangian of the theory while some cannot. In particular, conformal symmetry and the  $\mathcal{N} = 4$  supersymmetry which together give rise to *superconformal symmetry* are symmetries of the Lagrangian (1.4). The full set of generators of the symmetries of the MSYM Lagrangian is quoted in Appendix C.

Scattering amplitudes in MSYM, as any other quantity in this theory, transform appropriately under the actions of the above mentioned symmetries and satisfy the relevant Ward identities. Some of these properties will be discussed below and further in detail in Chapter 2 when explicit expressions for scattering amplitudes are provided.

### 1.1.2 Scattering in MSYM

This Section aims to give a brief overview of the special properties of scattering amplitudes in MSYM. Some of these properties immediately follow from the symmetries of the Lagrangian of the theory, but some have a much more non-trivial origin.

The Lagrangian symmetries of MSYM have some immediate consequences on the scattering amplitudes. For instance, the defining property of MSYM is the supersymmetry generated by sixteen supercharges, the maximum allowed in four dimensions and it sets stringent conditions on scattering amplitudes. SUSY is not broken perturbatively and thus the scattering amplitudes obey non-anomalous, homogeneous SUSY Ward identities. As a result, the scattering amplitudes with less than 2 negative-helicity gluons vanish:

$$Q_i^A \mathcal{A} = 0 \Rightarrow \begin{cases} \mathcal{A}(1^\pm, 2^\pm, \dots, n^\pm) = 0 \\ \mathcal{A}(1^\pm, 2^\pm, \dots, n^\pm) = 0 \end{cases} \quad (1.7)$$

As mentioned in the previous Section, at tree level, QCD gluon amplitudes are kinematically indistinguishable from those of MSYM and the implications of Ward identities also apply to tree-level QCD amplitudes [25]. Hence, while QCD amplitudes with zero or one odd helicity gluons do not vanish at the loop level, they do not exist in MSYM.

In general, all scattering amplitudes of processes for which the  $R$ -charge is not conserved, such as  $\phi_{12}\phi_{12} \rightarrow \phi_{12}\phi_{34}$ , vanish.

Moreover, SUSY relates the amplitudes of diverse particle species to each other allowing the amplitudes to be packaged in supermultiplets as described in Section 2.1 of the following Chapter.

The scattering amplitudes of MSYM are known to have conformal symmetry, at least at tree level [26]. Since the theory is massless the loop amplitudes are IR divergent and have to be regulated. With the scale introduced by the regulators, conformal symmetry of amplitudes is broken. However, the IR-safe observables respect all of the superconformal symmetries of the theory [27].

There are other special properties of scattering amplitudes in MSYM which do not directly follow from the Lagrangian.

An extremely curious property of MSYM amplitudes at loop level is the so-called “maximal transcendentality”. All known amplitudes in this theory are made out of polylogarithm functions and transcendental numbers which have uniform degree of transcendentality  $2L$  at  $L$  loops. This is expected to be the case for all MHV amplitudes however to break down for the 10-gluon amplitude with 5 positive and 5 negative-

helicity gluons at two loops. This amplitude is given in terms of a elliptic integral - a class of functions which appear in many QCD computations with massive internal particles, see for example the two-loop self energies computed in [28].

There are diverse formulations of scattering amplitudes in MSYM which make certain properties more transparent. In [26] it was shown that, when transformed into twistor space, the  $L$ -loop,  $N^k$ MHV scattering amplitudes in MSYM have support on holomorphic curves of degree  $k + L + 1$ . This has been one of the first geometric ways of understanding the simplicity of MHV amplitudes.

Later further geometric pictures have emerged in which they are defined in the Grassmannian space [29], or as polyhedra in twistor space [30]. These Grassmannian integrals can be written down as a solution of the all-loop recursion relations, using a prescription from three equivalent pictures, namely on-shell diagrams with trivalent vertices, permutations and polyhedra. They reproduce scattering amplitudes in MSYM to an arbitrary number of loops, or the integrals thereof, once a correct contour is chosen for the Grassmannian integral. In the Grassmannian formalism, the Yangian symmetry of the theory is manifest [31].

Although the advances in QCD often lag behind those in MSYM due to the complication of the computations, the two theories are not as unrelated as one might expect. Despite all the differences between MSYM and QCD, there exist surprising results that link the amplitudes in the two theories.

As the most trivial example, the tree amplitudes of gluons in two theories have the same kinematical dependence as they share the same Yang-Mills action (apart from the number of colours) and the matter fields play a role only at loop level. Moreover, surprising results at loop level indicate interesting connections between MSYM and QCD. In some known cases, such as form factors, anomalous dimensions and Wilson coefficients [32], the maximally-transcendental parts of the QCD quantities, which are the parts with transcendentality weight  $2L$  for an  $L$ -loop quantity, coincide with the corresponding quantity in MSYM. For example, a two-loop form factor of a BPS operator with three gluons captures the maximally transcendental part of a  $H \rightarrow ggg$  scattering amplitude in QCD [33].

### 1.1.3 Hidden symmetries of scattering amplitudes in MSYM

Besides of the symmetries that can be derived from the Lagrangian of this theory, there is another set of symmetry transformations that realise a copy of the superconformal

algebra and leave the scattering amplitudes in MSYM invariant.

This symmetry is called the dual conformal symmetry and it first emerged in a strong coupling computation of scattering amplitudes [34]. In the AdS/CFT picture, the computation of scattering amplitudes is mapped to the problem of computing the expectation value of a light-like Wilson loop. This is achieved by a T-duality transformation, which acts on the boundary spacetime where MSYM lives and leaves the AdS bulk unchanged.

The AdS bulk spacetime has  $SO(2, 4)$  symmetry, corresponds to a conformal symmetry of the boundary theory. It is very important that the conformal symmetry of the dual Wilson loop is independent of the conformal symmetry of the original scattering picture.

The duality was confirmed to hold for one-loop perturbative Wilson loops and MHV scattering amplitudes with four and five gluons in [35] and for all MHV amplitudes in [36]. Since the Wilson loop expectation values have conformal symmetry, the duality explicitly confirms the dual conformal symmetry for scattering amplitudes.

The dual symmetry of all-loop perturbative scattering amplitudes / Wilson loops relies on the co-variance of the tree-level prefactor multiplying dual conformal invariant integral functions. It was conjectured in [37] and it was proven in [38] that all MHV and non-MHV- tree scattering amplitudes transform co-variantly under the dual symmetry.

The dual transformations act on 't Hooft region momenta  $x_i$  which are defined such that:

$$x_i - x_{i+1} = p_i \quad (1.8)$$

and the fermionic analogues thereof such that:

$$\theta_{i\alpha}^A - \theta_{i+1\alpha}^A = \lambda_{i\alpha} \eta_i^A. \quad (1.9)$$

The momenta  $p_i$  form a closed polygon with vertices  $x_i$ . Such a construction is possible if and only if  $\sum_{i=1}^n p_i = 0$ , ie when all the momenta of the particles in the asymptotics state sum to zero - which is not the case for form factors.

An obvious freedom in the definition of the region momenta  $x_i$  is the choice of the origin. Overall shifts of the region momenta generated by

$$P = \sum_{i=1}^n \frac{\partial}{\partial x_{\alpha\dot{\alpha}}^i} \quad (1.10)$$

do not change the momentum. Similar to  $P$ , the other generators of the dual superconformal transformations acting on the dual space coordinates coordinates  $x_i$ ,  $\lambda_i$  and  $\theta_i$  are defined in analogy to the ordinary space as if these were ordinary spatial coordinate. The explicit forms of the dual superconformal symmetry generators are quoted in Appendix C.

The dual conformal symmetry has important consequences on the scattering amplitudes that have this symmetry. As explained in Chapter 2, it is very useful to be able to expand scattering amplitude in terms of an integrand basis. If the theory has a dual conformal symmetry, integrals not invariant under dual conformal symmetry, which amount to a big majority of integrands one can think of, should be discarded.

Dual conformal symmetry also clarifies the remarkable iterative structure observed [39] in MSYM, namely The BDS Ansatz. Motivated by the resummation of the infrared divergences, the BDS Ansatz predicts the *all-loop* scattering amplitude for an  $n < 6$  particle process in an exponential form, which kinematically only depends on the 1-loop scattering amplitude. This astonishing resummation can be explained by realising that the BDS Ansatz the unique solution to the dual conformal Ward identities for  $n < 6$  [40]. The prediction of [39] was based on the known two-loop results [41] and a three loop computation in that paper. It has been explicitly checked up to four loops for  $n = 4$  [42–44] and up to two loops for  $n = 5$  [45].

When the number of particles  $n$  is equal to or greater than 6, it is possible to define kinematical variables

$$u_{ij} := \frac{x_{i,j+1}^2 x_{i+1,j}^2}{x_{ij}^2 x_{i+1,j+1}^2} \quad (1.11)$$

which are invariant dual conformal transformations, including inversions  $x_i \mapsto x_i/x_i^2$ .

This makes it possible to define a function, that depends non-trivially on the kinematical variables and also annihilated by the generator of dual conformal transformations, because any function of the  $u_{ij}$  variables would be invariant under such transformations and be a homogeneous solution of the dual conformal Ward identity [35].

As a consequence of the existence of dual conformal invariant cross ratios for  $n \geq 6$ , the amplitude can be modified by a homogeneous solution to the Ward identity. These functions are called *remainder functions* and they have been computed numerically with a large number of legs [46] and analytically up to four loops for  $n = 6$  [7, 24, 47]. The remainder functions for higher number of particles have not yet been computed.

The dual superconformal symmetry of scattering amplitudes together with the ordinary superconformal symmetry generate a Yangian algebra [48]. The Yangian is an

infinite dimensional algebra and it is argued that it is linked to the integrability of the scattering amplitudes of MSYM [49]. Supporting this, it is possible to find Yangian invariants using integrability techniques and identify these as scattering amplitudes [19–23]. However, finding Yangian invariants is not enough to construct scattering amplitudes because the scattering amplitudes are made of non-trivial combinations of Yangian invariants<sup>3</sup>. The construction of a scattering amplitude in terms of Yangian invariants needs further input. For a Yangian invariant to be identified as a scattering amplitude, it must have the required factorisation properties and this input comes from recursion relations.

## 1.2 ABJM

From the string theory perspective, MSYM is the effective field theory of a stack of D3 branes. The field theory lives on the 3+1 dimensional world volume of the brane and the gauge fields correspond to the open strings attached to these branes. String theory however, arises from compactifications of M theory, which only involves M2 and M5 branes. From this point of view, it is a very natural question to ask what the field theory living on the world volume of M2 branes is.

The answer turns out to be [51] a 2+1 dimensional theory with two Chern-Simons gauge fields [52] of level  $k$  and additional matter fields such that the theory has  $\mathcal{N} = 6$  supersymmetry. The Chern-Simons gauge fields transform under two independent  $SU(N)$  rotations, making the gauge symmetry of the theory  $SU(N) \times SU(N)$ . The matter fields consist of four fermions and four scalars. Each matter field comes in two types, those transforming as  $(N, \bar{N})$  and those transforming as  $(\bar{N}, N)$  representations to this gauge group. These two types couple to each other such that they are the antiparticles of each other.

The 4+4 scalar degrees of freedom can be interpreted as the transverse motion of an M2 brane, which is a 2+1 dimensional object embedded in a 10+1 dimensional spacetime. This is largely analogous of the role played by the six scalars of the MSYM theory. The fermions are the supersymmetric partners of these degrees of freedom.

Although in ABJM theory, as described above, the two independent gauge transformations are representations of the same special unitary group, it is possible to have these groups with unequal ranks [53] i.e.,  $SU(N) \times SU(N')$  instead of  $SU(N) \times SU(N)$ . In this theory, which is referred to as the ABJ theory, the matter fields are  $N \times N'$

---

<sup>3</sup>This is compatible with the observation made in [50], namely that conformal and dual conformal symmetries do not constrain the amplitudes entirely.

Field	$SU(N)$	$SU(N')$
$A_\mu$	$\mathbf{N}$	$\mathbf{1}$
$\hat{A}_\mu$	$\mathbf{1}$	$\mathbf{N}'$
$\phi, \psi$	$\mathbf{N}$	$\bar{\mathbf{N}}'$
$\bar{\phi}, \bar{\psi}$	$\bar{\mathbf{N}}$	$\mathbf{N}'$

Table 1-A: The field content of ABJ(M) theories.  $\mathbf{1}$  stands for a singlet,  $\mathbf{N}$ ,  $\mathbf{N}'$  for the fundamental and  $\bar{\mathbf{N}}$ ,  $\bar{\mathbf{N}}'$  for the anti-fundamental representation of the gauge group they are written under. For ABJM theory, the ranks of the two gauge groups are equal to each other:  $N = N'$ .

non-square matrices in colour space.

The field content of ABJM and ABJ theories can be summarised as shown in table 1-A. The string/M theory interpretation of ABJ theory is a stack of  $N' - N$  M2 branes fixed at the singularity of the manifold  $\mathbb{C}/\mathbb{Z}^k$  manifold and  $N$  M2 branes move unrestrictedly, where without loss of generality  $N' > N$  is assumed.

Although this thesis is mainly concerned with form factors in ABJM theory, the notation is used for the colour degrees of freedom of the fields is suitable to describe the ABJ generalisation. For the fundamental (anti-fundamental)  $SU(N)$  indices of a particle labelled  $m$  the indices  $i_m$  ( $i_m$ ) are used, while for the fundamental (anti-fundamental)  $SU(N)$  indices of such a particle are indicated by  $\bar{i}_m$  ( $\bar{i}_m$ ). The indices  $i_m$  run from 1 to  $N$ , whereas  $\bar{i}_m$  run from 1 to  $N'$ . To recover the ABJM case,  $N'$  is simply set to  $N$ .

### 1.2.1 Comparison to MSYM

If one is unaware of the string/M theory origin of the two theories, at a first glance at ABJM theory is quite unrelated to MSYM: it is defined in 2+1 dimension instead of 3+1, it has two Chern-Simons gauge fields instead of a Yang-Mills gauge field and the matter fields transform under the bi-fundamental representation of the gauge group.

One would also not necessarily expect similarities for the scattering amplitudes, either. Spinor-helicity in three dimensions is essentially different to that in four dimensions, as there is no helicity in three dimensions. There is a single type of spinors that correspond to on-shell momenta and there are no MHV amplitudes.

Nevertheless, the  $2n$ -point scattering amplitudes of ABJM theory behave similarly to the scattering amplitudes of MSYM with equal number of negative and positive helicities, as if the barred fields had one helicity and the unbarred the other. Thus the four point scattering amplitudes, have the simplicity of an MHV amplitude, six point

amplitudes that of an NMHV amplitude and so on.

To some surprise, the two-loop, four-point scattering amplitude, which is purely of transcendentality weight 2 turns out to have the exact same functional form as the one-loop scattering amplitude in MSYM theory [54]. Moreover, the two-loop six-point scattering amplitude has the same BDS part [55]. This is actually not so surprising as the ABJM amplitudes possess an anomalous dual conformal symmetry and the anomalous Ward identities they satisfy are the same [55]. As a result the unique special solution to the anomalous Ward identities are the same as in MSYM. However the remainder functions are not constrained by the Ward identity and indeed they differ in these theories.

### 1.3 Form factors

At a first glance, form factors are objects in the middle of scattering amplitudes and correlation functions. Scattering amplitudes are the overlap of an in-state with an out state. Correlation functions are the vacuum expectation values of operators inserted at space-time points. Form factors on the other hand, are expectation values of operators between multi-particle states.

More precisely, the objects of interest have the following form:

$$\tilde{F}(p_i; x) = \langle 0 | \mathcal{O}(x) | \text{m.p. state} \rangle, \quad (1.12)$$

where  $|\text{m.p. state}\rangle$  is a multi-particle state with,  $n$  particles and the (composite) operator  $\mathcal{O}$  is chosen to be a protected (BPS) operator such that it does not get renormalised. The ket state can involve any of the particles in the theory considered, for the form factor to be non-zero, it must involve fields that saturate the elementary fields that make up  $\mathcal{O}$ .

For the computation of the form factor  $F$ , it is more convenient to write its spacetime dependence of  $F$  in momentum space. This is done as follows. One first Fourier transforms  $x$

$$\tilde{F}(p_i; q) = \int dx \exp(iq \cdot x) \tilde{F}(x) \quad (1.13)$$

and then translates the operator to the origin with the finite generators of translations

$$\mathcal{O}(x) = \exp(i\hat{P} \cdot x) \mathcal{O}(0) \exp(-i\hat{P} \cdot x) \quad (1.14)$$

and acts with the translation generators on  $\langle 0 |$  and  $| \text{m.p. state} \rangle$ . One obtains:

$$\tilde{F}(q) = \delta \left( q - \sum_{i=1}^n p_i \right) F(p_i), \quad (1.15)$$

where

$$F(p_i) = \langle 0 | \mathcal{O}(0) | \text{m.p. state} \rangle \quad (1.16)$$

and  $p_i, i, \dots, n$  are the momenta of the particles in  $| \text{m.p. state} \rangle$ , such that

$$\sum_{i=1}^n p_i = q. \quad (1.17)$$

In quantum field theory, form factors appear in several interesting places. For example they appear in the cross sections of hadrons scattering off hadrons or other particles. One such process is deep inelastic scattering (DIS), where a lepton probes a hadron by interacting with its constituents by a boson exchange and also producing some particles in the final state. Another one is a Drell-Yann process, in which two hadrons collide and several different particles are produced.

The hadrons are non-perturbative objects and it is very hard to treat them entirely in a hadron - lepton collision process governed by a perturbative model of quarks, gluons and leptons. Considering DIS for definiteness, one can instead assume that the lepton and the hadron interact via a boson exchange and inside of the hadron, the boson couples to a parton which is found in the hadron with a certain probability. The amplitude corresponding to this process is the matrix element of a quark current, which the exchanged boson couples to. The initial state in this matrix element is the QCD vacuum as hadrons do not exist in perturbative QCD and the final state is the one with several unobserved particles.

The Sudakov form factor, which is the matrix element of an operator with a two-particle state, can be used to compute the universal infrared divergences of (colour-ordered) scattering amplitudes and the anomalous dimensions that control these soft and collinear divergences. For example in the planar MSYM theory the infrared divergences are particularly simple and they factorise as follows [39]:

$$\mathcal{A}(p_i) = \prod_i^n \left[ F^{1 \rightarrow 2}(s_{i,i+1}) \right]^{\frac{1}{2}} h(p_i), \quad (1.18)$$

where  $F^{1 \rightarrow 2}$  is the Sudakov form factor and  $h$  is a finite hard function. The main feature of the IR singularities of planar MSYM is that they only arise from kinematical

limits of neighbouring particles, as is apparent from the momentum dependence of the IR-divergent parts of (1.18).

Furthermore, it is also an interesting question how much one can achieve in the computation of “off-shell” quantities using “on-shell” techniques. They certainly drastically simplify the computation of scattering amplitudes, in which all the fields are on-shell. One would be encouraged to attempt to utilise these methods for computing correlation functions. Indeed, it has been possible to compute correlation functions of protected operators in MSYM and results form factors have been central in this [56].

In [57], on-shell techniques have been successfully applied to some form factors in MSYM at tree and one-loop level. Using recursion relations it was possible to show that there is a subclass of form factors, which can be classified as MHV and resemble the MHV scattering amplitudes with their simplicity and resemblance to the Parke-Taylor form of MHV scattering amplitudes (1.2). Moreover, using unitarity methods it has been possible to derive known and unknown one-loop results using unitarity cuts.

Other old and new works on the form factors of this type include the two-loop Sudakov form factor in MSYM [58], two-loop computations of the form factors of the operators that appear in the stress-tensor multiplet in component formalism [59], and in superspace [60]. The Sudakov form factor in MSYM has also been computed up to three loops [61].

More general form factors have been considered in a recent paper [62]. These form factors are constructed with longer BPS operators such as  $\text{Tr}(\phi^k)$  have a recursive structure which links form factors with different values of  $k$ .

# 2 On-shell methods

This Chapter contains the review of the techniques used in Chapters 3 and 4 to compute form factors of protected operators in MSYM and ABJM. Example calculations are provided at the end of the Chapter.

Some of the results quoted here are among the important milestones of amplitude computations in MSYM and ABJM. Using recursion techniques, it is extremely easy to derive certain tree-level scattering amplitudes with an arbitrary number of particles, a task impossible using the traditional Feynman diagram approach. At loop level, (generalised) unitarity is a very powerful method. This is especially true at one loop, where it is possible to expand any gauge theory amplitude into an non-over-complete integral basis and to find the coefficients in a straightforward way. Thanks to this method, certain gauge theory amplitudes, in particular the one-loop MHV superamplitude in MSYM, can be easily computed also with an arbitrary number of particles.

Furthermore, these results are an important ingredient of the computations presented in Chapters 3 and 4. The tree-level and loop-level factorisation diagrams of form factors contain simpler form factors as well as scattering amplitudes. Due to the colour structure of form factors, the loop level form factor computations require not only the leading  $N_c$  parts of scattering amplitudes but also the sub-leading ones, which is not the case for scattering amplitudes.

The methods (and results) discussed in this Chapter are restricted by their practical relevance for the form factor computations that are the subject of this thesis. For further details on these methods one may consult to several detailed review articles available on the subject: [25, 63–65].

This Chapter is organised such that the technical background reviewed at the beginning without many examples. Explicit computations of amplitudes using a number these techniques are included at the end of the Chapter.

## 2.1 Supersymmetry multiplets of scattering amplitudes

Especially in MSYM, SUSY has very constraining consequences and is responsible for many simple results for scattering amplitudes in this theory. These properties can be made manifest by not considering amplitudes that are related to each other through SUSY as multiplets in a superspace.

To study supersymmetric multiplets of scattering amplitudes, it is necessary to have an on-shell representation of the supersymmetry algebra, in which the on-shell multi-particle states transform. Such a representation was constructed for MSYM in [66].

The on-shell superalgebra can be constructed starting from the off-shell algebra. The maximal supersymmetry algebra in four dimensions is:

$$\{Q_\alpha^A, \bar{Q}_{\dot{\alpha},B}\} = p_{\alpha\dot{\alpha}}\delta_B^A, \quad (2.1)$$

where  $A, B$  are the R symmetry indices and  $\alpha, \dot{\alpha}$  are Weyl spinor indices for the two kinds of spinor representations of four-dimensional Lorenz algebra.  $p_{\alpha\dot{\alpha}}$  is the momentum of a massless one-particle state dotted with the matrices  $\sigma_{\alpha\dot{\alpha}}$  defined in Appendix A.

For massless single-particle states, the momentum can be decomposed into one left- and one right-handed spinor, as described in Appendix A:

$$p_{\alpha,\dot{\alpha}} = \lambda_\alpha \tilde{\lambda}_{\dot{\alpha}}, \quad (2.2)$$

such that  $p \cdot p = 0$ . Moreover, the supermomentum generators can be projected onto the spinors corresponding to the momentum of an on shell particle as follows:

$$Q_\alpha^A = q^A \lambda_\alpha + Q_\alpha^{\perp,A}, \quad \bar{Q}_{\dot{\alpha},B} = \bar{Q}_B \tilde{\lambda}_{\dot{\alpha}} + \bar{Q}_{B,\dot{\alpha}}^{\perp}. \quad (2.3)$$

The supersymmetry generators  $Q_\alpha^A$  and  $\bar{Q}_{\dot{\alpha},B}$  are indeed proportional to the spinors  $\lambda_\alpha$  and  $\tilde{\lambda}_{\dot{\alpha}}$  associated with the momentum  $p^\mu$  of the one-particle state, as can be seen by dotting equation (2.1) with these spinors. Therefore the perpendicular components  $Q_\alpha^{\perp,A}$  and  $\bar{Q}_{B,\dot{\alpha}}^{\perp}$  can be set to zero.

Substituting the decompositions into the supersymmetry algebra (2.1) one finds the following anti-commutation relation for  $Q^A$  and  $\bar{Q}_B$ :

$$\{Q^A, \bar{Q}_B\} = \delta_B^A, \quad (2.4)$$

which can be represented using four anti-commuting variables  $\eta^A$ :

$$Q^A = \eta^A, \quad \bar{Q}_A = \frac{\partial}{\partial \eta^A}. \quad (2.5)$$

Supersymmetry relates different field configurations that can appear as an external state of an amplitude. This is realised by organising the fields in a supermultiplet  $\Phi$  in the  $\eta^A$  superspace:

$$\Phi = G^+ + \eta^A \psi_A + \frac{1}{2} \eta_A \eta_B \phi^{AB} + \frac{1}{3!} \epsilon_{ABCD} \eta^A \eta^B \eta^C \psi^D + \frac{1}{4!} \epsilon_{ABCD} \eta^A \eta^B \eta^C \eta^D G^- \quad (2.6)$$

on which the representations of the on-shell SUSY generators (2.5) act naturally.

For multi-particle states, the representation of the superalgebra is just a product of the single-particle representations. In particular, multiplets of scattering amplitudes are polynomials in the  $\eta$  variables corresponding to the particles involved, as explained further below.

Types of particles in a scattering process are transformed into each other via supersymmetric and it is possible to package these amplitudes in a multiplet of amplitudes, called the *superamplitude*. Superamplitudes have an overall supermomentum-conserving delta function of the sum of the supermomenta carried by the particles involved in the process. An  $L$ -loop superamplitude in MSYM is defined as

$$\mathcal{M}_n^{(L)} = \frac{\delta^{(8)} \left( \sum_{i=1}^n \eta_i^A \lambda_{i,\alpha} \right) \delta^{(4)}(p_{\alpha\dot{\alpha}})}{\langle 12 \rangle \langle 23 \rangle \cdots \langle n1 \rangle} \mathcal{P}_n^{(L)}, \quad (2.7)$$

where  $\mathcal{P}$  is a sum of monomials of Grassmann degree  $4k$ . Each term in  $\mathcal{P}_n^{(L)}$  is equal to the ratio of an  $N^k$ MHV amplitude to an MHV, with the first term being equal to one.

The delta function  $\delta^{(8)} \left( \sum_{i=1}^n \eta_i^A \lambda_{i,\alpha} \right)$  involves the fermionic variables  $\eta_i^A$ , thus the superamplitude is a polynomial of a limited degree. The component amplitudes can be extracted from it as the monomial with the correct powers of  $\eta_i^A$  according to the multiplet (2.6). For instance, the scattering amplitude of

1. A gluon with + helicity
2. A gluon with - helicity
3. A scalar  $\phi_{12}$
4. A scalar  $\phi_{34}$

would be the coefficient of  $(\eta_1)^0(\eta_2)^4\eta_3^1\eta_3^2\eta_4^3\eta_4^4$  in the superamplitude  $\mathcal{M}_4$  where

$$(\eta_i)^4 = \frac{1}{4}\epsilon_{ABCD}\eta_i^A\eta_i^B\eta_i^C\eta_i^D. \quad (2.8)$$

A superamplitude of the form (2.7) is annihilated by the supersymmetry generators. The  $q$  symmetry is manifest by the holomorphic (chiral) fermionic delta function appearing in the numerator.

The  $\bar{Q}$  symmetry is similarly easy to see. When  $\bar{Q}_{A,\dot{\alpha}} = \tilde{\lambda}_{\dot{\alpha}}\frac{\partial}{\partial\eta^A}$  acts on the fermionic delta function in (2.51), it converts the  $\eta$ 's to  $\tilde{\lambda}$ 's and the resulting expression is proportional to  $\sum \lambda\tilde{\lambda}$  which is equivalent to zero by the momentum conserving delta function.

In four dimensions, the on-shell superalgebra (2.4) can be realised using only one kind of of fermionic variable  $\eta^A$ . Therefore, the representation of on-shell  $\mathcal{N} = 4$  supersymmetry is *chiral*. This is not the case many other supersymmetric gauge theories with less supersymmetry [67].

Also in ABJM theory, it is possible to package the on-shell fields of ABJM theory into two chiral Nair [66] superfields which depend only on the chiral half of the superspace:

$$\Phi(l, \eta) = \phi^4(l) + \eta^A\psi_A(l) + \frac{1}{2}\epsilon_{ABC}\eta^A\eta^B\phi^C(l) + \frac{1}{3!}\epsilon_{ABC}\eta^A\eta^B\eta^C\psi_4(l), \quad (2.9)$$

$$\bar{\Phi}(l, \eta) = \bar{\psi}^4(l) + \eta^A\bar{\phi}_A(l) + \frac{1}{2}\epsilon_{ABC}\eta^A\eta^B\bar{\psi}^C(l) + \frac{1}{3!}\epsilon_{ABC}\eta^A\eta^B\eta^C\bar{\phi}_4(l), \quad (2.10)$$

where the indices  $A, B, \dots$  take values between 1 and 3. This breaks the manifest  $SU(4)$  R symmetry to  $SU(3)$ . However the theory still retains the full  $SU(4)$  symmetry and the breaking is only a notational issue.

The superfields  $\Phi$  behave like even variables while  $\bar{\Phi}$  behave like odd ones. The two superfields carry the antiparticles of each other and unsurprisingly the superamplitude in ABJM theory is always a function of *pairs* of superfields  $\bar{\Phi}_{2i-1}\Phi_{2i}$ ,  $i \in \mathbb{N}^+$ :

$$\mathcal{M} = \mathcal{M}(\bar{\Phi}_1, \Phi_2, \dots, \bar{\Phi}_{n-1}\Phi_n). \quad (2.11)$$

Whether one starts writing a colour-ordered superamplitude with a barred field or an unbarred one is a matter of convention.

## 2.2 Colour ordering

In gauge theories, like Yang-Mills theories and Chern-Simons theories, where fields transform under an internal symmetry group (such as the colour symmetry) as well as the symmetry group the scattering amplitudes depend on the colour configuration of the particles involved in the scattering as well as their kinematics.

An immediate simplification in the computation of scattering amplitudes is achieved when the dependence on colour is decoupled from the dependence on kinematics. This is done by expanding the scattering amplitude in all the possible colour structures. The coefficients of these colour structures are called “colour-ordered amplitudes”. They can be computed using either colour-ordered Feynman rules or using their factorisation properties under unitarity cuts and recursion techniques. In this thesis, and commonly in the literature, the colour-ordered amplitudes are referred to as just amplitudes.

### 2.2.1 Colour structures in MSYM

In MSYM theory in four dimensions, which is an  $SU(N_c)$  gauge theory, the fields are in the adjoint representation of the gauge group. Therefore the scattering amplitude has one free adjoint index  $a_i = 1, \dots, N_c^2 - 1$  for each particle. A suitable basis for expanding these is the traces of generators of the  $SU(N_c)$  symmetry group in the adjoint representation.

At tree level, the scattering amplitude, or a superamplitude, can be expanded into single-trace factors, i.e.,

$$\mathcal{M}(\{p_i, h_i, a_i\}) = \sum_{\sigma} \text{Tr}(T^{a_{\sigma(1)}} \dots T^{a_{\sigma(n)}}) \mathcal{A}(\sigma(1), \sigma(2), \dots, \sigma(n)) \quad (2.12)$$

where  $\sigma$  belongs to the set of permutations of the  $n$  particles. It turns out that this is a more than adequate, even much redundant decomposition due to the identities amongst the amplitudes.

The first constraint comes from the  $U(1)$  decoupling identity, also known as the dual Ward identity, which follows from the statement that the amplitude must vanish whenever an external particle is a neutral photon, instead of a charged gluon. This identity relates [68] the amplitudes in the following way:

$$\sum_{\sigma} A(1, \sigma(2), \sigma(3), \dots, \sigma(n)) = 0, \quad (2.13)$$

hence they reduce the number of independent amplitudes to  $(n - 1)!$  in an  $n$ -particle scattering process.

The  $U(1)$  decoupling identity discussed above follows from considering the  $U(1) \times SU(N_c)$  subgroup of an  $U(N_c)$  gauge group. More general identities, called Kleiss-Kuijf identities, can be obtained by considering a more general case, namely an  $SU(N_1) \times SU(N_2)$  embedded in a  $U(N_1 + N_2)$ . They reduce the number of independent amplitudes to  $(n - 2)!$ . In fact, an alternative colour decomposition [69] for gauge theory amplitudes, which uses the structure constants of the colour algebra instead of the fundamental generators unlike in (2.12), has already  $(n - 2)!$  independent terms:

$$\mathcal{A}(\{p_i, h_i, a_i\}) = \sum_{\sigma} \text{Tr}(T^{a_{\sigma(1)}} \dots T^{a_{\sigma(n)}}) A(1, \sigma(2), \sigma(3), \dots, \sigma(n-1), n) , \quad (2.14)$$

where  $\sigma$  are the permutations of the legs  $2, \dots, n - 1$ . It can be shown that (2.14) results from imposing the Kleiss-Kuijf relations to the decomposition (2.12) [70].

The kinematical Jacobi identities that were observed in [71] and they are known as BCJ relations. At loop level, these relations imply structures between the numerators of the integrand level which are analogous to the usual Jacobi identities satisfied by the colour factors. The BCJ relations reduce the number of independent amplitudes to  $(n - 3)!$ .

At loop level, the colour decomposition is slightly more involved. In general, planar amplitudes come with leading contributions in the number of colours whereas non-planar amplitudes come with subleading contributions. Two ways of organising these colour structures will be presented below. One can either use the adjoint generators used in the tree-level colour decomposition and the sub-leading-colour contributions would be manifestly separated. Alternatively, one could use the fundamental generators, where the leading and sub-leading terms are treated on an equal footing. The latter is particularly useful for deriving form factor integrands from generalised unitarity cuts.

Using the adjoint generators, the the one-loop amplitude is decomposed as follows [72]:

$$\begin{aligned} \mathcal{M}_n = & N_c \sum_{\sigma \in S_n / \mathbb{Z}_n} \text{Tr}(T^{a_{\sigma(1)}} \dots T^{a_{\sigma(n)}}) \mathcal{A}_n^{(1)}(\sigma(1), \dots, \sigma(n)) \\ & + \sum_{c=2}^{\lfloor n/2 \rfloor + 1} \sum_{\sigma \in S_n / S_{n;c}} \text{Tr}(T^{a_{\sigma(1)}} \dots T^{a_{\sigma(c-1)}}) \text{Tr}(T^{a_{\sigma(c)}} \dots T^{a_{\sigma(n)}}) \mathcal{A}_{n,c}^{(1)}(\sigma(1), \dots, \sigma(n)) \end{aligned} \quad (2.15)$$

where  $S_{n,c}$  is the subset of the permutations of  $\{1, 2, \dots, n\}$  which leave the double-trace structure  $\text{Tr}(T^{a_{\sigma(1)}} \dots T^{a_{\sigma(c-1)}}) \text{Tr}(T^{a_{\sigma(c)}} \dots T^{a_{\sigma(n)}} \dots T^{a_{\sigma_n}})$  invariant. Indeed, in

in this formalism, the non-planar amplitudes  $\mathcal{A}_{n,c}^{(1)}(\sigma(1), \dots, \sigma(n))$  are explicitly lacking a factor of  $N_c$  compared to the planar amplitudes  $\mathcal{A}_n^{(1)}(\sigma(1), \dots, \sigma(n))$ .

In the expansion using the fundamental generators of [70], it is possible to package (2.14) into a single sum. In this formalism, the one-loop full amplitude can be written as

$$\mathcal{M}(1, \dots, n) = \sum_{\sigma \in S_n / (\mathbb{Z}_n \times \mathcal{R})} \text{Tr}(F^{a_{\sigma_1}} \dots F^{a_{\sigma_1}}) \mathcal{A}(\sigma(1), \sigma(2), \dots, \sigma(n)), \quad (2.16)$$

where  $F_{bc}^a$  are the adjoint generators. In this colour decomposition, one sums over the permutations modulo the reflections  $\mathcal{R}$  which reverse the ordering of the momenta. Thus the number of independent terms is  $(n - 1)!/2$ .

## 2.2.2 Colour structures in ABJM

Colour-ordered amplitudes in ABJM can be defined in a similar fashion. The difference in ABJM is that the fields carry bifundamental indices. The colour factors can be constructed using Kronecker deltas such as  $\delta_{i_k}^{i'_k} \delta_{\bar{i}_k}^{\bar{i}'_k}$  where  $i_k$  and  $\bar{i}'_k$  are indices that belong to a barred particle, whereas  $i_k$  and  $\bar{i}_k$  are indices that belong to an unbarred one.

Thus, the colour decomposition of an  $n$ -particle tree superamplitude would be as follows [73, 74]

$$\mathcal{M}^{(0)}(\bar{1}, 2, \dots, n) = \sum_{\mathcal{P}_n} \text{sgn}(\sigma) \mathcal{A}^{(0)}(\sigma(\bar{1}), \sigma(2), \sigma(\bar{3}), \dots, \sigma(n)) [\sigma(\bar{1}), \sigma(2), \sigma(\bar{3}), \dots, \sigma(n)], \quad (2.17)$$

where  $\mathcal{P}_n := (S_{n/2} \times S_{n/2})/C_{n/2}$  are permutations of  $n$  sites that only mix even (bosonic) and odd (fermionic) particles among themselves, modulo cyclic permutations by two sites. The function  $\text{sgn}(\sigma)$  is equal to  $-1$  if  $\sigma$  involves an odd permutation of the odd (fermionic) sites, and  $+1$  otherwise.  $\mathcal{A}^{(0)}(\bar{1}, 2, \bar{3}, \dots, n)$  are colour-ordered tree superamplitudes. It is also useful define the following shorthand notation for the strings of Kronecker deltas:

$$[\bar{1}, 2, \bar{3}, \dots, n] := \delta_{i_2}^{\bar{i}_1} \delta_{i_3}^{\bar{i}_2} \delta_{i_4}^{\bar{i}_3} \dots \delta_{i_1}^{\bar{i}_n}. \quad (2.18)$$

At loop level, certain colour structures are of leading order in the large- $N_c$  expansion. These are the ones that are made of a single string of Kronecker deltas such as  $[\sigma(\bar{1}), \sigma(2), \sigma(\bar{3}), \dots, \sigma(n)]$ , and not products of such colour singlet such as  $[\sigma(\bar{1}), \sigma(2), \sigma(\bar{3}), \dots, \sigma(k)] [\sigma(k \bar{+} 1), \sigma(k + 2), \sigma(k \bar{+} 3), \dots, \sigma(n)]$ .

The symmetry properties of the full superamplitude imply relations among the colour ordered amplitudes. Because of the barred superfields are Grassmann odd and the unbarred ones are Grassmann even, some care is necessary in deriving these properties.

The spin-statistics theorem requires that the full amplitude  $\mathcal{M}$  should be odd under the exchange of fermionic superfields. With the conventions of the colour decomposition (2.17), this implies that the  $L$ -loop colour-ordered amplitudes should satisfy [75]:

$$\mathcal{A}^{(L)}(\bar{1}, 2, \bar{3}, 4, \dots, n) = (-1)^{\frac{n}{2}-L} \mathcal{A}^L(\bar{3}, 4, \dots, \bar{1}, 2) \quad (2.19a)$$

and

$$\mathcal{A}^{(L)}(\bar{1}, 2, \bar{3}, 4, \dots, n) = (-1)^{\frac{n(n-2)}{8}+L} \mathcal{A}(\bar{1}, n, \overline{n-1}, n-2, \dots, \bar{3}, 2). \quad (2.19b)$$

## 2.3 Tree-level recursion

The complication of computing scattering amplitudes at tree level is mainly due to the increasing number of Feynman diagrams with the number of external particles. Consider for example the scattering of six gluons. There are about  $6!$  Feynman diagrams that contribute to this amplitude, where the exact number depends on the gauge choice. Interestingly, all these diagrams sum up to zero for cases with one or less particles of opposite helicity compared to the others, to one simple term for two such particles and finally to three very simple terms when half of the particles are of one helicity and the other half are of the other.

To provide insight into this phenomenon and compute tree-level amplitudes with just complication expected from their helicity structure, analytic continuation of scattering amplitudes to complex momenta is very useful, as it is the case for loop amplitudes. Under a certain complex-valued shift of the momenta, which is demonstrated below and known as the “BCFW-shift”, the tree level amplitudes have poles in complex kinematics where an internal propagator becomes on-shell. Around this pole, the tree amplitude factorises to two lower-point scattering amplitudes. The recursion relations not only make the computation simpler but also helps one to understand the simplicity of tree-level results.

To realise what kind of singularities the tree-level amplitudes might have, it is useful to think about Feynman diagrams. The amplitudes are constructed from external and internal propagators, vertex terms and polarisation vectors which are in the appropriate representation of the Lorentz group that are attached to the external propagators. At

tree level, internal propagators are of the form

$$\frac{i}{P_{i,j}^2 + i\epsilon}, \quad P_{i,j} = p_i + p_{i+1} + \cdots + p_j \quad (2.20)$$

and they are the only source for any poles that a diagram might have. These poles are called multi-particle singularities corresponding to the configuration in which sum of the momenta of particles from  $i$  to  $j$ ,  $p_i + \cdots + p_j$  is light-like.

The multiparticle singularities can be used to derive recursion relations between tree level scattering amplitudes [76]. Consider the behaviour of a tree level amplitude near a multi-particle singularity. One can check that the residue at this pole becomes the sum of the products of two amplitudes with the propagator replaced by all possible external diagrams. Schematically this can be expressed as

$$P_{ij}^2 A_n \rightarrow \sum_h A_L^h A_R^{-h} \quad \text{as} \quad P_{i,j}^2 \rightarrow 0 \quad (2.21)$$

where the amplitude  $A_L$  ( $A_R$ ) is the amplitude of particles to the left (right) of the propagator and one extra particle carrying the momentum  $P_{i,j}$  and helicity  $h$ . This behaviour is known as factorisation.

### 2.3.1 Recursion in four dimensions

In [2] it was realised that the factorisation properties lead to recursion relations between tree-level amplitudes. The conjecture of [2] was proved in [76] using a particular, complex parameter to parametrise the multi-particle limit  $P_{i,j}^2 \rightarrow 0$  together with Cauchy's theorem. These relations are known as the BCFW relations due to the authors of [76].

The derivation of the BCFW relations is as follows. Consider a complex “shift” of the momenta of two particles<sup>1</sup>:

$$\hat{p}_i(z) = p_i - z\eta, \quad \hat{p}_j(z) = p_j + z\eta \quad (2.22)$$

by some momentum  $\eta$ . Note that this shift of momenta still respects the momentum conservation. If  $\eta$  is chosen as:

$$\eta = \lambda_i \tilde{\lambda}_j \quad (2.23)$$

then the light-likeness of the spinors is preserved as well. Such a shift often denoted as

<sup>1</sup>Although in principle one can shift the spinors of any two particles, for the example presented the most convenient choice turns out to be that of adjacent ones. However, this choice has an effect on the large- $z$  behaviour.

the  $[ij]\rangle$  shift because it essentially corresponds to shifting the spinors of two particles:

$$\tilde{\lambda}_i = \tilde{\lambda}_i - z\tilde{\lambda}_j, \quad \lambda_{\hat{j}} = \lambda_j + z\lambda_i. \quad (2.24)$$

The shift (2.24) can also be written in the matrix form

$$\begin{pmatrix} \hat{\lambda}_i \\ \hat{\lambda}_j \end{pmatrix} = \begin{pmatrix} 1 & z \\ 0 & 1 \end{pmatrix} \begin{pmatrix} \lambda_i \\ \lambda_j \end{pmatrix}, \quad \begin{pmatrix} \hat{\tilde{\lambda}}_i \\ \hat{\tilde{\lambda}}_j \end{pmatrix} = \begin{pmatrix} 1 & 0 \\ -z & 1 \end{pmatrix} \begin{pmatrix} \tilde{\lambda}_i \\ \tilde{\lambda}_j \end{pmatrix}, \quad (2.25)$$

which sets the notation for the three-dimensional shifts discussed in Section 2.3.2 of this Chapter. The momentum conservation implies that the shift is a unitary transformation.

For simplicity we will employ an adjacent  $[n1]\rangle$  shift or a  $\langle n1]$ , wherever possible. Adjacent shifts commonly reduce the number of recursion diagrams. This choice between the two shifts is important for the large- $z$  behaviour of the sifted amplitude.

Focusing on the  $[n1]\rangle$  shift it can be noted that this modifies the propagator momenta which include either  $p_n$  or  $p_1$ . The propagators that include only  $p_1$  or only  $p_n$  become functions of  $z$ , too:

$$\frac{i}{P_{1,j}^2} \rightarrow \frac{i}{\hat{P}_{1,j}^2(z)} = \frac{i}{P_{1,j}^2 - z\langle n|P_{1,j}|1\rangle}. \quad (2.26)$$

With the shifted momenta the amplitude can be considered as a meromorphic function  $\hat{A}(z)$  with simple poles only. Its poles are at

$$z_{1j} = \frac{P_{1,j}^2}{\langle n|P_{1,j}|1\rangle}. \quad (2.27)$$

At this pole the propagator momentum  $P_{ij}(z)$  becomes light-like.

Now consider the integral of  $A(z)/z$  along a closed contour at infinity where for the moment we assume that the amplitude vanishes. Therefore, the integral along this contour is zero. This means that the value at the origin  $A(0)$  and the contributions from other poles have to cancel each other and an expression for  $A(0)$  in terms of the factorised amplitudes at the poles is obtained:

$$0 = \frac{1}{2\pi i} \oint_{C_\infty} dz \frac{A(z)}{z} = A(0) + \sum_{z_{1j} \neq 0} \text{Res} \left[ \frac{A(z)}{z} \right]_{z_{1j}} \quad (2.28)$$

where  $z_{1j}$  are the poles of the shifted amplitude  $A(z)$ . The residues can be computed

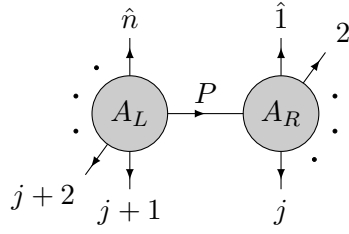


Figure 2.1: Diagrammatic representation of equation (2.30)

using the factorisation property of the amplitude that was sketched in equation (2.21).

$$\begin{aligned} \text{Res}(A(z), z_{1j}) &= \lim_{z \rightarrow z_{1j}} (z - z_{1j}) A(z) \\ &= - \sum_{\text{particles}} A_L(P, j+1, \dots, n) \Big|_{z_{1j}} i \frac{z_{1j}}{P_{1j}^2} A_R(1, \dots, j, P) \Big|_{z_{1j}}, \end{aligned} \quad (2.29)$$

where the sum represents all possible particles of both helicities that could be running between  $A_L$  and  $A_R$ . Plugging the residues in equation (2.28) it is possible to express the physical amplitude  $A(0)$  in terms of some other lower point amplitudes evaluated at the poles:

$$A(0) = \sum_{z_{1j}} \sum_{\text{particles}} A_L(P, j+1, \dots, n) \Big|_{z_{1j}} i \frac{1}{P_{1j}^2} A_R(1, \dots, j, P) \Big|_{z_{1j}} \quad (2.30)$$

This equality can be represented by diagrams depicted in Figure 2.1.

The derivation assumes that the amplitude vanishes as  $z \rightarrow \infty$ . Polarisation vectors have  $z$  dependence as well as the propagators (see Appendix A). It is possible to make a similar construction whenever a suitable choice of shifted spinors assures vanishing at infinity. For gluon amplitudes, shifts of the type  $[-+]$ ,  $[++]$  and  $[--]$  are good in this sense while  $[+-]$  is not.

The above construction is valid for any gauge theory, given that the large- $z$  behaviour is good. In theories with supersymmetry, it is possible to write the supersymmetric versions of equation (2.30), which relate superamplitudes to each other. In the case of MSYM, the supersymmetrisation of the BCFW recursion is particularly simple and takes the form [77]

$$\mathcal{A} = \sum_P \int d^4 \eta_P \mathcal{A}_L(z_P) \frac{i}{P^2} \mathcal{A}_R(z_P) \quad (2.31)$$

where  $\int d^4 \eta_P$  is over the four supersymmetric coordinates that appear in the internal legs.

### 2.3.2 Recursion in three dimensions

There is no obstacle for applying the BCFW recursion to amplitudes in ABJM theory. The amplitudes exhibit the required factorisation properties and they can be reconstructed from their singularities. However the shifts in three dimensions are necessarily non-linear as explained below and this makes the application of recursion relations slightly more laboursome.

When a shift like (2.24) is applied to the three dimensional spinors, a solution to the on-shell condition  $P_{ij}(z) = 0$  cannot be found assuming that the transformation matrix is linear in  $z$ . The solution to this technical obstacle is circumvented by giving up the linearity assumption [78] and shifting the spinor that corresponds to the momenta  $p_i$  and  $p_j$  as

$$\begin{pmatrix} \hat{\lambda}_i \\ \hat{\lambda}_j \end{pmatrix} = \begin{pmatrix} \frac{z+z^{-1}}{2} & -\frac{z-z^{-1}}{2i} \\ \frac{z-z^{-1}}{2i} & \frac{z+z^{-1}}{2} \end{pmatrix} \begin{pmatrix} \lambda_i \\ \lambda_j \end{pmatrix}. \quad (2.32)$$

The ABJM amplitude  $\mathcal{A}(z)$  shifted through the map (2.32) reduces to the original amplitude at  $z = 1$ , unlike in four dimensions, where the amplitude is recovered at  $z = 0$ . Therefore, for ABJM amplitudes can be computed by summing all the residues of  $\mathcal{A}/(z - 1)$  apart from the one at  $z = 1$ .

The three-dimensional analogue of (2.31) was derived in [78] as:

$$\mathcal{A}^{(0)}(z = 1) = -\frac{1}{2\pi i} \sum_f \int d^3\eta H(z_{1,f}, z_{2,f}) \mathcal{A}_L^{(0)}(z_{1,f}, \eta) \frac{1}{p_f^2} \mathcal{A}_R^{(0)}(z_{1,f}, \eta) + z_{1,f} \rightarrow z_{2,f}, \quad (2.33)$$

where the for the factorisation channels in which  $p_f = p_1 + \dots + p_l$  with  $l$  even. The function  $H(z_1, z_2)$ , which defined as

$$H(z_1, z_2) = \frac{z_1(z_2^2 - 1)}{z_1^2 - z_2^2}, \quad (2.34)$$

is present because the propagators are not linear in the deformation parameter  $z$ , and therefore the the poles are not simple poles. The sum over  $f$  represents the sum over all factorisation channels. (2.33). A factorisation channel  $f$  is shown in Figure 2.2, in which the momenta  $K_1$  and  $K_2$  are defined as:

$$K_1 = p_{i+1} + p_{i+2} + \dots + p_n \quad K_2 = p_3 + p_4 + \dots + p_i \quad (2.35)$$

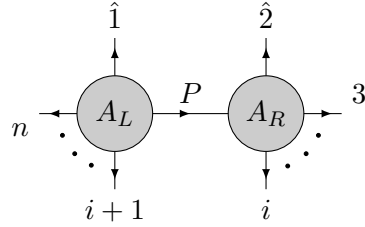


Figure 2.2: A factorisation channel of a tree-level amplitude in ABJM

The recursion relation was cast into a refined form in [79]:

$$\mathcal{A}^{(0)}(z = 1) = \sum_f \frac{1}{\sqrt{K_1^2 K_2^2}} \int \frac{d^4 \eta_f}{z_1 - z_1^{-1}} \mathcal{A}_L^{(0)}(z_{1,f}, \eta) \mathcal{A}_R^{(0)}(z_{1,f}, \eta) + z_{1,f} \rightarrow z_{2,f}. \quad (2.36)$$

Not that in (2.36), the unpleasant factors of  $H(z_1, z_2)$  and the propagator are replaced by the factor  $1/(z_1 - z_1^{-1})$ .

As an example, the derivation of the six-particle amplitude in ABJM from the recursion relation (2.36) is sketched in Section 2.5.3.

The ABJM scattering amplitudes also allow an all-loop generalisation of the recursion relation which has a Grassmannian interpretation like in MSYM. In the case for the ABJM amplitudes, the Grassmannian is the positive orthogonal Grassmannian [80, 81].

## 2.4 Unitarity

Unitarity is not only a property that physical quantum field theories are mostly assumed to have, but also the name of an approach to perform loop-level computations.

Much like the tree-level recursion relations, the unitarity-based techniques rely on the factorisation properties of scattering amplitudes. To compute loop corrections to scattering amplitudes, clearly one integrates the loop momenta over the whole domain, which also includes on-shell values. In other words, there exist a hyperspace inside the  $D \times L$ -dimensional space of loop momenta which is defined by the condition that some of the internal propagators carry light-like momentum. Such configurations of loop momenta, where a scattering amplitude is divided into two or more pieces, bridged by on-shell loop momenta are called “cuts”. In these isolated points in the integration domain, the scattering amplitude, or its integrand, factorises into individual pieces.

The idea of (generalised) unitarity techniques is to revert this process and construct the amplitude, or its integrand from, all possible factorisation channels. This can be made

in an algorithmic way in which one writes down an Ansatz as a linear combination of some basis of integrals that contribute to a scattering amplitude and solves a system of equations for the coefficients of these integrals. For simpler cases, it is possible to write down all possible factorisation channels and manually identify the integrals that would make up the amplitude.

### 2.4.1 Traditional Unitarity

Unitarity is a basic assumption of quantum theories. A state  $|\psi\rangle$  evolves to another state as

$$|\psi'\rangle = S|\psi\rangle \quad (2.37)$$

and the statement is that  $S$  is a unitary operator. This follows from the expectation that the  $|\psi'\rangle$  is still an element of the same Hilbert space as the one that  $|\psi\rangle$  belongs to.

This can be shown by recalling that the inner product

$$\mathcal{M}_{\text{in} \rightarrow \text{out}} = \langle \text{out} | S | \text{in} \rangle, \quad (2.38)$$

i.e. the matrix elements of the operator  $S$ , is interpreted as the probability *amplitude* of a state  $|\text{in}\rangle$  to evolve in time and to be observed as  $|\text{out}\rangle$ . The probability is obtained by squaring the modulus of the probability amplitude. If one should expect that the sum of such probability over all possible  $|\text{out}\rangle$  states is unity, then the condition

$$S^\dagger S = \mathbb{1} \quad (2.39)$$

is imposed on  $S$ . Unitarity of the  $S$  operator has useful consequences on the analytic structure of scattering amplitudes which are discussed in Section 2.4.1. When the ideas of unitarity techniques are applied to the integrand of a scattering amplitude by considering more constrained kinematical configurations, where several intermediate particles are treated as on-shell states, they go under the name generalised unitarity and such techniques are briefly discussed in Section 2.4.2.

Historically, the use of unitarity cuts have started by studying the analytic structure of the scattering amplitude itself, and not its integrand. In a scattering process, the momenta are real-valued and therefore so are the kinematical invariants  $s_{i,j,\dots} = (p_i + p_j \dots)^2$ . However it is common that one gains substantial insight and computational power when scattering amplitudes are analytically continued to complex values of kinematical invariants. These are analytically continued to complex values

and to study the analytic properties of the scattering amplitudes as a function of complex kinematical invariants. Unitarity of the  $S$  matrix implies that near the branch cuts, (the imaginary part of) the scattering amplitudes can be written as a product of two other scattering amplitudes. This has useful consequences in perturbation theory.

The unitarity of the  $S$  matrix (2.39) implies

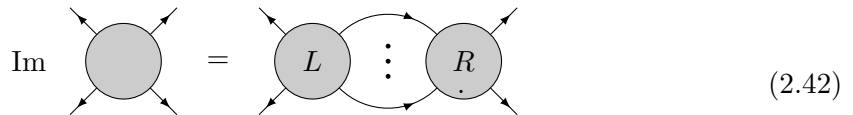
$$i(T^\dagger - T) = T^\dagger T \quad (2.40)$$

on the  $T$  matrix, defined as  $S - 1$ . The  $T$  matrix is essentially the non-trivial part of the  $S$  matrix. Then for non-trivial scattering amplitudes, defined using the  $T$  matrix, the following relation holds:

$$2 \operatorname{Im} M = \sum_n \langle \text{in} | T^\dagger | n \rangle \langle n | T | \text{out} \rangle, \quad (2.41)$$

where the sum over  $n$  denotes the sum over all states of the theory. The object  $\langle n | T | \text{out} \rangle$  is the non-trivial scattering amplitude of a state  $|n\rangle$  producing a state  $|n\rangle$  whereas the object  $\langle \text{in} | T^\dagger | n \rangle$  is the complex conjugate of the same quantity but the out state is replaced with  $|\text{in}\rangle$ . Using the CPT theorem, this can be related to the scattering of the state  $|\bar{n}\rangle$  into  $|\text{in}\rangle$  state with the anti-particles of  $|n\rangle$  with reversed momenta.

For the scattering of four particles, this relation becomes schematically



$$\operatorname{Im} = \text{Diagram with shaded circle and four external lines} = \text{Diagram with shaded circles L, \dots, R and curved line} \quad (2.42)$$

The ellipsis represent the many particles that may appear in the intermediate state. The lines representing these intermediate particles are drawn in a way, such that they connect the two amplitudes and remind the fact that the particles at the both ends of the line are antiparticles of each other and carry the opposite momentum.

The relation (2.42) is not a perturbative statement, however it becomes particularly useful in perturbation theory. When the amplitude in the LHS is wanted up to some certain number of loops, the intermediate states can contain a limited number of particles, and furthermore the amplitudes in the RHS are of at least one-less loop order.

Once the imaginary part of the amplitude is computed, the full amplitude can be

constructed through dispersion integrals. The assumption of an analytic  $S$  matrix, i.e. the absence of singularities other than the branch cuts implied by unitarity allows these integrals to be performed in practice. This procedure is one of the most basic examples of “bootstrap procedures” in computing scattering amplitudes.

### 2.4.2 Generalised unitarity cuts of the integrand

A loop correction to a scattering amplitude is a sum of some Feynman integrals with a fixed number of loops and external legs. Instead of considering a cut of the amplitude such as in equation (2.42), one can consider the *cut of the integrands* that compute it. This approach is more efficient than computing dispersion relations but there is a subtlety coming from the dimension of the spacetime the loop momenta live in.

In most cases, even if the scattering amplitude is UV-finite, the integrals one has to compute are divergent due to IR-effects which arise in regions in the integration domain where the loop momentum becomes collinear with one of the external legs (the collinear limit), or its magnitude tends to zero (the soft limit). These divergences have to be regularised and the most common method to do so is to compute the integrals not in four dimensions but in  $D = 4 - 2\epsilon$  dimension.

This raises the question whether on-shell loop momenta have to be in four or  $D$ -dimensions. Indeed, to compute the  $\mathcal{O}(\epsilon)$  terms, one has to consider the  $-2\epsilon$  dimensional components of the loop momenta. However, as long as one is interested in up to  $\mathcal{O}(1)$  terms in the  $\epsilon$  expansion, four-dimensional cuts are adequate.

At one loop, the unitarity method is particularly efficient. At this level, the integral cannot contain irreducible numerators. This means that an arbitrary one-loop integral with an arbitrary numerator can be written in terms of scalar integrals with the same or lower number of external legs. This leads to an integral basis, in which one-loop scattering amplitudes can be expanded. Schematically, one can write:

$$\mathcal{M} = \sum c_i I_i + \text{Rational terms} \quad (2.43)$$

where  $I_i$  stands for integrals of box, triangle and bubble topologies. The coefficient  $c_i$  are, in general, functions of kinematical invariants. These integrals contain branch cuts in the kinematic variables and they constitute the “cut constructable” part of the scattering amplitude. The rational terms, which are non-zero for example in QCD, do not have branch cuts and their computation requires further considerations, such as [82]. In supersymmetric theories, they are zero.

Starting from two loops, a systematic expansion of an amplitude into an integral basis is not straightforward anymore since finding a basis of integrals at two loops is a difficult task. At two loops, it is always possible to find a basis for the Feynman integrals that appear in an amplitude but this basis would most likely be overcomplete.

One can also proceed in a less-systematic way and consider cuts of an integrand in various channels and hope to detect all integrals contributing the amplitude in this way [83]. The cuts will detect only a limited number of integrals, namely those that have propagators in the cut channel with some coefficients. Therefore one has to cut the amplitude all possible ways and build an Ansatz for the scattering amplitude (or the form factor) which is compatible with all possible unitarity cuts. In the computation of the two-loop Sudakov form factor in ABJM theory, which is presented in Chapter 4, this method has been employed used.

## 2.5 Some results for scattering amplitudes

In this section some results for the scattering amplitudes in four and three dimensions are presented. As well as they serve as examples for the technical background reviewed earlier in this Chapter, these amplitudes are important ingredients of the results presented in Chapters 3 and 4.

### 2.5.1 Tree-level $n$ -point MHV in four dimensions

One of the most remarkable results in scattering amplitudes is arguably  $n$ -point tree-level MHV amplitude in four dimensional Yang-Mills theories. This amplitude has a famously simple form which led to research in finding ever simpler structures in scattering amplitudes, many of which are non-manifest in the Feynman diagram approach.

The component amplitude for the scattering of  $n$  gluons, where only the gluons  $i$  and  $j$  have negative helicity is

$$A_n^{(0)} = ig^{n-2} \frac{\langle ij \rangle^4}{\langle 12 \rangle \langle 23 \rangle \dots \langle n1 \rangle} \delta^{(4)} \left( \sum_{i=1}^n P_{1,n} \right), \quad (2.44)$$

where

$$p_{1,n} = \sum_{i=1}^n \lambda_i \tilde{\lambda}_i \quad (2.45)$$

is the total momentum of the scattering particles and the spinor brackets  $\langle kl \rangle$  are

defined in Appendix A.

The Feynman diagram computation of  $A_n^{(0)}$  involves  $\mathcal{O}(n!)$  Feynman diagrams however complexity of the answer remains the same. For any  $n$ , the proof of (2.44) by induction using induction is extremely simple using the BCFW recursion relations. To demonstrate this, it is practical to assume  $1 < i < j - 1 < n$ . Other cases can be treated similarly.

Under the shift  $[ii+1]$  applied to (2.44) there is a single factorisation channel (pole in the  $z$  plane):

$$\begin{aligned} A_n &= A_{n-1}(1^+, \dots, \hat{i}^-, \hat{P}^+, \dots, j^-, \dots, n) \frac{1}{P_{i+1, i+2}^2} A_3(\widehat{i+1}, i+2, \hat{P}) \\ &= \frac{\langle ij \rangle^4}{\langle 12 \rangle \dots \langle i \hat{P} \rangle \langle \hat{P}, i+3 \rangle \dots} \frac{1}{\langle i+1 i+2 \rangle \langle i+1 i+2 \rangle} \frac{[i+1 i+2]^4}{[i+1 i+2][i+2, \hat{P}][\hat{P} i+1]}, \end{aligned} \quad (2.46)$$

where the hatted quantities are evaluated at the pole:

$$z_* = \frac{\langle i+1 i+2 \rangle}{\langle i+2 i \rangle}. \quad (2.47)$$

At this pole, the shifted momentum  $\hat{P}$  is

$$\hat{P} = P_{i+1} + P_{i+2} + \frac{\langle i+1 i+2 \rangle}{\langle i+2 i \rangle} \lambda_i \tilde{\lambda}_{i+1}. \quad (2.48)$$

Using (2.48),  $\hat{P}$  can be eliminated from the brackets in (2.46). In particular one can write:

$$\langle i \hat{P} \rangle [\hat{P} i+2] = \langle i i+1 \rangle [i+1 i+2] \quad (2.49a)$$

$$\langle i+3 \hat{P} \rangle [\hat{P} i+1] = \langle i+3 i+2 \rangle [i+2 i+1]. \quad (2.49b)$$

With the help of (2.49a), the only residue (2.46) yields the  $n$ -point MHV gluon amplitude (2.44).

The proof by induction is completed by computing the three-point MHV amplitude either by Feynman diagrams or by deriving it from physical constraints to be:

$$A_3(1^-, 2^-, 3^+) = ig \frac{\langle 12 \rangle^4}{\langle 12 \rangle \langle 23 \rangle \langle 31 \rangle} \quad A_3(1^-, 2^+, 3^+) = ig \frac{[23]^4}{[12][23][31]}. \quad (2.50)$$

In MSYM, this amplitude is just a component of the MHV superamplitude,

$$\mathcal{A}_n = \frac{\delta^{(4)}(P) \delta^{(8)}(Q_{1,n})}{\langle 12 \rangle \langle 23 \rangle \cdots \langle n1 \rangle}, \quad (2.51)$$

where

$$Q_{1,n} = \sum_{i=1}^n = \lambda_i \eta_i \quad (2.52)$$

is the total supermomentum of the  $n$  particles. The apparently missing factor of  $\langle ij \rangle^4$  in the numerator is the coefficient of the relevant term in the  $\eta$  expansion of the supermomentum-conserving delta function  $\delta^{(8)}(q)$ .

The action on superconformal symmetry on amplitudes and its anomaly can be seen from the superamplitude. It does not depend on antiholomorphic variables  $\tilde{\lambda}$  and it may seem like it should be annihilated by any of the generators that contain  $\frac{\partial}{\partial \tilde{\lambda}}$ . However when the momenta are real and the left and right handed spinors are complex conjugates of each other,

$$\frac{\partial}{\partial \tilde{\lambda}} \frac{1}{\langle \lambda \mu \rangle} \quad (2.53)$$

is proportional to  $\delta(\langle \lambda \mu \rangle)$  and is nonzero when the two spinors become collinear. In the collinear limit the amplitude is proportional to another amplitude with one less particle. This problem can be cured by redefining the symmetry operators by subtracting the anomalous piece from the symmetry generator and considering the symmetry as acting on the whole S-matrix rather than just one amplitude [84].

### 2.5.2 The colour-ordered one-loop MHV superamplitude in four MSYM

One-loop amplitudes can be computed using general unitarity cuts, which are discussed in section 2.4.2. The MHV superamplitude in MSYM for any number of external legs is exceptionally constrained due to supersymmetry and is computed relatively easily using this method [85]. Here the derivation of this quantity is presented closely following [85].

The maximal number of cuts allowed in strictly four dimensions is four. This is because the loop momentum is assumed to be four-dimensional and only four constraints can be simultaneously imposed upon it. Therefore the cut diagram is a chain of four superamplitudes connected by four propagators set on-shell.

The cut diagrams that can contribute to the MHV superamplitude are highly constrained. Firstly, for the cut of the MHV superamplitude, only diagrams with two MHV and two  $\overline{\text{MHV}}$  vertices can contribute. This follows from the fact that the MHV

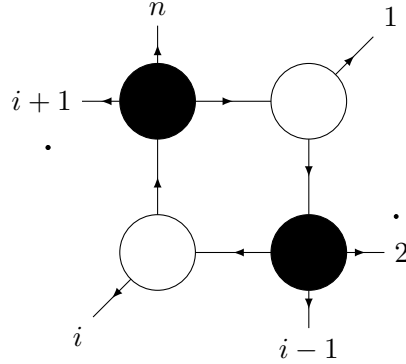


Figure 2.3: An sample generalised cut of the one-loop MHV amplitude in MSYM. The white and black blobs represent MHV and  $\overline{\text{MHV}}$  tree amplitudes, respectively.

amplitude has Grassmann degree eight and it should be proportional to the overall supermomentum-conserving delta function:

$$\mathcal{A}_n^{(1)} \propto \delta^{(8)}(Q_{1,n}), \quad (2.54)$$

where the shorthand

$$Q_{i,j} = \sum_{k=1}^j \lambda_k \eta_k \quad (2.55)$$

is used for convenience. Four four-dimensional Grassmann integrals at the edges remove in total 16 fermionic degrees of freedom. Therefore, the cut diagram must have 24 fermionic degrees of freedom before the fermionic integrals are preformed. Recalling that all MHV or  $\overline{\text{MHV}}$  amplitudes have Grassmann degree 8, with the exception of the three-particle  $\overline{\text{MHV}}$  amplitude, which has Grassmann degree 4, it is easy to realise that this can only be constructed if two of the vertices are MHV and two of the vertices are three-particle  $\overline{\text{MHV}}$  amplitudes. This guarantees that only two-mass-easy box integral topologies contribute to the one-loop MHV superamplitude. The numerator, which turns out to be independent of the loop momenta and therefore is merely a coefficient for the scalar box function, is given by the cut diagram evaluated at both of the solutions.

An example for the type of cut diagrams that give the coefficient of the relevant box function is depicted in Figure 2.3. The box function detected by this cut has massless momenta 1 and  $i$  and its coefficient  $c_{(1|i)}$  is the product of four tree-level amplitudes evaluated at the solution to the cut conditions.

$$c_{(1|i)} = \frac{1}{2} \sum \int d^{16} \eta \mathcal{A}_a \mathcal{A}_b \mathcal{A}_c \mathcal{A}_d, \quad (2.56)$$

where  $\mathcal{A}_{a,b,c,d}$  are superamplitudes depicted in figure. The white blobs indicate MHV superamplitudes whereas shaded blobs indicate  $\overline{\text{MHV}}$  super amplitudes. The product of these tree amplitudes is

$$\frac{\delta^{(4)}(Q_a)}{[1P_1][P_1P_4][P_41]} \frac{\delta^{(8)}(Q_b)}{\langle 23 \rangle \cdots \langle i-2 \ i-1 \rangle} \frac{\delta^{(4)}(Q_c)}{[iP_3][P_3P_2][P_2i]} \frac{\delta^{(8)}(Q_d)}{\langle i+1 \ i+2 \rangle \cdots \langle n-1 \ n \rangle}, \quad (2.57)$$

where the supermomenta  $Q_{a,b,c,d}$  are defined as

$$Q_a = \eta_1[P_1P_4] + \eta_{P_1}[P_4, 1] + \eta_{P_4}[1P_1], \quad (2.58a)$$

$$Q_b = Q_{2,i-1} + \eta_{P_1}\lambda_{P_2} - \eta_{P_4}\lambda_{P_1}, \quad (2.58b)$$

$$Q_c = \eta\lambda_1 + \eta_{P_1}\lambda_{P_4} - \eta_{P_4}\lambda_{P_3} \quad (2.58c)$$

$$Q_d = \eta_i[P_3P_2] + \eta_{P_3}[P_2, i] + \eta_{P_2}[iP_3], \quad (2.58d)$$

where the internal variables  $\eta_{P_i}$  are to be integrated.

The integrations over the internal  $\eta$  variables can be performed one after the other. Each of the internal  $\eta$  variables are contained in the delta functions belonging to two neighbouring vertices. For example for the  $\eta_{P_1}$  integration, the relevant delta functions are  $\delta^{(4)}(Q_a)$  and  $\delta^{(8)}(Q_b)$ :

$$\int d\eta_{P_1} \delta^{(4)}(Q_a) \delta^{(8)}(Q_b). \quad (2.59)$$

On the support of the four-dimensional delta function, the eight-dimensional delta function can be freed of the integration variable and the integral (2.59) can be rewritten as:

$$\int d^4\eta_{P_1} \delta^{(4)}(Q_a) \delta^{(8)}(Q_{1,i-1} + \lambda_{P_2}\eta_{P_2} - \lambda_{P_4}\eta_{P_4}). \quad (2.60)$$

Then, the argument of  $\delta^{(4)}(Q_a)$  can be solved for  $\eta_{P_1}$  and so that the  $\eta_{P_4}$  becomes trivial. After this manipulation (2.54) becomes

$$\int d^4\eta_{P_1} [P_41]^4 \delta^{(4)}(\eta_{P_1} + \cdots) \delta^{(8)}(Q_{1,i-1}) = [P_41]^4 \delta^{(8)}(Q_{1,i-1}), \quad (2.61)$$

where the factor  $[P_{P_4}1]^4$  comes as the Jacobian of the change of variables inside the delta function. The ellipsis denotes terms that do not depend on  $\eta_{P_4}$ .

After an identical procedure the  $\eta_{P_3}$  integral gives:

$$\int d\eta_{P_3} \delta^{(4)}(Q_c) \delta^{(8)}(Q_d) = [P_2i]^4 \delta^{(8)}(Q_{i,n} + \lambda_{P_4}\eta_{P_4} - \lambda_{P_2}\eta_{P_2}) \quad (2.62)$$

After working (2.61) and (2.62), the total Grassmann integral reduces to:

$$\int d^{16}\eta \delta^{(4)}(Q_a)\delta^{(8)}(Q_b)\delta^{(4)}(Q_c)\delta^{(8)}(Q_d) = [P_2i]^4[P_41]^4 \int d^4\eta_{P_2} d^4\eta_{P_4} \delta^{(8)}(Q_{1,i-1})\delta^{(8)}(Q_{i,n}). \quad (2.63)$$

The remaining integrals can be done very easily by noting that

$$\delta^{(8)}(Q_{1,i-1} + \lambda_{P_2}\eta_{P_2} - \lambda_{P_4}\eta_{P_4}) \delta^{(8)}(Q_{i,n} + \lambda_{P_4}\eta_{P_4} - \lambda_{P_2}\eta_{P_2}) = \delta^{(8)}(Q_{1,n}) \delta^{(8)}(Q_{i,n} + \lambda_{P_2}\eta_{P_2} - \lambda_{P_4}\eta_{P_4}) \quad (2.64)$$

and

$$\delta^{(8)}(Q_{i,n} + \lambda_{P_2}\eta_{P_2} - \lambda_{P_4}\eta_{P_4}) = \langle P_2 P_4 \rangle^4 \delta^{(4)}(\eta_{P_4} + \dots) \delta^{(4)}(\eta_{P_2} + \dots). \quad (2.65)$$

Combining all the steps together, the result of the Grassmann integration becomes:

$$\int d^{16}\eta \delta^{(4)}(Q_a)\delta^{(8)}(Q_b)\delta^{(4)}(Q_c)\delta^{(8)}(Q_d) = [P_2i]^4[P_41]^4 \langle P_2 P_4 \rangle^4 = [i|P_2 P_4|1]^4 \quad (2.66)$$

After performing the Grassmann integrations, the coefficient for the box function becomes

$$c_{1,i} = \mathcal{A}_n^{\text{tree}} \langle i-1 | i \rangle \langle i | i+1 \rangle \langle n | 1 \rangle \langle 1 | 2 \rangle \frac{[1|P_4 P_2|i]}{\langle i-1 | P_2 P_3 | i+1 \rangle \langle 2 | P_1 P_4 | n \rangle}, \quad (2.67)$$

where the tree-level MHV superamplitude presented in equation (2.51) has been pulled out. Using the fact that the loop momenta are null on the cut and the constraints imposed thereon by the  $\overline{\text{MHV}}$  vertices,

$$|P_1\rangle \propto |P_4\rangle \propto |1\rangle, \quad |P_2\rangle \propto |P_3\rangle \propto |i\rangle, \quad (2.68)$$

the coefficients can be simplified to:

$$\begin{aligned} c_{1,i} &= \mathcal{A}_n^{\text{tree}} [P_1 P_4] \langle P_4 P_2 \rangle [P_2 P_3] \langle P_3 P_1 \rangle \\ &= P_{2,i-1}^2 P_{i+1,n}^2 - st, \end{aligned} \quad (2.69)$$

with

$$s = P_{2,i-1}, \quad \text{and} \quad t = P_{i+1,n}. \quad (2.70)$$

In writing the second line one relies on the fact that the loop momenta are null  $P_i^2 = 0$ . Therefore, the coefficients of integrals detected by a particular unitarity cut are defined up to terms proportional to  $P_i^2$ . However, in this case the four particle cuts are considered. These cuts can only come from box functions and terms such as  $P_i^2$  would cancel a propagator, turning the integral into a triangle. Therefore in generalised unitarity with maximal cuts, this ambiguity does not arise. However when non-maximal

cuts are considered, such as the ones considered in Section 4.2.2.1.

### 2.5.3 Tree-level amplitudes in ABJM

#### Four particles

The simplest non-trivial superamplitude in ABJM theory is the four-particle tree amplitude. This amplitude can be expanded into the following colour factors:

$$\mathcal{M}_4^{(0)}(\bar{1}, 2, \bar{3}, 4) = \mathcal{A}_4^{(0)}(\bar{1}, 2, \bar{3}, 4)[1, 2, 3, 4] + \mathcal{A}_4^{(0)}(\bar{1}, 4, \bar{3}, 2)[1, 4, 3, 2]. \quad (2.71)$$

The relative sign of the two different colour structures is plus since we chose to write the amplitudes by exchanging bosonic sites.

The colour-ordered tree amplitude has the following peculiar form: [86],

$$\mathcal{A}_4^{(0)}(\bar{1}, 2, \bar{3}, 4) = i \frac{\delta^{(6)}(Q)\delta^{(3)}(P)}{\langle 1 2 \rangle \langle 2 3 \rangle}. \quad (2.72)$$

Although does not manifest the cyclic symmetry of ABJM amplitudes, it is not hard to confirm this by noting that the  $\langle 2 \rangle \langle 2 \rangle$  in the denominator is in fact the momentum  $p_2$ . Using momentum conservation of four particles,

$$p_2 = -p_1 - p_3 - p_4, \quad (2.73)$$

and the fact that  $p_i$  annihilates  $|i\rangle$ , one can rewrite (2.72) and then perform the cyclic rotation of the momenta to obtain:

$$\mathcal{A}_4^{(0)}(\bar{1}, 2, \bar{3}, 4) = -i \frac{\delta^{(6)}(q)\delta^{(3)}(p)}{\langle 1 4 \rangle \langle 4 3 \rangle} \xrightarrow{p_i \rightarrow p_{i+2}} -i \frac{\delta^{(6)}(q)\delta^{(3)}(p)}{\langle 1 2 \rangle \langle 2 3 \rangle}, \quad (2.74)$$

in accordance with the relations (2.19) satisfied by the colour-ordered amplitudes.

A further symmetry of the amplitude (2.72) implied by the relations (2.19) that it is mapped to minus itself under the exchange of the momenta of the bosonic particles, ie  $p_2 \leftrightarrow p_4$ :

$$\mathcal{A}_4^{(0)}(\bar{1}, 2, \bar{3}, 4) = \mathcal{A}_4^{(0)}(\bar{1}, 4, \bar{3}, 2), \quad \mathcal{A}_4^{(0)}(\bar{1}, 2, \bar{3}, 4) = -\mathcal{A}_4^{(0)}(\bar{3}, 2, \bar{1}, 4) \quad (2.75)$$

Similarly, this can be checked by sending  $p_2$  to  $p_4$  in (2.72) and using momentum conservation (2.73) to replace  $p_2$  with  $p_4$  inside the denominator.

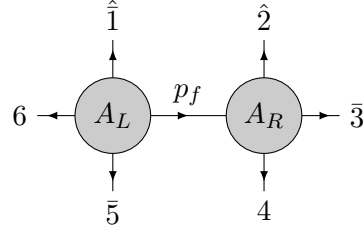


Figure 2.4: BCFW recursion of the six-particle superamplitude in ABJM

Using this relation the full tree amplitude can be rewritten in a more compact form:

$$\mathcal{M}_4^{(0)}(\bar{1}, 2, \bar{3}, 4) = \mathcal{A}_4^{(0)}(\bar{1}, 2, \bar{3}, 4) ([1, 2, 3, 4] - [1, 4, 3, 2]). \quad (2.76)$$

This amplitude is the main ingredient for the unitarity cuts that are used to derive the full one-loop scattering amplitude in Section 2.5.4.

### Six particles

The six-particle amplitude  $\mathcal{A}_6(\bar{1}, 2, \bar{3}, 4, \bar{5}, 6)$  can be derived from the four-particle colour ordered amplitude using the recursion relation (2.36).

Closely following [78], one can choose to shift particles 1 and  $\bar{2}$  according to (2.25)

$$\hat{\lambda}_1 = \frac{z+z^{-1}}{2} \lambda_1 - \frac{z-z^{-1}}{2i} \lambda_2 \quad (2.77a)$$

$$\hat{\lambda}_2 = \frac{z-z^{-1}}{2i} \lambda_1 + \frac{z+z^{-1}}{2} \lambda_2 \quad (2.77b)$$

such that the only factorisation channel will be the one shown in Figure 2.4. The shifted propagator in the only factorisation channel is

$$P_{6,1,2} = p_6 + p_1(z) + p_2(z) = \lambda_6 \lambda_6 + \hat{\lambda}_1 \hat{\lambda}_1 + \hat{\lambda}_2 \hat{\lambda}_2 \quad (2.78)$$

and the kinematical configuration where factorisation should occur is such that

$$P_{6,1,2}^2(z) = az^2 + b + cz^{-2} = 0 \quad (2.79)$$

with

$$a = P_{56} \cdot q, \quad b = -P_{34} \cdot P_{56}, \quad c = P_{56} \cdot \tilde{q}, \quad (2.80)$$

where it is convenient to define the null momenta  $q$  and  $\tilde{q}$  such that:

$$\lambda_q = \lambda_1 + i\lambda_2, \quad \lambda_{\tilde{q}} = \lambda_1 - i\lambda_2. \quad (2.81)$$

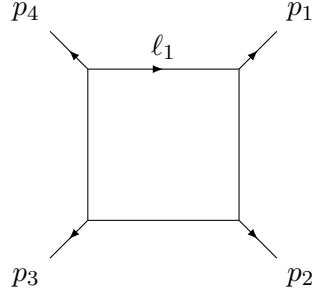


Figure 2.5: The one-loop box function in (2.85).

The two solutions of this quadradic equation (2.79) for  $z^2$  are given simply as [78]:

$$z_{\pm}^2 = \frac{P_{34} \cdot P_{56} \pm \langle 34 \rangle \langle 56 \rangle}{\langle \lambda_1 + i\lambda_2 | P_{34} | \lambda_1 - i\lambda_2 \rangle}. \quad (2.82)$$

Evaluating the residues at these poles, one obtains the six-particle superamplitude in ABJM [79]:

$$\mathcal{M}_6^{(0)} = \frac{\delta^{(3)}(p)\delta^{(6)}(q)}{P_{24}} \left[ \frac{\delta^{(3)}(\epsilon_{ijk}\langle jk \rangle \eta_i - \epsilon_{i\bar{j}\bar{k}}\langle j\bar{k} \rangle)}{(\langle 2|P_{34}|5\rangle + i\langle 34 \rangle \langle 61 \rangle)(\langle 1|P_{23}|4\rangle + i\langle 23 \rangle \langle 56 \rangle)} \right. \\ \left. + \frac{\delta^{(3)}(\epsilon_{ijk}\langle jk \rangle \eta_i - \epsilon_{i\bar{j}\bar{k}}\langle j\bar{k} \rangle)}{(\langle 2|P_{34}|5\rangle - i\langle 34 \rangle \langle 61 \rangle)(\langle 1|P_{23}|4\rangle - i\langle 23 \rangle \langle 56 \rangle)} \right] \quad (2.83)$$

#### 2.5.4 The complete one-loop four-point amplitude in ABJM

In this section the result for the complete four-point amplitude at one loop in ABJM is presented. This amplitude will be needed in order to construct the two-particle cuts of the two-loop form factor since the colour structure of the tree-level form factor amplifies some subleading colour structures when glued to a scattering amplitude in a unitarity cut.

The one-loop colour-ordered four-point superamplitude with the leading-color structure is equal to:

$$\mathcal{A}^{(1)}(\bar{1}, 2, \bar{3}, 4) = i\mathcal{A}^{(0)}(\bar{1}, 2, \bar{3}, 4) N I(1, 2, 3, 4), \quad (2.84)$$

where the one-loop integral  $I(1, 2, 3, 4)$  is defined by

$$I(1, 2, 3, 4) := \int \frac{d^D \ell}{i\pi^{D/2}} \frac{s_{12} \text{Tr}(\ell p_1 p_4) + \ell^2 \text{Tr}(p_1 p_2 p_4)}{\ell^2 (\ell - p_1)^2 (\ell - p_1 - p_2)^2 (\ell + p_4)^2}, \quad (2.85)$$

with  $D = 3 - 2\epsilon$ .  $s_{ij}$  denote the usual Mandelstam invariants  $(p_i + p_j)^2$ .

As opposed to [87], where the normalisation for the loop measure is  $1/(2\pi)^D$  per loop, in this thesis the integrals have been computed with a factor  $1/(i\pi^{D/2})$ . Note that  $\text{Tr}(abc) = 2\epsilon(a, b, c) := 2\epsilon_{\mu\nu\rho}a^\mu b^\nu c^\rho$ .

Explicit evaluation of the right-hand side of (2.84) shows that  $\mathcal{A}^{(1)}(\bar{1}, 2, \bar{3}, 4)$  is of  $\mathcal{O}(\epsilon)$ , and hence vanishes in three dimensions [87]. This is consistent with the fact that all one-loop amplitudes in ABJM can be expanded in terms of one-loop triangle functions [75], as expected from dual conformal invariance. The vanishing of the four-point amplitude then follows since one-mass (and two-mass) triangles vanish in three dimensions. Very interestingly, the box function with the particular numerator in (2.85) is also dual conformal invariant, as was demonstrated in [87] using a five-dimensional embedding formalism. Furthermore, the expression for  $\mathcal{A}^{(1)}(\bar{1}, 2, \bar{3}, 4)$  given in (2.84) is correct to all orders in the dimensional regularisation parameter  $\epsilon$ . The integrand of (2.85) will be the main ingredient that is responsible for the appearance of the particular numerators that appear in the unitarity cut computation of the Sudakov form factor.

The complete one-loop four-point amplitude is given by the sum of a planar and non-planar contribution, which can be written in terms of the integral (2.85):

$$\tilde{\mathcal{A}}^{(1)}(\bar{1}, 2, \bar{3}, 4) = \mathcal{A}_P^{(1)}(\bar{1}, 2, \bar{3}, 4) + \mathcal{A}_{NP}^{(1)}(\bar{1}, 2, \bar{3}, 4), \quad (2.86)$$

where

$$\mathcal{A}_P^{(1)}(\bar{1}, 2, \bar{3}, 4) = i N \mathcal{A}^{(0)}(\bar{1}, 2, \bar{3}, 4) I(1, 2, 3, 4) \left( [1, 2, 3, 4] + [1, 4, 3, 2] \right), \quad (2.87)$$

and

$$\begin{aligned} \mathcal{A}_{NP}^{(1)}(\bar{1}, 2, \bar{3}, 4) = & -2i \mathcal{A}^{(0)}(\bar{1}, 2, \bar{3}, 4) \left[ \left( I(1, 2, 3, 4) - I(4, 2, 3, 1) \right) [1, 2][3, 4] \right. \\ & \left. - \left( I(2, 3, 4, 1) - I(1, 3, 4, 2) \right) [1, 4][3, 2] \right]. \end{aligned} \quad (2.88)$$

Note that the part  $[1, 2]$  of the double-trace structure  $[1, 2][3, 4]$  is a short hand for two Kronecker deltas:

$$[1, 2] = \delta_{i_2}^{\bar{i}_1} \delta_{i_1}^{i_2}. \quad (2.89)$$

The complete one-loop amplitude can also be written in the following way,

$$\begin{aligned} \frac{\tilde{\mathcal{A}}^{(1)}(\bar{1}, 2, \bar{3}, 4)}{\mathcal{A}^{(0)}(\bar{1}, 2, \bar{3}, 4)} = & i \left\{ I(1, 2, 3, 4) \left[ N([1, 2, 3, 4] + [1, 4, 3, 2]) - 2[1, 2][3, 4] - 2[1, 4][3, 2] \right] \right. \\ & \left. + 2 \left[ I(4, 2, 3, 1)[1, 2][3, 4] - I(1, 3, 4, 2)[1, 4][3, 2] \right] \right\}. \end{aligned} \quad (2.90)$$

### Symmetry properties of the one-loop amplitude

Before discussing the derivation of (2.86), it is instructive to prove that  $\mathcal{A}_P^{(1)}$  and  $\mathcal{A}_{NP}^{(1)}$  are antisymmetric under the swap  $\bar{1} \leftrightarrow \bar{3}$ . In order to show this one needs to use (2.75) and the following relations satisfied by the one-loop box (2.85):

$$I(a, b, c, d) = -I(b, c, d, a) , \quad I(a, b, c, d) = -I(c, b, a, d) , \quad (2.91)$$

which can be directly checked from its definition.

These relations state that by cyclically shifting the labels of the external legs of the box function (2.85) by one unit one picks a minus sign; and similarly if one swaps two non-adjacent legs. Both relations are straightforward to prove using the definition (2.85) of the box function. One then finds,

$$\begin{aligned} I(3, 2, 1, 4) - I(4, 2, 1, 3) &= I(2, 3, 4, 1) - I(1, 3, 4, 2) , \\ I(2, 1, 4, 3) - I(3, 1, 4, 2) &= I(1, 2, 3, 4) - I(4, 2, 3, 1) . \end{aligned} \quad (2.92)$$

Using (2.92) one obtains

$$\begin{aligned} \mathcal{A}_P^{(1)}(\bar{1}, 2, \bar{3}, 4) &= -\mathcal{A}_P^{(1)}(\bar{3}, 2, \bar{1}, 4) , \\ \mathcal{A}_{NP}^{(1)}(\bar{1}, 2, \bar{3}, 4) &= -\mathcal{A}_{NP}^{(1)}(\bar{3}, 2, \bar{1}, 4) . \end{aligned} \quad (2.93)$$

Notice the presence of a minus sign between the two non-planar colour structure  $[1, 2][3, 4]$  and  $[1, 4][3, 2]$  appearing in the non-planar one-loop amplitude (2.88).

### Derivation of the complete one-loop amplitude from cuts

The outline of the strategy for the derivation of the complete one-loop amplitude (2.86), which is very similar to that in MSYM<sup>2</sup>, is as follows. One considers the two-particle cuts of the complete one-loop amplitude, which are obtained by merging two tree-level amplitudes summed over all possible colour structures and internal particle species. Each of these cuts can be re-expressed in terms of cuts of sums of box functions (2.85). The sum over internal species is (partially) performed via an integration over the Grassmann variables  $\eta_{\ell_1}$  and  $\eta_{\ell_2}$  associated to the cut momenta. If one of the particles crossing is bosonic and the other is fermionic one also has to add to this the same expression with  $\ell_1 \leftrightarrow \ell_2$  – this is necessary only for the  $s$ - and  $t$ -cuts. For instance, the  $s$ -cut

---

<sup>2</sup>see for example [88]

integrand of the one-loop amplitude is<sup>3</sup>

$$\mathcal{M}^{(1)}(\bar{1}, 2, \bar{3}, 4)|_{s\text{-cut}} = \frac{1}{2} \int d^3\eta_{\ell_1} d^3\eta_{\ell_2} \mathcal{M}^{(0)}(\bar{1}, 2, -\bar{\ell}_2, -\ell_1) \times \mathcal{M}^{(0)}(\bar{3}, 4, \bar{\ell}_1, \ell_2) + \ell_1 \leftrightarrow \ell_2. \quad (2.94)$$

The one-loop amplitude has cuts in the  $s$ -,  $t$ - and  $u$ -channels, for which one finds the following integrands:

$$\begin{aligned} \mathcal{M}^{(1)}(\bar{1}, 2, \bar{3}, 4)|_{s\text{-cut}} &= \frac{i}{2} \mathcal{A}^{(0)}(\bar{1}, 2, \bar{3}, 4) c_s \mathcal{S}_{12} I(1, 2, 3, 4)|_{s\text{-cut}}, \\ \mathcal{M}^{(1)}(\bar{1}, 2, \bar{3}, 4)|_{t\text{-cut}} &= \frac{i}{2} \mathcal{A}^{(0)}(\bar{1}, 2, \bar{3}, 4) c_t \mathcal{S}_{23} I(1, 2, 3, 4)|_{t\text{-cut}}, \\ \mathcal{M}^{(1)}(\bar{1}, 2, \bar{3}, 4)|_{u\text{-cut}} &= \frac{i}{2} \mathcal{A}^{(0)}(\bar{1}, 2, \bar{3}, 4) c_u \mathcal{S}_{13} I(3, 1, 2, 4)|_{u\text{-cut}}, \end{aligned} \quad (2.95)$$

where the colour factors  $c_s$ ,  $c_t$ ,  $c_u$  are

$$\begin{aligned} c_s &= N[1, 2, 3, 4] + N[1, 4, 3, 2] - 2[1, 2][3, 4], \\ c_t &= N[1, 2, 3, 4] + N[1, 4, 3, 2] - 2[1, 4][3, 2], \\ c_u &= 2[1, 2][3, 4] - 2[1, 4][3, 2], \end{aligned} \quad (2.96)$$

and recalling that  $\mathcal{A}^{(0)}(\bar{1}, 2, \bar{3}, 4)$  denotes the colour-ordered four-point superamplitude. Furthermore,  $\mathcal{S}_{ab} I(a, b, c, d)|_{s_{ab}\text{-cut}}$  indicates the  $s_{ab}$ -cut of the one-loop box function  $I(a, b, c, d)$  in (2.85), symmetrised in the cut loop momenta  $\ell_1$  and  $\ell_2$ , which are defined such that  $\ell_1 + \ell_2 = p_a + p_b$ ,

$$\begin{aligned} \mathcal{S}_{12} I(1, 2, 3, 4)|_{s\text{-cut}} &= \frac{s \text{Tr}(\ell_1 p_1 p_4)}{(\ell_1 - p_1)^2 (\ell_1 + p_4)^2} + \ell_1 \leftrightarrow \ell_2, \\ \mathcal{S}_{23} I(1, 2, 3, 4)|_{t\text{-cut}} &= \frac{(-t) \text{Tr}(\ell_1 p_1 p_2)}{(\ell_1 - p_1)^2 (\ell_1 + p_2)^2} + \ell_1 \leftrightarrow \ell_2, \\ \mathcal{S}_{13} I(3, 1, 2, 4)|_{u\text{-cut}} &= \frac{u \text{Tr}(\ell_2 p_3 p_4)}{(\ell_2 - p_3)^2 (\ell_2 + p_4)^2} + \ell_1 \leftrightarrow \ell_2. \end{aligned} \quad (2.97)$$

It should be stressed here that despite the simplified notation the cut momenta  $\ell_1$  and  $\ell_2$  are different for the three distinct channels under considerations. For instance,  $\ell_1 + \ell_2 = p_1 + p_2$  for the  $s$ -cut, while  $\ell_1 + \ell_2 = p_2 + p_3$  in the  $t$ -cut and  $\ell_1 + \ell_2 = p_1 + p_3$  in the  $u$ -cut. Recall that the symmetrisation in the cut momenta in the  $s$ - and  $t$ -channel coefficients originates from summing over all possible particle species that can propagate on the cut legs, while in the  $u$  cut there is a single configuration allowed, and the result turns out to be automatically symmetric in  $\ell_1$  and  $\ell_2$ .

---

<sup>3</sup>For convenience, a factor of  $\frac{1}{2}$  is included in the definition of the (symmetrised) cuts. In practice it means that one takes the average of the two contributions in the  $s$ - and  $t$ -cuts, and multiply the  $u$ -cut with a symmetry factor as two identical (super)particles cross the cut.

Next one merges the cuts into box functions. For the planar structures  $[1, 2, 3, 4]$  and  $[1, 4, 3, 2]$  this is immediate as the only function consistent with the  $s$ - and  $t$ -cuts in (2.95) and vanishing  $u$ -cut is  $I(1, 2, 3, 4)$ . Hence, the corresponding planar amplitude is

$$i \mathcal{A}^{(0)}(\bar{1}, 2, \bar{3}, 4) N([1, 2, 3, 4] + [1, 4, 3, 2]) I(1, 2, 3, 4) , \quad (2.98)$$

thus arriving at the expression (2.87) for the planar part of the full one-loop amplitude.<sup>4</sup> For the non-planar terms  $[1, 2][3, 4]$  and  $[1, 4][3, 2]$ , it is useful to notice a property of the box integral (2.85):

$$\mathcal{S}_{ab} I(a, b, c, d)|_{s_{ab}-\text{cut}} = \mathcal{S}_{ab} I(a, b, d, c)|_{s_{ab}-\text{cut}} . \quad (2.99)$$

The relation (2.99) means that if one exchanges two momenta of the two adjacent legs  $p_c$  and  $p_d$  of the ABJM box integral, then the cut *integrand* of the resulting integrand would be the *equivalent* to the cut *integrand* of the original integral in channel  $s_{ab}$ .

Obviously, the cut integral - with the phase space integration performed - depends only on  $s_{ab}$  and it depends on any transformation that leaves  $s_{ab}$  invariant would leave the cut invariant. However, the statement above applies for the cut integrand. It is crucial that the equivalence can be proved only by symmetrising the integrand with respect to different relabellings of the loop momentum.

This can easily be proved explicitly by considering the symmetrised cut of (2.85) and the same integral with  $p_3$  and  $p_4$  exchanged. In the  $s_{12}$  channel cut of the original integrand (2.85):

$$\begin{aligned} \mathcal{S}_{12} I(1, 2, 3, 4) &= I(1, 2, 3, 4) \Big|_{s_{12}-\text{cut}} + p_1 \leftrightarrow p_2 \\ &= \frac{s_{12}\langle 41 \rangle}{\langle 4|\ell_1|1 \rangle} + \frac{s_{12}\langle 41 \rangle}{\langle 4|\ell_2|1 \rangle} \end{aligned} \quad (2.100)$$

Using  $\langle 4|\ell_1 + \ell_2|1 \rangle = \langle 4|2|1 \rangle$  it is possible to write the symmetrised cut as:

$$\mathcal{S}_{12} I(1, 2, 3, 4) = \frac{s_{12}\langle 41 \rangle\langle 4|2|1 \rangle}{\langle 4|\ell_1|1 \rangle\langle 4|\ell_2|1 \rangle} , \quad (2.101)$$

Under the exchange  $p_3 \leftrightarrow p_4$  the symmetrised cut integrand becomes:

$$\mathcal{S}_{12} I(1, 2, 4, 3) = \frac{s_{12}\langle 31 \rangle\langle 3|2|1 \rangle}{\langle 3|\ell_1|1 \rangle\langle 3|\ell_2|1 \rangle} . \quad (2.102)$$

It is easy to check that the two expressions (2.101) and (2.102) are equal using momen-

---

<sup>4</sup>Note that at the level of the integral one can simply replace  $\mathcal{S}_{12}I(1, 2, 3, 4)$  by  $2I(1, 2, 3, 4)$ .

tum conservation on  $3\rangle\langle 3$  that appears in (2.102).

An immediate consequence of this result is that

$$\mathcal{S}_{23} I(2, 3, 4, 1)|_{t\text{-cut}} - \mathcal{S}_{23} I(2, 3, 1, 4)|_{t\text{-cut}} = 0, \quad (2.103)$$

in other words the combination  $I(2, 3, 4, 1) - I(2, 3, 1, 4)$ , symmetrised in the loop momenta  $\ell_1$  and  $\ell_2$ , with  $\ell_1 + \ell_2 = p_2 + p_3$ , has a vanishing  $t$ -channel cut as expected for the coefficient of the  $[1, 2][3, 4]$  colour structure (see (2.84)). For the same combination one finds, using  $I(2, 3, 4, 1) = -I(1, 2, 3, 4)$ , the symmetrised  $s$ -cut

$$- \mathcal{S}_{12} I(1, 2, 3, 4)|_{s\text{-cut}}, \quad (2.104)$$

and similarly, for the symmetrised  $u$ -cut one obtains

$$\mathcal{S}_{13} I(3, 1, 4, 2)|_{u\text{-cut}} = \mathcal{S}_{13} I(3, 1, 2, 4)|_{u\text{-cut}}, \quad (2.105)$$

where the identity  $I(2, 3, 1, 4) = -I(3, 1, 4, 2)$  and (2.99) were used, which allow one to swap the last two legs on the symmetrised  $u$ -cut. Comparing with (2.95) and (2.96) one can uniquely fix the coefficient of the non-planar structure  $[1, 2][3, 4]$ :

$$2i \mathcal{A}^{(0)}(\bar{1}, 2, \bar{3}, 4) [1, 2][3, 4] \left[ I(2, 3, 4, 1) - I(2, 3, 1, 4) \right], \quad (2.106)$$

or, using the first relation of (2.91),

$$- 2i \mathcal{A}^{(0)}(\bar{1}, 2, \bar{3}, 4) [1, 2][3, 4] \left[ I(1, 2, 3, 4) - I(4, 2, 3, 1) \right]. \quad (2.107)$$

One can proceed similarly for the coefficient of the other non-planar structure  $[1, 4][3, 2]$ , arriving at the result quoted earlier in (2.88). Note that in that result one uses the freedom to rename loop momenta in order to eliminate the various symmetrisations introduced by the operation  $\mathcal{S}_{ab}$  above.

# 3 Form factors in four dimensions

In this Chapter tree and loop-level form factors of protected, half-BPS operators in MSYM are considered. Thanks to the factorisation properties, form factors admit recursion relations very similar to those of scattering amplitudes.

In particular, it is possible to derive more complicated form factors using MHV rules. Such derivations are presented with a focus on the NMHV and the  $N^2$ MHV cases. Also, BCFW recursion relations can be efficiently applied to form factors. The solution to the BCFW recursion relations for the split-helicity case is given in terms of a diagrammatic procedure.

The operators which the form factors are constructed from, belong to chiral supermultiplets of MSYM and using these it is possible to construct supermultiplets of form factors, or super form factors. The super form factors are objects very similar to superamplitudes and encode form factors of various operators and particles which belong to different supermultiplets in an expansion in Grassmann variables. This construction also allows the supersymmetrisation of the recursion relations.

## 3.1 MHV form factors of $\text{Tr } \phi_{12}\phi_{12}$

MHV tree-level amplitudes can famously be written as a single term with the Parke-Taylor denominator. Apart from the aesthetic advantage of this form, the simplicity of MHV amplitudes, which is irrespective of the number of particles involved, makes them practically useful seeds of recursion relations of more complicated scattering amplitudes.

Similarly, the concept of maximal helicity violation exists for form factors, in the sense that for certain helicity configurations of the particles in the asymptotic state, they become remarkable simple and can be written with a Parke-Taylor denominator, very similar to tree-level MHV amplitudes.

For example, the tree-level form factor of  $\text{Tr } \phi_{12}\phi_{12}$  with two scalars  $\phi_{12}$  and  $n$  positive

helicity gluons is [57]:

$$\begin{aligned} & \int d^4x e^{-iqx} \langle g^+(p_1) \cdots \phi_{12}(p_i) \cdots \phi_{12}(p_j) \cdots g^+(p_n) | \text{Tr}(\phi_{12}\phi_{12})(x) | 0 \rangle \\ &= g^{n-2} (2\pi)^4 \delta^{(4)} \left( \sum_{k=1}^n \lambda_k \tilde{\lambda}_k - q \right) F_{\text{MHV}} , \end{aligned} \quad (3.1)$$

where

$$F_{\text{MHV}} = \frac{\langle ij \rangle^2}{\langle 12 \rangle \cdots \langle n1 \rangle} . \quad (3.2)$$

Here  $p_m := \lambda_m \tilde{\lambda}_m$  are on-shell momenta of the external particles, and  $q := \sum_{m=1}^n p_m$  is the momentum carried by the operator insertion.

One can verify that the little-group weights for the gluons and scalars are correct on the right hand side of (3.1). It can be easily derived by induction through BCFW recursion in the exact same way as the derivation of the tree-level MHV amplitude presented in Section 2.3.1, with the only difference being that for form factors it is possible to recurse down to a two-particle object, the Sudakov form factor:

$$F^{(0)}(1_{\phi_{12}}, 2_{\phi_{12}}) = 1 . \quad (3.3)$$

The computational details of the recursion of form factors are given in Sections 3.2.2.1 with focus on the split-helicity case.

## 3.2 Tree-level bootstrap in four dimensions

### 3.2.1 MHV diagrams

As an initial example of how the form factors can be used as vertices in an MHV diagram expansion [3] of non-MHV form factors, the NMHV form factors of the simplest class of operators in  $\mathcal{N} = 4$  SYM, namely the half-BPS operators  $\text{Tr}(\phi_{12}\phi_{12})$  are constructed in this Section. These NMHV form factors take the following form:

$$\langle g^+(p_1) \cdots \phi_{12}(p_i) \cdots \phi_{12}(p_j) \cdots g^+(p_{n-1}) g^-(p_n) | \text{Tr}(\phi_{12}\phi_{12})(x) | 0 \rangle , \quad (3.4)$$

Although only tree-level calculations are considered here, the extension to loop level, following [89], is straightforward and this will be considered in Section 3.5.

To make use of MHV diagrams to compute form factors of the half-BPS operator, one simply augments the set of usual MHV vertices for amplitudes by including a new family

of MHV vertices, obtained by continuing off shell the tree-level MHV form factors of the half-BPS operators.

For the computation of the above NMHV form factor, it is enough to include the MHV form factors given by equation (3.2) as a vertex. Since (3.2) is a holomorphic function of the spinor variables, the MHV form factors are localised on a complex line in twistor space, similarly to the MHV amplitudes [26].

Using localisation as an inspiration, it is proposed to use an appropriate off-shell continuation of (3.2) as a new vertex to construct the perturbative expansion of non-MHV form factors of the operator  $\text{Tr}(\phi_{12}\phi_{12})$ . The off-shell continuation is the standard one introduced in [3]. The momentum  $L$  of an internal, off-shell particle is decomposed as  $L = l + z\xi$ , where  $l = \lambda_L \tilde{\lambda}_L$  is an on-shell momentum and  $\xi$  an arbitrary reference null momentum. The off-shell continuation of [3] consists then in using the spinor  $\lambda_L$  as the spinor variable associated with the internal leg of momentum  $L$ , where

$$\lambda_{L,\alpha} = \frac{L_{\alpha\dot{\alpha}} \tilde{\xi}^{\dot{\alpha}}}{[\tilde{\lambda}_L, \tilde{\xi}]} . \quad (3.5)$$

The denominator in the right-hand side of (3.5) will be irrelevant for our applications since each MHV diagram is invariant under rescalings of the internal spinor variables. Hence, it will be discarded and simply replaced as  $\lambda_{L,\alpha} \rightarrow L_{\alpha\dot{\alpha}} \tilde{\xi}^{\dot{\alpha}}$ .

### 3.2.1.1 NMHV form factors

The NMHV form factor can be derived using the MHV rules outlined in the previous Section. Specifically, the simplest NMHV form factor -which is not dual to an MHV form factor under parity- is

$$F_{\text{NMHV}}(1_{\phi_{12}}, 2_{\phi_{12}}, 3_{g^-}, 4_{g^+}) := \langle \phi_{12}(p_1)\phi_{12}(p_2)g^-(p_3)g^+(p_4) | \text{Tr}(\phi_{12}\phi_{12})(0) | 0 \rangle . \quad (3.6)$$

There are four MHV diagrams contributing to (3.6), depicted in Figure 3.1. A short

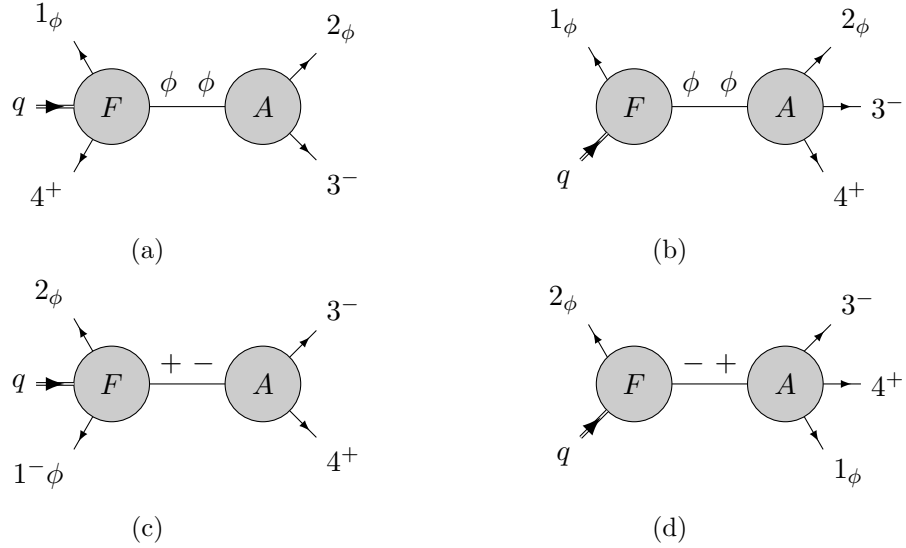


Figure 3.1: The four MHV diagrams contributing to the NMHV form factor (3.6).

calculation shows that these are given by the following expressions:

$$\begin{aligned}
 \text{Diagram (a)} &= \frac{[2\xi]}{[\xi 3]} \frac{1}{[32]\langle 41 \rangle} \frac{\langle 1|q-p_4|\xi \rangle}{\langle 4|q-p_1|\xi \rangle}, \\
 \text{Diagram (b)} &= \frac{\langle 23 \rangle}{\langle 34 \rangle s_{234}} \frac{\langle 3|p_2+p_4|\xi \rangle^2}{\langle 2|p_3+p_4|\xi \rangle \langle 4|p_2+p_3|\xi \rangle}, \\
 \text{Diagram (c)} &= \frac{\langle 12 \rangle}{[43]} \frac{[\xi 4]^3}{[3\xi]} \frac{1}{\langle 2|p_3+p_4|\xi \rangle \langle 1|p_3+p_4|\xi \rangle}, \\
 \text{Diagram (d)} &= \frac{1}{s_{341}} \frac{\langle 13 \rangle^2}{\langle 34 \rangle \langle 41 \rangle} \frac{\langle 3|p_4+p_1|\xi \rangle}{\langle 1|p_3+p_4|\xi \rangle}.
 \end{aligned} \tag{3.7}$$

It has been checked that the sum of all MHV diagrams is independent of the choice of the reference spinor  $\tilde{\xi}$ . A particularly convenient choice of  $\tilde{\xi}$  is  $\tilde{\xi} = \tilde{\lambda}_4$ , in which case one obtains

$$\begin{aligned}
 F_{\text{NMHV}}(1_{\phi 12}, 2_{\phi 12}, 3_{g^-}, 4_{g^+}) &= \frac{[24]}{[34]} \frac{1}{\langle 4|p_2+p_3|4 \rangle} \left[ \frac{\langle 1|q|4 \rangle}{\langle 23 \rangle \langle 41 \rangle} + \frac{[24]\langle 23 \rangle^2}{\langle 34 \rangle} \frac{1}{s_{234}} \right] \\
 &+ \frac{\langle 13 \rangle^2 [14]}{\langle 41 \rangle \langle 34 \rangle [43]} \frac{1}{s_{341}}.
 \end{aligned} \tag{3.8}$$

It is straightforward to apply this procedure to more general form factors. All results derived in the next subsection using recursion relations have been compared with formulae obtained from MHV diagrams finding a perfect match in all cases.

### 3.2.2 Recursion relations

In this Section, the application of recursion relations to the derivation of tree-level form factors is studied. As a warm-up, the NMHV form factor in (3.6) is re-derived, finding agreement with (3.8), which is followed by more general cases including split-helicity configurations. Since form factors contain a single operator insertion, it is clear that every recursive diagram will contain one amplitude and one form factor as the factorisation properties used in the case of tree-level recursions for amplitudes also apply to tree-level form factors. This is the only modification to the on-shell recursion relations of [2]. In Section 3.4 the behaviour of form factors under large complex deformations is discussed, and the validity of the calculations below is confirmed, i.e. it is shown that under the shifts used the form factors vanish sufficiently quickly as  $z \rightarrow \infty$ .

The re-derivation of the NMHV form factor (3.6) using recursion relations works as follows:

Under a  $[34\rangle$  shift, namely

$$\hat{\tilde{\lambda}}_3 := \tilde{\lambda}_3 + z\tilde{\lambda}_4, \quad \hat{\lambda}_4 := \lambda_4 - z\lambda_3, \quad (3.9)$$

there are two recursive diagrams, depicted in Figure 3.2 below. Note that the momentum insertion is not included in the colour ordering. A short calculation shows that

$$\begin{aligned} \text{Diagram (a)} &= \frac{[24]^2}{[23][34]} \frac{1}{s_{234}} \frac{\langle 1|q|4]}{\langle 1|q|2]} , \\ \text{Diagram (b)} &= \frac{\langle 13\rangle^2}{\langle 34\rangle\langle 41\rangle} \frac{1}{s_{341}} \frac{\langle 3|q|2]}{\langle 1|q|2]} , \end{aligned} \quad (3.10)$$

so that

$$F_{\text{NMHV}}(1_{\phi_{12}}, 2_{\phi_{12}}, 3_{g^-}, 4_{g^+}) = \frac{1}{\langle 1|q|2]} \left[ \frac{[24]^2}{[23][34]} \frac{1}{s_{234}} \langle 1|q|4] + \frac{\langle 13\rangle^2}{\langle 34\rangle\langle 41\rangle} \frac{1}{s_{341}} \langle 3|q|2] \right]. \quad (3.11)$$

It is interesting to note that the  $1/\langle 1|q|2]$  pole is in fact spurious. This can be shown by using the identities

$$\begin{aligned} \langle 1|q|p_4|3\rangle + \langle 1|q|p_2|3\rangle &= \langle 13\rangle s_{234} , \\ [4|p_3 q|2] + [4|p_1 q|2] &= [42] s_{341} , \end{aligned} \quad (3.12)$$

which allow to recast the form factor in the alternative form

$$F_{\text{NMHV}}(1_{\phi 12}, 2_{\phi 12}, 3_{g^-}, 4_{g^+}) = \frac{1}{s_{34} [23] \langle 41 \rangle} \left[ \frac{\langle 14 \rangle \langle 23 \rangle [24]^2}{s_{234}} + \frac{[41] [32] \langle 13 \rangle^2}{s_{341}} + [24] \langle 13 \rangle \right]. \quad (3.13)$$

The result (3.13) has been checked against the form factor derived using MHV diagrams, (3.8) and they are in perfect agreement.

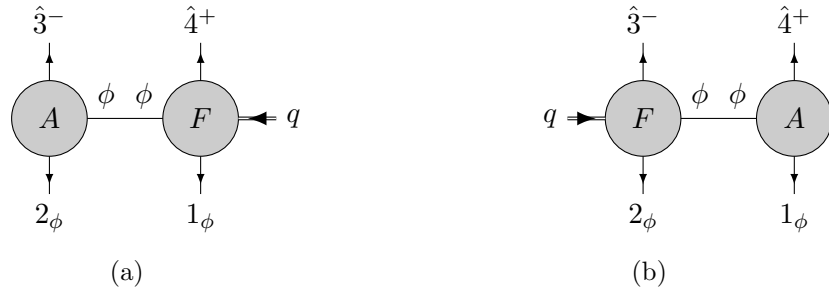


Figure 3.2: The two recursive diagrams contributing to the NMHV form factor (3.6).

### 3.2.2.1 Recursion relations for the split-helicity form factor

In the previous section it was observed that the BCFW recursion relation for the NMHV form factor with a  $[3, 4]$  shift has just two diagrams. This property in fact holds for all form factors of the form  $F_{\phi^2; q-2, n-q}(1_\phi, 2_\phi, 3^-, \dots, q^-, (q+1)^+, \dots, n^+)$ , which are henceforth called *split-helicity*. As is shown shortly, performing a  $[q, q+1]$  shift leads to a general, closed-form solution of the BCFW recursion relations for this special class of form factors. Note that all split-helicity gluon scattering amplitudes were computed in [90] – a similar solution for form factors is constructed here.

Each recursive diagram with a  $[q, q+1]$  shift contains a three-point amplitude and an  $(n-1)$ -point form factor. The three-point amplitude and the propagator can be neatly combined in a prefactor to write<sup>1</sup>

$$\begin{aligned} F_{q-2, n-q} &= \frac{[q-1] q+1}{[q-1] q [q q+1]} F_{q-3, n-q}(1_\phi, 2_\phi, 3^-, \dots, \widehat{q-1}^-, \widehat{q+1}^+, \dots, n^+) \quad (3.14) \\ &+ \frac{\langle q q+2 \rangle}{\langle q q+1 \rangle \langle q+1 q+2 \rangle} F_{q-2, n-q-1}(1_\phi, 2_\phi, 3^-, \dots, \widehat{q}^-, \widehat{q+2}^+, \dots, n^+), \end{aligned}$$

where the shifted spinors of the external momenta that appear in the lower-point form

<sup>1</sup>For the rest of this Section it is always assumed that the operator  $\mathcal{O} = \text{Tr}(\phi_{12} \phi_{12})$  is inserted and it will not be mentioned explicitly. Although the solution is presented for this particular insertion, the construction can be generalised to form factors involving other operators.

factors are

$$\lambda_{\widehat{q+1}} = \frac{[q-1|P_{q,q+1}]}{[q-1\,q+1]}, \quad (3.15a)$$

$$\tilde{\lambda}_{\widehat{q}} = \frac{P_{q,q+2}|q+2\rangle}{\langle q\,q+2\rangle}, \quad (3.15b)$$

with  $P_{a,b} = p_a + \dots + p_b$ . Furthermore, the shifted spinors associated with internal legs are relabelled as

$$\lambda_{\hat{P}_{q-1\,q}}(z = z_{q-1\,q}) \rightarrow \lambda_{\widehat{q-1}} = \frac{P_{q,q+1}|q+1]}{[q-1\,q+1]}, \quad (3.16a)$$

$$\tilde{\lambda}_{\hat{P}_{q+1\,q+2}}(z = z_{q+1\,q+2}) \rightarrow \tilde{\lambda}_{\widehat{q+2}} = \frac{\langle q|P_{q,q+2}}{\langle q\,q+2\rangle}, \quad (3.16b)$$

so that the notation remains compatible with subsequent recursions. Crucially, all lower-point form factors appearing in (3.14) are of split-helicity form, so that the split helicity form factors are closed under recursions. Once one has reduced the form factor to expressions that involve only MHV and  $\overline{\text{MHV}}$  terms, one can insert the shifted momenta.

It is useful to illustrate the structure of the recursion relations for split-helicity form factors using a square lattice as in Figure 3.3. Consider for example the form factor  $F_{2,2}$ . In this case, the first iteration using equation (3.14) relates  $F_{2,2}$  to the form factors  $F_{2,1}$  and  $F_{1,2}$ , which however are neither MHV nor  $\overline{\text{MHV}}$ . The next iteration leads to an expression involving one  $F_{2,0}$ , two  $F_{1,1}$ 's and one  $F_{0,2}$  evaluated at some shifted momenta. A final iteration would then allow us to express the answer in terms of MHV and  $\overline{\text{MHV}}$  form factors alone, or even to reduce everything down to  $F_{0,0}$ . It is also easy to see that this pattern generalises to arbitrary split-helicity form factors and that each term generated by subsequent recursions corresponds to a unique path between the form factor and the MHV or  $\overline{\text{MHV}}$  edges of the lattice, as illustrated in Figure 3.3.

In principle, all one needs to do to compute a split-helicity form factor is to collect all prefactors picked up at each step of the recursion process and follow the iterated momentum shifts along a particular path on the lattice.

### 3.2.2.2 Solution for the split-helicity form factor

A very efficient way to organise the recursion is in terms of *zig-zag diagrams*, like those introduced in [90] for split-helicity gluon amplitudes. It is natural to split the terms of the solution into those corresponding to paths ending on the MHV or  $\overline{\text{MHV}}$  lines,

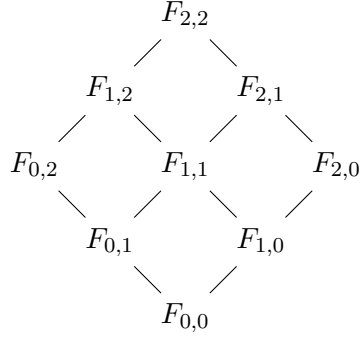


Figure 3.3: The iterative structure of split-helicity form factors illustrated by a square lattice. The three coloured paths ending on the MHV line are in one-to-one correspondence with terms that appear in the iterated recursion of  $F_{2,2}$ . Similarly there will be three paths (terms) that end on the  $\overline{\text{MHV}}$  line.

respectively.

Zig-zag diagrams that correspond to recursion terms with an MHV form factor will be denoted as MHV zig-zags and the ones with an  $\overline{\text{MHV}}$  form factor as  $\overline{\text{MHV}}$  zig-zags. Note that there are therefore two types of diagrams, in contrast to the case of amplitudes in [90]. One can make this separation also for amplitudes as it only means that the iterated recursion terminates once it reaches an  $\overline{\text{MHV}}$  term, instead of recursing it further down to  $F_{0,0}$  (or  $A_{2,2}$  for the case of amplitudes). In the path picture of the previous section, this separation corresponds to the fact that there is a unique path between any  $\overline{\text{MHV}}$  form factor and  $F_{0,0}$ , hence one can replace that part of the recursion directly with an  $\overline{\text{MHV}}$  form factor. Because the MHV zig-zags defined below are not compatible with two point objects such as  $F_{0,0}$ , this formalism with two types of diagrams is preferred. This has the added advantage that it makes the parity symmetry of  $F_{q-2,q-2}$  form factors manifest.

The MHV zig-zags are parameterised with  $2k + 1$  labels

$$2 \leq a_1 < \dots < a_k < q - 1 \quad \text{and} \quad n \geq b_1 > \dots > b_{k+1} > q, \quad k \geq 0,$$

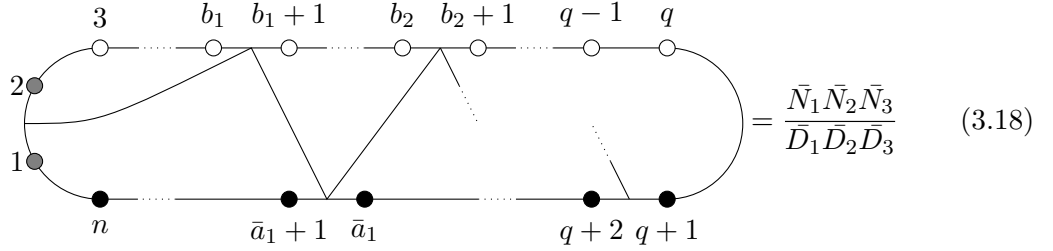
representing expressions in the following manner

$$= \frac{N_1 N_2 N_3}{D_1 D_2 D_3} \quad (3.17)$$

while the  $\overline{\text{MHV}}$  zig-zags are parameterised with  $2k + 1$  labels

$$2 \leq \bar{b}_1 < \dots < \bar{b}_{k+1} < q \quad \text{and} \quad n \geq \bar{a}_1 > \dots > \bar{a}_k > q + 1, \quad k \geq 0,$$

representing expressions, similarly shown below



where  $N_{1,2,3}$  and  $D_{1,2,3}$  are defined as

$$\begin{aligned} N_1 &= \langle 1 | P_{2,b_1} P_{a_1+1,b_1} P_{a_1+1,b_2} P_{a_2+1,b_2} \cdots P_{q,b_{k+1}} | q \rangle \\ &\quad \times [2 | P_{a_1+1,b_1} P_{a_1+1,b_2} P_{a_2+1,b_2} \cdots P_{q,b_{k+1}} | q ]^2 \\ N_2 &= \langle b_1 + 1 | b_1 \rangle \langle b_2 + 1 | b_2 \rangle \cdots \langle b_{k+1} + 1 | b_{k+1} \rangle \\ N_3 &= [a_1 a_1 + 1] \cdots [a_k a_k + 1] \\ D_1 &= P_{2,b_1}^2 P_{a_1+1,b_1}^2 P_{a_1+1,b_2}^2 P_{a_2+1,b_2}^2 \cdots P_{q,b_{k+1}}^2 \\ D_2 &= Z_{q,1} \bar{Z}_{2,q-1} \\ D_3 &= [2 | P_{2,b_1} | b_1 + 1 \rangle \langle b_1 | P_{a_1+1,b_1} | a_1 ] [a_1 + 1 | P_{a_1+1,b_2} | b_2 + 1 \rangle \cdots \langle b_{k+1} | P_{q,b_{k+1}} | q - 1 ] \end{aligned} \quad (3.19a)$$

$$\begin{aligned} \bar{N}_1 &= [q + 1 | P_{\bar{b}_{k+1}+1,q+1} | \dots, P_{\bar{b}_2+1,\bar{a}_2}, P_{\bar{b}_2+1,\bar{a}_1}, P_{\bar{b}_1+1,\bar{a}_1} | 1 ]^2 \\ &\quad \times [q + 1 | P_{\bar{b}_{k+1}+1,q+1} | \dots, P_{\bar{b}_2+1,\bar{a}_2}, P_{\bar{b}_2+1,\bar{a}_1}, P_{\bar{b}_1+1,\bar{a}_1} P_{\bar{b}_1+1,1} | 2 ] \\ \bar{N}_2 &= [\bar{b}_1 \bar{b}_1 + 1] \cdots [\bar{b}_{k+1} \bar{b}_{k+1} + 1] \\ \bar{N}_3 &= \langle \bar{a}_1 + 1 | \bar{a}_1 \rangle \cdots \langle \bar{a}_k + 1 | \bar{a}_k \rangle \\ \bar{D}_1 &= P_{\bar{b}_1+1,1}^2 P_{\bar{b}_1+1,\bar{a}_1}^2 P_{\bar{b}_2+1,\bar{a}_1}^2 \cdots P_{\bar{b}_k+1,q+1}^2 \\ \bar{D}_2 &= \bar{Z}_{2,q+1} Z_{q+2,1} \\ \bar{D}_3 &= \langle 1 | P_{\bar{b}_1+1,1} | \bar{b}_1 \rangle [\bar{b}_1 + 1 | P_{\bar{b}_1+1,\bar{a}_1} | \bar{a}_1 + 1 \rangle \langle \bar{a}_1 | P_{\bar{b}_2+1,\bar{a}_1} | \bar{b}_2 \rangle \dots [\bar{b}_k + 1 | P_{\bar{b}_k+1,q+1} | q + 2 \rangle, \end{aligned} \quad (3.19b)$$

with

$$Z_{i,j} = \langle i | i + 1 \rangle \cdots \langle j - 1 | j \rangle, \quad \bar{Z}_{i,j} = [i | i + 1] \cdots [j - 1 | j]. \quad (3.19c)$$

The split-helicity form factor is then the sum of all recursion terms, or equivalently

the sum of all possible MHV and  $\overline{\text{MHV}}$  zig-zags, which is equal to

$$F_{q-2,n-q-2} = \sum_{\{a_i, b_i\}} \frac{N_1 N_2 N_3}{D_1 D_2 D_3} + \sum_{\{\bar{a}_i, \bar{b}_i\}} \frac{\bar{N}_1 \bar{N}_2 \bar{N}_3}{\bar{D}_1 \bar{D}_2 \bar{D}_3}. \quad (3.20)$$

Notice that for the form factors with equal number of negative and positive helicity gluons, the  $\overline{\text{MHV}}$  zig-zags can be obtained from the MHV ones by changing  $(2, 3, \dots, q) \rightarrow (1, n, \dots, q+1)$  and  $\langle ij \rangle \rightarrow [ji]$ .

Let us now explain the precise relation between the zig-zag diagrams and the paths on the split-helicity form factor lattice. Let a path with  $r_1$  steps to the right,  $l_1$  steps to the left followed by  $r_2$  steps to the right etc. be represented by

$$R^{r_k} \dots R^{r_2} L^{l_1} R^{r_1}. \quad (3.21)$$

Then an MHV zig-zag labelled by  $\{a_i, b_i\}$  corresponds to the path:

$$L^{a_1-1} R^{b_1-b_2} \dots L^{a_k-a_{k-1}} R^{b_k-b_{k+1}} L^{q-1-a_k} R^{b_k-(q+1)},$$

while an  $\overline{\text{MHV}}$  zig-zag labelled by  $\{\bar{a}_i, \bar{b}_i\}$  corresponds to the path:

$$R^{\bar{a}_1+1} L^{\bar{b}_2-\bar{b}_1} \dots R^{\bar{a}_k-\bar{a}_{k-1}} L^{\bar{b}_{k+1}-\bar{b}_k} R^{\bar{a}_k-q-1} L^{q-\bar{b}_{k+1}-1}.$$

Note that if there are no  $a_i$  indices in the MHV zig-zag diagram  $a_1$  is set to  $a_1 = 1$ ; and if there are no  $\bar{a}_i$  in the  $\overline{\text{MHV}}$  zig-zag diagram, it is set to  $\bar{a}_1 = n$ . All powers in the above formulae are modulo  $n$ .

### 3.2.2.3 Examples

Here, some examples are listed to demonstrate that the solution (3.20) reproduces indeed the correct expressions.

#### MHV case

The zig-zag diagrams collapse onto a point between 1 and 2 as there are neither  $b_i$  nor  $\bar{a}_i$ . Hence, the only contributions are  $N_1 = \langle 12 \rangle$  and  $D_2 = F_{2,1}$  and

$$F_{1,n-3}(1_\phi, 2_\phi, 3^+, \dots, n^+) = \frac{\langle 12 \rangle}{\langle 23 \rangle \langle 34 \rangle \dots \langle n1 \rangle}, \quad (3.22)$$

as required. The situation for MHV amplitudes is similar [90]. An equivalent calculation for the  $\overline{\text{MHV}}$  zig-zag gives the  $\overline{\text{MHV}}$  form factor.

## NMHV case

At four points, there is exactly one MHV and one  $\overline{\text{MHV}}$  zig-zag, representing one move to the left and one move to the right, making the application of the zig-zag diagrams a simple reiteration of the BCFW recursion relation presented in the previous Section. In the zig-zag picture, the form factor  $F(1_{\phi_{12}}, 2_{\phi_{12}}, 3^-, 4^+)$  as a sum of two terms represented by two single-step moves that reach the edge of the lattice:

$$F(1_{\phi_{12}}, 2_{\phi_{12}}, 3^-, 4^+) = \begin{array}{c} F_{1,1} \\ \diagup \quad \diagdown \end{array} + \begin{array}{c} F_{1,1} \\ \diagdown \quad \diagup \end{array} \quad (3.23)$$

Comparing with equations (3.17) and (3.18) one can read off  $b_1 = 4$  for the MHV zig-zag and  $\bar{b}_1 = 2$  for the  $\overline{\text{MHV}}$  zig-zag.

$$\begin{array}{c} F_{1,1} \\ \diagup \quad \diagdown \end{array} = \begin{array}{c} \text{circle with vertices 1, 2, 3, 4} \\ \text{red line from 1 to 2} \\ \text{red line from 3 to 4} \end{array} = \frac{[24]^2}{[32][43]} \frac{\langle 1|q|4 \rangle}{\langle 1|q|2 \rangle} \frac{1}{s_{234}} \quad (3.24)$$

$$\begin{array}{c} F_{1,1} \\ \diagdown \quad \diagup \end{array} = \begin{array}{c} \text{circle with vertices 1, 2, 3, 4} \\ \text{blue line from 2 to 3} \\ \text{blue line from 4 to 1} \end{array} = \frac{\langle 13 \rangle^2}{\langle 34 \rangle \langle 41 \rangle} \frac{\langle 3|q|2 \rangle}{\langle 1|q|2 \rangle} \frac{1}{s_{341}} \quad (3.25)$$

This result is in agreement with the previous section.

In general, for the NMHV form factors, there is one  $\overline{\text{MHV}}$  zig-zag corresponding to the path which proceeds along the NMHV line until it reaches the  $\overline{\text{MHV}}$  edge of the lattice, and  $n - 3$  MHV zig-zags where the path shifts onto the MHV edge before it arrives at the  $\overline{\text{MHV}}$  edge. The MHV paths and the corresponding zig-zags are shown in Figure 3.4.

An  $\mathbf{N^2MHV}$  example

The  $\mathbf{N^2MHV}$  form factor  $F(1_{\phi_{12}}, 2_{\phi_{12}}, 3^-, 4^+, 5^+)$  is the first non-trivial example, where using the direct solution in terms of zig-zag diagrams is more convenient than successive applications of BCFW recursion relations.

As it can be seen from the lattice in Figure 3.3, there are three MHV and three  $\overline{\text{MHV}}$

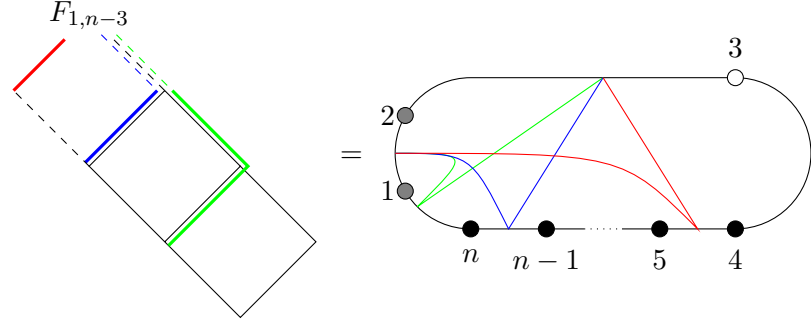


Figure 3.4: Correspondence of lattice paths and MHV zig-zags for NMHV form factors.

terms in the recursion of the six-point split-helicity form factor:

$$F(1_{\phi 12}, 2_{\phi 12}, 3^-, 4^+, 5^+) = F_{LL} + F_{RLL} + F_{LRL} + F_{RR} + F_{LRR} + F_{RLR}, \quad (3.26)$$

where the diagrammatic representation of each term is given below together with its value. The subscripts encode the shape of the path as described earlier. For example,  $F_{RLL}$  is the term which corresponds to the path that starts with a step to right and terminates at the MHV edge with two steps to the left. The MHV terms are:

- $b_1 = 5$ , no  $a$ :

$$F_{LL} = \text{Diagram with 6 points (1, 2, 3, 4, 5, 6) and a zig-zag path from 1 to 5.} = -\frac{[25]^2}{[23][34][45]\langle 61 \rangle} \frac{1}{P_{2,5}^2} \frac{[5|P_{2,4}|1\rangle}{[2|P_{2,5}|6\rangle} \quad (3.27a)$$

- $b_1 = 6$ , no  $a$ :

$$F_{RLL} = \text{Diagram with 6 points (1, 2, 3, 4, 5, 6) and a zig-zag path from 1 to 6.} = \frac{1}{\langle 45 \rangle \langle 56 \rangle [23]} \frac{1}{P_{2,6}^2 P_{4,6}^2} \frac{\langle 1|P_{2,6}P_{4,6}|4\rangle [2|P_{4,6}|4\rangle^2}{[2|P_{2,6}|1\rangle \langle 6|P_{4,6}|3\rangle} \quad (3.27b)$$

- $b_1 = 6, b_2 = 5, a_1 = 2$ :

$$F_{LRL} = \text{Diagram} = \frac{1}{[34][45]} \frac{1}{P_{2,6}^2 P_{3,6}^2 P_{3,5}^2} \frac{\langle 1|P_{2,6}P_{3,6}P_{3,5}|5][2|P_{3,6}P_{3,5}|5]^2}{[2|P_{2,6}|1]\langle 6|P_{3,6}1|2][3|P_{3,5}|6]} \quad (3.27c)$$

The  $\overline{\text{MHV}}$  terms are:

- $\bar{b}_1 = 3$ , no  $\bar{a}$

$$F_{RR} = \text{Diagram} = \frac{\langle 14\rangle^2}{\langle 45\rangle\langle 56\rangle\langle 61\rangle[23]} \frac{1}{P_{4,1}^2} \frac{\langle 4|P_{4,1}|2]}{\langle 1|P_{4,1}|3]} \quad (3.28a)$$

- $\bar{b}_1 = 2$ , no  $\bar{a}$

$$F_{LRR} = \text{Diagram} = \frac{1}{[34][45]\langle 61\rangle} \frac{1}{P_{3,5}^2 P_{3,1}^2} \frac{\langle 1|P_{3,5}|5]^2[5|P_{3,5}P_{3,1}|2]}{\langle 1|P_{3,1}|2][3|P_{3,5}|6]} \quad (3.28b)$$

- $\bar{b}_1 = 2, b_2 = 3, \bar{a}_1 = 6$

$$F_{RLR} = \text{Diagram} = \frac{1}{\langle 45\rangle\langle 56\rangle} \frac{1}{P_{3,1}^2 P_{3,6}^2 P_{4,6}^2} \frac{\langle 4|P_{4,6}P_{3,1}|1]^2\langle 5|P_{4,6}P_{3,6}P_{3,1}|2]}{\langle 1|P_{3,1}|2][3|P_{3,6}|1]\langle 6|P_{4,6}|3][4|P_{4,6}|6]} \quad (3.28c)$$

This result has been checked against an MHV diagram calculation and both methods yield the same result.

### 3.3 Supersymmetric multiplets of form factors

The superamplitude formalism, reviewed in Section 2.1, is a very convenient tool which packages all the scattering amplitudes in a supersymmetric theory as the coefficients of its Taylor expansion in superspace coordinates. Superamplitudes are particularly useful when amplitudes are fed into recursion relations. Summation over several internal particles can be replaced by a simple integration over the odd variables, see for example [38].

It is also possible to construct such supermultiplets of form factors of protected operators. The construction involves not only the supersymmetrisation of multi-particle states, but also the supersymmetrisation of the operator of the form factor. Similar to superamplitudes, the super form factors have a supermomentum-conserving delta function alongside a momentum-conserving one. This supermomentum-conserving delta function equates the total on-shell supermomentum of the particles to the supermomentum carried by the operator and the form factors of the component fields can be extracted from an expansion in fermionic variables.

The derivation of form factors presented here is very close to the derivation of superamplitudes and it uses the supersymmetry Ward identities for correlation functions of the form  $\langle 0|\Phi(1)\cdots\Phi(n)\mathcal{O}|0\rangle$ . These Ward identities impose that the form factor must be equal to a supermomentum-conserving delta function multiplied by a bosonic factor which can be easily derived for MHV form factors.

#### 3.3.1 BPS Multiplets in MSYM

In a supersymmetric quantum field theory, there is a very important special operators, namely BPS operators. Such operators are annihilated by a subset of the supersymmetry generators. MSYM is a theory with 16 supercharges and operators which are annihilated by half of these are called half-BPS. For instance, the operators

$$\text{Tr } \phi_{12}\phi_{12}(x), \quad (3.29)$$

which is considered in the whole of the present chapter is such an operator. Since the SUSY variation of a scalar operator is

$$\delta_\xi \phi^{AB} = -i\sqrt{2} (\xi^{\alpha,A} \lambda_\alpha^B - \xi^{\alpha,B} \lambda_\alpha^A - \epsilon^{ABCD} \bar{\xi}_{\dot{\alpha},C} \bar{\lambda}_D^{\dot{\alpha}}), \quad (3.30)$$

half of the possible to find non-zero transformation parameters  $\xi$  leave the operator  $\text{Tr}\phi_{12}\phi_{12}$  invariant. Other operators, which are annihilated by a smaller fraction of all possible SUSY transformations are called 1/8-BPS, etc. depending on the number of such directions in the transformation parameter space.

BPS operators are also called *protected* operators, since supersymmetry protects them from renormalisation. They are not renormalised and do their scaling dimensions do not receive anomalous corrections.

The operator  $\text{Tr}\phi_{12}\phi_{12}$  is embedded in the chiral half of the stress-tensor multiplet together with the on-shell Lagrangian and other fermionic fields. This multiplet is explicitly given as [91]:

$$\begin{aligned}\mathcal{T}(x, \theta^+) = & \text{Tr}(\phi^{++}\phi^{++}) + i2\sqrt{2}\theta_a^{+a}\text{Tr}(\lambda_a^{+\alpha}\phi^{++}) \\ & + \theta_a^{+a}\epsilon_{ab}\theta_b^{+b}\text{Tr}\left(\lambda^{+c(\alpha}\lambda_c^{+\beta)} - i\sqrt{2}F^{\alpha\beta}\phi^{++}\right) \\ & - \theta_a^{+a}\epsilon^{\alpha\beta}\theta_b^b\text{Tr}\left(\lambda_{(a}^{+\gamma}\lambda_{b)\gamma}^{+} - g\sqrt{2}[\phi_{(a}^{+C}, \bar{\phi}_{C+b)}]\phi^{++}\right) \\ & - \frac{4}{3}(\theta^+)_a^{3a}\text{Tr}\left(F_\beta^\alpha\lambda_a^{+\beta} + ig[\phi_a^{+B}, \bar{\phi}_{BC}]\lambda^{C\alpha}\right) + \frac{1}{3}(\theta^+)^4\mathcal{L}.\end{aligned}\quad (3.31)$$

Notice that the  $(\theta^+)^0$  component is nothing but the scalar operator  $\text{Tr}(\phi^{++}\phi^{++})$ , whereas the  $(\theta^+)^4$  component is the on-shell Lagrangian. The field  $\phi^{++}$  is related to the scalar  $\phi_{AB}$  through projection onto harmonic variables:

$$\phi^{++} = -\frac{1}{2}u_A^{+a}\epsilon_{ab}u_B^{+b}\phi^{AB}.\quad (3.32)$$

The operator  $\mathcal{T}(x, \theta^+)$  is the chiral part of the full stress-tensor multiplet operator,  $\mathcal{T}(x, \theta^+, \bar{\theta}_-, u)$ , obtained by setting  $\theta_- = 0$ . The full multiplet can be written in terms of the vector multiplet of MSYM as

$$\begin{aligned}\mathcal{T}(x, \theta^+, \tilde{\theta}_-) := & \text{Tr}(W^{++}W^{++}) \\ = & e^{i\theta^+Q_++i\tilde{\theta}_-\bar{Q}^-}\text{Tr}(\phi^{++}\phi^{++})(x)e^{-i\theta^+Q_+-i\tilde{\theta}_-\bar{Q}^-} \\ = & \text{Tr}(\phi^{++}\phi^{++}) + (\theta^+)^4\mathcal{L} + (\tilde{\theta}_-)^4\tilde{\mathcal{L}} + (\theta^+\sigma^\mu\tilde{\theta}_-)(\theta^+\sigma^\nu\tilde{\theta}_-)T_{\mu\nu} + \dots,\end{aligned}\quad (3.33)$$

where only some terms of the full multiplet are indicated in the expansion in the chiral as well as anti-chiral variables  $\theta^+$  and  $\tilde{\theta}_-$ .

The advantage of the chiral part over the full multiplet is that the supersymmetry algebra closes on this multiplet without the need of imposing the equations of motion, whereas this is not true for the full multiplet. However, as far as the tree-level form

factors are concerned, this does not raise any problems.

The multiplet  $\mathcal{T}(x, \theta^+, \tilde{\theta}_-)$  takes its name from its spin-2 component which is the stress-tensor of MSYM, which is not present in  $\mathcal{T}(x, \theta^+)$  since it is obtained from  $\mathcal{T}(x, \theta^+, \tilde{\theta}_-)$  by setting  $\tilde{\theta}_- = 0$ .

The full stress-tensor multiplet  $\mathcal{T}(x, \theta^+, \bar{\theta}_-)$  is an example in a series of half-BPS operators which are constructed from the vector multiplet of MSYM

$$\text{Tr} \left[ (W^{++} W^{++})^k \right], \quad (3.34)$$

which have a composite operator as their lowest component that transforms in the  $[0 \ k \ 0]$  representation of  $\text{SU}(4)$ . In accordance with this, the operator  $\text{Tr} \phi_{12} \phi_{12}$  belongs to the 20-dimensional  $[0 \ 2 \ 0]$  representation of the  $\text{SU}(4)$  R-symmetry.

### 3.3.2 Form factor of the chiral stress-tensor multiplet

In this Section, the form factors of the chiral supersymmetric operator  $\mathcal{T}(x, \theta^+)$  are considered. This is a special case of the form factors of operators belonging to the full multiplet.

Just as it is the case for the amplitudes, [68, 92–94], Ward identities can be used to constrain the form of the form factors. They require that the form factors are non-vanishing only under the support of certain delta functions, such as supermomentum-conserving delta functions for supersymmetry. This functional form plays the central role in the construction of the multiplets.

Ward identities associated with a certain symmetry generator  $s$  which leaves the vacuum invariant are obtained in a standard way by expanding the identity

$$0 = \langle 0 | [s, \Phi(1) \cdots \Phi(n) \mathcal{O}] | 0 \rangle, \quad (3.35)$$

or

$$0 = \langle 0 | \Phi(1) \cdots \Phi(n) [s, \mathcal{O}] | 0 \rangle + \sum_{i=1}^n \langle 0 | \Phi(1) \cdots [s, \Phi(i)] \cdots \Phi(n) \mathcal{O} | 0 \rangle. \quad (3.36)$$

For instance, by considering  $s$  to be the momentum generator  $\mathcal{P}$  and using  $[\mathcal{P}_\mu, \mathcal{O}(x)] = -i\partial_\mu \mathcal{O}(x)$  as well as the the action of  $Q$  on a single-particle Nair superstate,  $q|i\rangle =$

$\eta_i \lambda_i |i\rangle$ , one obtains

$$-i \langle 0 | \Phi(1) \cdots \Phi(n) \partial_\mu \mathcal{O}(x) | 0 \rangle + \left( \sum_{i=1}^n p_i \right) \langle 0 | \Phi(1) \cdots \Phi(n) \mathcal{O}(x) | 0 \rangle = 0 . \quad (3.37)$$

Fourier transforming  $x$  to  $Q$  and integrating by parts one obtains

$$(q - \sum_{i=1}^n p_i) F(q; 1, \dots, n) = 0 , \quad (3.38)$$

where

$$F(q; 1, \dots, n) := \int d^4x e^{-iqx} \langle 1 \cdots n | \mathcal{O}(x) | 0 \rangle . \quad (3.39)$$

From this, it follows that

$$F(q; 1, \dots, n) = \langle 0 | \Phi(1) \cdots \Phi(n) \mathcal{O}(0) | 0 \rangle = \delta^{(4)}(q - \sum_{i=1}^n p_i) \langle 1 \cdots n | \mathcal{O}(0) | 0 \rangle , \quad (3.40)$$

where the action of the momentum operator on the operator and the states has been used to get rid of the space dependence on the matrix element, namely:

$$\langle 1 \cdots n | \mathcal{O}(x) | 0 \rangle = \langle 1 \cdots n | \exp(iP) \mathcal{O}(0) \exp(-iP) | 0 \rangle . \quad (3.41)$$

and

$$\langle 1 \cdots n | \exp(iP) = \exp \left( i \sum_{i=1}^n p_i \right) \langle 1 \cdots n | . \quad (3.42)$$

Then the relation (3.40) immediately follows from the Fourier transform of a phase.

Similarly, for the Ward identities for the harmonic projections  $Q_{\pm a}^\alpha$ ,  $a = 1, 2$ , of the  $Q$ -supersymmetry generators one obtains

$$0 = \langle 0 | \Phi(1) \cdots \Phi(n) [Q_\pm, \mathcal{T}(x, \theta^+)] | 0 \rangle + \sum_{i=1}^n \langle 0 | \Phi(1) \cdots [Q_\pm, \Phi(i)] \cdots \Phi(n) \mathcal{T}(x, \theta^+) | 0 \rangle . \quad (3.43)$$

It is now necessary to discuss how supersymmetry acts on the chiral part of  $\mathcal{T}(x, \theta^+)$  as well as on the states.

In general the supersymmetry algebra closes only up to gauge transformations and equations of motion, however gauge-invariant operators such as  $\mathcal{T}$  which, furthermore, are made only of a subset of all fields, namely  $\phi^{AB}$ ,  $\lambda_\alpha^A$  and  $F_{\alpha\beta}$  are considered here.

It is an important fact that the algebra of the  $Q$ -generators closes off shell on the chiral part of  $\mathcal{T}$  [91], and hence these generators can be realised as differential operators. Of

course, representing the  $\bar{Q}$ -generators in terms of differential operators is, in general, problematic, because the full supersymmetry algebra closes only on shell.

Moreover, restricting to  $\theta^- = 0$  in order to obtain the chiral operator  $\mathcal{T}(x, \theta^+)$  breaks the  $\bar{Q}^-$  symmetry, hence this operator does not have a representation. For the  $Q_\pm$ -variation of  $\mathcal{T}(x, \theta^+)$ , which is unbroken, one can write have,

$$[Q_-, \mathcal{T}(x, \theta^+)] = 0, \quad [Q_+, \mathcal{T}(x, \theta^+)] = i \frac{\partial}{\partial \theta^+} \mathcal{T}(x, \theta^+). \quad (3.44)$$

Note that since the chiral part of the stress-tensor multiplet is considered,  $\bar{\theta}$  is set to zero and hence the  $\bar{\theta}$ -dependent terms are dropped in the realisation of  $Q$  and  $\bar{Q}$ . Then the first relation is obvious since  $\mathcal{T}(x, \theta^+)$  is independent of  $\theta^-$ . This also makes manifest the fact that all component operators of  $\mathcal{T}(x, \theta^+)$  are annihilated by  $Q_{-a}^\alpha$  [91]. On the other hand,  $Q_{+a}^\alpha$  relates different components of the supermultiplet, as the second relation in (3.44) shows.

The super form factor is defined as the super Fourier transform of the matrix element  $\langle 1 \cdots n | \mathcal{T}(x, \theta^+) | 0 \rangle$ , i.e.

$$\mathcal{F}_\mathcal{T}(q, \gamma_+; 1, \dots, n) := \int d^4x d^4\theta^+ e^{-(iqx + i\theta_\alpha^{+a} \gamma_{+a}^\alpha)} \langle 1 \cdots n | \mathcal{T}(x, \theta^+) | 0 \rangle, \quad (3.45)$$

where  $\gamma_{+a}^\alpha$  is the Fourier-conjugate variable to  $\theta_\alpha^{+a}$ . Note that there is no  $\gamma_{-a}^\alpha$  variable, since  $\theta_\alpha^{-a}$  has been set to zero in order to define the chiral part of the stress-tensor multiplet. The Ward identities (3.43) can then be recast as

$$\begin{aligned} \left( \sum_{i=1}^n \lambda_i \eta_{-,i} \right) \mathcal{F}_\mathcal{T}(q, \gamma_+; 1, \dots, n) &= 0, \\ \left( \sum_{i=1}^n \lambda_i \eta_{+,i} - \gamma_+ \right) \mathcal{F}_\mathcal{T}(q, \gamma_+; 1, \dots, n) &= 0, \end{aligned} \quad (3.46)$$

where

$$\eta_{\pm a,i} := \bar{u}_{\pm a}^A \eta_{A,i}, \quad (3.47)$$

has also been introduced.

The Ward identities (3.46) can be derived from the action on the  $Q_\pm$  operator on the multiplet  $\mathcal{T}(x, \theta^+)$ , (3.44), and using the fact that that  $Q|i\rangle = \eta_i \lambda_i |i\rangle$  for a Nair superstate  $|i\rangle$ .

To solve the Ward identities (3.46), the form factors must have the following functional

form:

$$\mathcal{F}_{\mathcal{T}}(q, \gamma_+; 1, \dots, n) = \delta^{(4)}(q - \sum_{i=1}^n \lambda_i \tilde{\lambda}_i) \delta^{(4)}(\gamma_+ - \sum_{i=1}^n \eta_{+,i} \lambda_i) \delta^{(4)}(\sum_{i=1}^n \eta_{-,i} \lambda_i) R, \quad (3.48)$$

for some function  $R$  which in principle depends on all bosonic and fermionic variables. The simplest example is that of the MHV form factor, where the function  $R$  has a particularly simple expression derived in [57], namely

$$R^{\text{MHV}} = \frac{1}{\langle 12 \rangle \cdots \langle n1 \rangle}. \quad (3.49)$$

Notice that for an  $N^k$ MHV form factor,  $R$  does depend on the fermionic coordinates with a fermionic degree of  $4k$ . Although, it is possible to further constrain  $R$  by using some of the  $\bar{Q}$ -supersymmetries.

More precisely, an inspection of the supersymmetry transformations of the fields reveals that a  $\bar{Q}^-$  transformation on the chiral part of the stress-tensor multiplet produces operators which are part of the full stress-tensor multiplet but not of its chiral truncation. Also, since  $[Q_-, \mathcal{T}(x, \theta^+)] = 0$  it is not possible to realise  $\bar{Q}^-$  such that its anticommutator with  $Q_-$  gives a translation. One could of course still write a Ward identity for  $\bar{Q}^-$ , but this would involve operators of the full multiplet.

On the other hand, the  $\bar{Q}^+$ -supersymmetry charge moves in the opposite direction of  $Q_+$  across the different components of  $\mathcal{T}(x, \theta^+)$ , and is therefore realised as  $\bar{Q}_\alpha^+ = -\theta^{+\alpha} \partial/\partial x^{\dot{\alpha}\alpha}$ .

It is necessary to stress at this point that the supersymmetry algebra on component fields closes only up to equations of motion and gauge transformations (the latter drop out for the gauge invariant operators considered here). An important exception is the subalgebra formed by the  $Q$ 's alone which does close off-shell for the fields appearing in  $\mathcal{T}(x, \theta^+)$  [91]. Now using the fact that matrix elements of terms proportional to equations of motion vanish at tree level, one can argue that for the tree-level form factors the algebra formed by  $Q_+$  and  $\bar{Q}^+$  does indeed close and, therefore, can be realised in the fashion described above. Thus, it is possible to consider the  $\bar{Q}^+$  Ward identity to constrain the function  $R$ . It implies, after integrating by parts and using the fact that  $\bar{Q}|i\rangle = \tilde{\lambda}_i \frac{\partial}{\partial \eta_i}|i\rangle$  for a Nair superstate  $|i\rangle$ ,

$$\left( \sum_{i=1}^n \tilde{\lambda}_i \frac{\partial}{\partial \eta_{+,i}} - q \frac{\partial}{\partial \gamma_+} \right) \mathcal{F}_{\mathcal{T}}(q, \gamma_+; 1, \dots, n) = 0. \quad (3.50)$$

Acting on (3.48), one obtains the following relation for  $R$ ,

$$\delta^{(4)}(q - \sum_{i=1}^n \lambda_i \tilde{\lambda}_i) \delta^{(4)}(\gamma_+ - \sum_{i=1}^n \eta_{+,i} \lambda_i) \delta^{(4)}(\sum_{i=1}^n \eta_{-,i} \lambda_i) \left[ \left( \sum_{i=1}^n \tilde{\lambda}_i \frac{\partial}{\partial \eta_{+,i}} - q \frac{\partial}{\partial \gamma_+} \right) R \right] = 0. \quad (3.51)$$

Notice that (3.51) implies a realisation of the supersymmetry generators on the form factor as

$$Q_{+a}^\alpha = \sum_{i=1}^n \lambda_i^\alpha \eta_{+,i} - \gamma_{+a}^\alpha, \quad Q_{-a}^\alpha = \sum_{i=1}^n \lambda_i^\alpha \eta_{-,i}, \quad (3.52)$$

whereas for  $\bar{Q}_{\dot{\alpha}}^{+a}$ ,

$$\bar{Q}_{\dot{\alpha}}^{+a} = \sum_{i=1}^n \tilde{\lambda}_{i,\dot{\alpha}} \frac{\partial}{\partial \eta_{+,i}} - Q_{\alpha\dot{\alpha}} \frac{\partial}{\partial \gamma_{\alpha+a}}. \quad (3.53)$$

### 3.3.3 Examples

In the previous Section, the general form of the supersymmetric form factor defined in (3.45) have been derived. This expression is given in (3.48), and was obtained by solving Ward identities related to translations and  $Q_\pm$ -supersymmetries. The use of  $\bar{Q}^+$  supersymmetry led to the constraint (3.51) on the function  $R$ . For the sake of illustration, a few examples of component form factors derived from (3.48) are presented below.

#### 3.3.3.1 Form factor of $\text{Tr}(\phi^{++}\phi^{++})$

The first example is the form factor of  $\text{Tr}(\phi^{++}\phi^{++})$ , which appears as the  $(\theta^+)^0$ -term in the expansion of  $\mathcal{T}(x, \theta^+)$  in (3.31). In this case, since

$$\int d^4\theta^+ e^{i\theta_{\alpha}^{+a} \gamma_{+a}^\alpha} = (\gamma_+)^4, \quad (3.54)$$

it is needed to extract the  $(\gamma_+)^4$  component of (3.48). This gives

$$\int d^4x e^{-iqx} \langle 1 \cdots n | \text{Tr}(\phi^{++}\phi^{++})(x) | 0 \rangle = \delta^{(4)}(q - \sum_{i=1}^n \lambda_i \tilde{\lambda}_i) \delta^{(4)}(\sum_{i=1}^n \eta_{-,i} \lambda_i^\alpha) R, \quad (3.55)$$

or

$$\langle 1 \cdots n | \text{Tr}(\phi^{++}\phi^{++})(0) | 0 \rangle = \delta^{(4)}(\sum_{i=1}^n \eta_{-,i} \lambda_i^\alpha) R. \quad (3.56)$$

Notice that with the help of (3.56) one can rewrite the supersymmetric form factor  $\mathcal{F}_{\mathcal{T}}(q, \gamma_+; 1, \dots, n)$  as

$$\mathcal{F}_{\mathcal{T}}(q, \gamma_+; 1, \dots, n) = \delta^{(4)}(q - \sum_{i=1}^n \lambda_i \tilde{\lambda}_i) \delta^{(4)}(\gamma_+ - \sum_{i=1}^n \eta_{+,i} \lambda_i) \langle 1 \cdots n | \mathcal{T}(0, 0) | 0 \rangle , \quad (3.57)$$

since  $\mathcal{T}(0, 0) := \text{Tr}(\phi^{++} \phi^{++})(0)$ . In other words, the function  $R$  appearing in the  $\mathcal{T}(x, \theta^+)$  form factor can be calculated from the form factor of its lowest component<sup>2</sup>  $\text{Tr}(\phi^{++} \phi^{++})(0)$ . Similar considerations apply to form factors of other half BPS operators such as  $\text{Tr}(\phi^{++})^n$  with  $n > 2$ .

### 3.3.3.2 Form factor of the on-shell Lagrangian

As a second important example, the form factor for the on-shell Lagrangian is presented. This operator is defined as: [91]

$$\mathcal{L} = \text{Tr} \left[ -\frac{1}{2} F_{\alpha\beta} F^{\alpha\beta} + \sqrt{2} g \lambda^{\alpha A} [\phi_{AB}, \lambda_{\alpha}^B] - \frac{1}{8} g^2 [\phi^{AB}, \phi^{CD}] [\phi_{AB}, \phi_{CD}] \right] . \quad (3.58)$$

Notice that it contains the self-dual part of  $\text{Tr}(F^2)$ . The on-shell Lagrangian appears as the  $(\theta^+)^4$  coefficient of the expansion of  $\mathcal{T}(x, \theta^+)$  in (3.31). The corresponding Fourier transform gives

$$\int d^4 \theta^+ e^{-i\theta_{\alpha}^{+a} \gamma_{+a}^{\alpha}} (\theta^+)^4 = 1 , \quad (3.59)$$

i.e. one has to take the  $\mathcal{O}(\gamma^0)$  component of (3.48). This is simply

$$\langle 1 \cdots n | \mathcal{L}(0) | 0 \rangle = \delta^{(8)} \left( \sum_{i=1}^n \eta_i \lambda_i \right) \cdot R . \quad (3.60)$$

It is interesting to note that for an MHV form factor, (3.60) is formally identical to the tree-level MHV superamplitude, except for a delta function of momentum conservation which now imposes  $\sum_{i=1}^n p_i = q$  rather than the usual momentum conservation of the particles. This allows us to make an interesting observation for the limit  $q \rightarrow 0$  in which this form factor reduces simply to the correspond scattering amplitude. Actually, it turns out that any form factor with the on-shell Lagrangian  $\mathcal{L}$  inserted reduces to the corresponding scattering amplitude in the  $q \rightarrow 0$  limit, since the insertion of the action corresponds to differentiating the path-integral for the amplitude with respect to the coupling [95–97].

<sup>2</sup>One could arrive at (3.57) in a much more straightforward way by noticing that  $\mathcal{T}(x, \theta_{\alpha}^{+a}) = \exp(i\mathcal{P}x) \exp(iQ_{+a}^{\alpha} \theta_{\alpha}^{+a}) \mathcal{T}(0, 0) \exp(-i\mathcal{P}x) \exp(-iQ_{+a}^{\alpha} \theta_{\alpha}^{+a})$  and using the invariance of the vacuum under supersymmetry and translations.

Another observation is that for the case of a gluonic state with MHV helicity configuration, (3.60) agrees with the Higgs plus multi-gluon or “ $\phi$ -MHV” amplitude considered in [98]. Indeed, if one has a gluonic state, one can effectively replace the on-shell Lagrangian (3.58) with its first term, the square of the self-dual field strength.

### 3.3.3.3 Why is the maximally non-MHV form factor so simple?

The simplest tree-level form factor is the MHV form factor, e.g.

$$\langle 1^+ 2^+ \cdots i^- \cdots j^- \cdots (n-1)^+ n^+ | \text{Tr}(F_{\text{SD}}^2)(0) | 0 \rangle = \frac{\langle ij \rangle^4}{\langle 12 \rangle \langle 23 \rangle \cdots \langle n-1 \rangle}. \quad (3.61)$$

Interestingly, there are non-MHV form factors whose expression is also remarkably simple. Consider for example that of the self-dual field strength with an all negative-helicity gluons state – which will be referred to as the “maximally non-MHV” form factor. The result for this quantity is [98]

$$\langle 1^- \cdots n^- | \text{Tr}(F_{\text{SD}}^2)(0) | 0 \rangle = \frac{q^4}{[1 \ 2][2 \ 3] \cdots [n \ 1]}. \quad (3.62)$$

In the following it is shown that the simplicity of (3.62) is determined by the supersymmetric Ward identity discussed earlier, and is linked to that of the MHV super form factor (3.49).

Recall from (3.57) that the super form factor of the chiral part of the stress-tensor multiplet  $\mathcal{T}(x, \theta^+)$  has the form

$$\mathcal{F}_{\mathcal{T}} = \delta^{(4)}(q - \sum_{i=1}^n \lambda_i \tilde{\lambda}_i) \delta^{(4)}(\gamma_+ - \sum_{i=1}^n \eta_{+,i} \lambda_i) \mathcal{F}_{\phi^2}, \quad (3.63)$$

where

$$\mathcal{F}_{\phi^2} := \langle 1 \cdots n | \text{Tr}(\phi^{++} \phi^{++})(0) | 0 \rangle = \delta^{(4)}\left(\sum_{i=1}^n \eta_{-,i} \lambda_i\right) R. \quad (3.64)$$

For the MHV helicity configuration, the function  $R^{\text{MHV}}$  is given in (3.49),

$$\mathcal{F}_{\phi^2}^{\text{MHV}} = \frac{\delta^{(4)}\left(\sum_{i=1}^n \eta_{-,i} \lambda_i\right)}{\langle 12 \rangle \cdots \langle n1 \rangle}. \quad (3.65)$$

One can now use this fact and perform a Grassmann Fourier transform in order to

derive the maximally non-MHV super form factor,

$$\mathcal{F}_{\phi^2}^{\text{NmaxMHV}} = \prod_{i=1}^n \int d^4 \tilde{\eta}_i e^{i\eta_{i,A} \tilde{\eta}_i^A} \frac{\delta^{(4)}(\sum_{i=1}^n \tilde{\eta}_i^+ \tilde{\lambda}_i)}{[12] \cdots [n1]} . \quad (3.66)$$

Thus, the maximally non-MHV super form factor for the chiral part of the stress-tensor multiplet is

$$\mathcal{F}_{\mathcal{T}}^{\text{NmaxMHV}} = \delta^{(4)}(q - \sum_{i=1}^n \lambda_i \tilde{\lambda}_i) \delta^{(4)}(\gamma_+ - \sum_{i=1}^n \eta_{+,i} \lambda_i) \mathcal{F}_{\phi^2}^{\text{NmaxMHV}} . \quad (3.67)$$

The following discussion focuses on the component corresponding to the self-dual field strength, which can be obtained from the coefficient of  $(\gamma_+)^0$ . This is given, omitting a trivial delta function of momentum conservation, by

$$\begin{aligned} & \delta^{(4)}\left(\sum_{i=1}^n \eta_{+,i} \lambda_i\right) \prod_{i=1}^n \int d^4 \tilde{\eta}_i e^{i\eta_{i,A} \tilde{\eta}_i^A} \frac{\delta^{(4)}(\sum_{i=1}^n \tilde{\eta}_i^+ \tilde{\lambda}_i)}{[12] \cdots [n1]} \\ &= \delta^{(4)}\left(\sum_{i=1}^n \eta_{+,i} \lambda_i\right) \frac{\sum_{i < j} [ij] \sum_{k < l} [kl]}{[12] \cdots [n1]} \eta_1^4 \cdots \eta_i^3 \cdots \eta_j^3 \cdots \eta_k^3 \cdots \eta_l^3 \cdots \eta_n^4 \\ &= \frac{\sum_{i < j} \langle ij \rangle [ij] \sum_{k < l} \langle kl \rangle [kl]}{[12] \cdots [n1]} \eta_1^4 \cdots \eta_n^4 \\ &= \frac{q^4}{[12] \cdots [n1]} \eta_1^4 \cdots \eta_n^4 . \end{aligned} \quad (3.68)$$

Equation (3.68) shows that there is a non-vanishing maximally non-MHV form factor for the self-dual field strength, whose expression is precisely given by (3.62).

### 3.3.4 Form factor of the complete stress-tensor multiplet

In this Section the form factor of the the full, non-chiral stress-tensor multiplet  $\mathcal{T}(x, \theta^+, \tilde{\theta}_-)$  is considered, which depends on both  $\theta^+$  and  $\tilde{\theta}_-$ . One can parallel this feature in the states by using a non-chiral description as in [99] with fermionic variables  $\eta_+$  and  $\tilde{\eta}_-$ . With this choice, the supersymmetry algebra is realised on states as

$$\begin{aligned} \langle i | Q_+ &= \langle i | \lambda_i \eta_{+,i} , & \langle i | Q_- &= \langle i | \lambda_i \frac{\partial}{\partial \tilde{\eta}_i^-} , \\ \langle i | \bar{Q}^- &= \langle i | \tilde{\lambda}_i \tilde{\eta}_i^- , & \langle i | \bar{Q}^+ &= \langle i | \tilde{\lambda}_i \frac{\partial}{\partial \eta_{+,i}} . \end{aligned} \quad (3.69)$$

This non-chiral representation can be obtained via a simple Fourier transform of half of the chiral superspace variables. In terms of the Nair description of states, this amounts to introducing a new super wavefunction,

$$\begin{aligned}\Phi(p, \eta_+, \tilde{\eta}^-) &:= \int d^2\eta_- e^{i\eta_- \tilde{\eta}^-} \Phi(p, \eta) \\ &= g^+(p)(\tilde{\eta}^-)^2 + \dots + \phi^{++}(\eta_+)^2(\tilde{\eta}^-)^2 + \phi^{--} + \dots + g^-(p)(\eta_+)^2.\end{aligned}\quad (3.70)$$

As a result, operators and superstates live in a non-chiral superspace. The non-chiral form factor in this representation is defined as

$$\mathcal{F}(q, \gamma_+, \tilde{\gamma}^-; 1, \dots, n) := \int d^4x d^4\theta^+ d^4\tilde{\theta}_- e^{-i(qx + \theta^+ \gamma_+ + \tilde{\theta}_- \tilde{\gamma}^-)} \langle 1 \dots n | \mathcal{T}(x, \theta^+, \tilde{\theta}_-) | 0 \rangle. \quad (3.71)$$

The Ward identities for (3.71) are written down by considering the action of supersymmetry generators on the operator  $\mathcal{T}(x, \theta^+, \tilde{\theta}_-)$ :

$$\begin{aligned}[Q_+, \mathcal{T}(x, \theta^+, \tilde{\theta}_-)] &= i \frac{\partial}{\partial \theta^+} \mathcal{T}(x, \theta^+, \tilde{\theta}_-) , \quad [Q_-, \mathcal{T}(x, \theta^+, \tilde{\theta}_-)] = -\tilde{\theta}_- \frac{\partial}{\partial x} \mathcal{T}(x, \theta^+, \tilde{\theta}_-) , \\ [\bar{Q}^-, \mathcal{T}(x, \theta^+, \tilde{\theta}_-)] &= -\frac{\partial}{\partial \tilde{\theta}_-} \mathcal{T}(x, \theta^+, \tilde{\theta}_-) , \quad [\bar{Q}^+, \mathcal{T}(x, \theta^+, \tilde{\theta}_-)] = i \theta^+ \frac{\partial}{\partial x} \mathcal{T}(x, \theta^+, \tilde{\theta}_-) .\end{aligned}\quad (3.72)$$

Following closely the derivation of the Ward identities described in the previous section, one arrives at the following relations for each supersymmetry generator,

$$Q_+ : \quad (\eta_+ \lambda - \gamma_+) \mathcal{F} = 0 , \quad Q_- : \quad \left( q \frac{\partial}{\partial \tilde{\gamma}^-} - \lambda \frac{\partial}{\partial \tilde{\eta}^-} \right) \mathcal{F} = 0 , \quad (3.73)$$

$$\bar{Q}^- : \quad (\tilde{\eta}^- \tilde{\lambda} - \tilde{\gamma}^-) \mathcal{F} = 0 , \quad \bar{Q}^+ : \quad \left( q \frac{\partial}{\partial \gamma_+} - \tilde{\lambda} \frac{\partial}{\partial \eta_+} \right) \mathcal{F} = 0 , \quad (3.74)$$

and hence the form factor in (3.71) takes the form

$$\mathcal{F} = \delta^{(4)}(q - \sum_{i=1}^n \lambda_i \tilde{\lambda}_i) \delta^{(4)}(\gamma_+ - \sum_{i=1}^n \eta_{+,i} \lambda_i) \delta^{(4)}(\tilde{\gamma}^- - \sum_{i=1}^n \tilde{\eta}_i^- \tilde{\lambda}_i) \mathcal{F}_{\phi^2}^{\text{nc}} , \quad (3.75)$$

for some function  $\mathcal{F}_{\phi^2}^{\text{nc}}$ .

A useful observation is that  $\mathcal{F}_{\phi^2}^{\text{nc}}$  can be obtained from the corresponding function introduced in (3.63) for the chiral form factor via a half-Fourier transform on the  $\eta$  and  $\tilde{\eta}$  variables, as

$$\mathcal{F}_{\phi^2}^{\text{nc}}(\lambda, \tilde{\lambda}, \eta_+, \tilde{\eta}^-) = \prod_{i=1}^n \int d^2\eta_{-,i} e^{i\eta_{-,i} \tilde{\eta}^-} \mathcal{F}_{\phi^2}(\lambda, \tilde{\lambda}, \eta_+, \eta_-) . \quad (3.76)$$

In the remaining part of this section a few applications of this formulation are presented.

The MHV case is the first example, for which one has:

$$\begin{aligned}\mathcal{F}_{\phi^2}^{\text{MHV, nc}} &= \prod_{i=1}^n \int d^2 \eta_{-,i} e^{i\eta_{-,i}\tilde{\eta}_i^-} \frac{\delta^{(4)}(\sum_{i=1}^n \eta_{-,i}\lambda_i)}{\langle 12 \rangle \cdots \langle n1 \rangle} \\ &= \frac{\langle kl \rangle^2}{\langle 12 \rangle \cdots \langle n1 \rangle} \prod_{i \neq k,l}^n (\tilde{\eta}_i^-)^2 + \cdots .\end{aligned}\quad (3.77)$$

The MHV form factor of  $\text{Tr}(\phi^+)^2$  is then obtained by extracting the coefficient of  $(\gamma_+)^4(\tilde{\gamma}^-)^4$  in (3.75), and thus it is immediately seen to give the correct answer. The form factor with an insertion of the chiral Lagrangian  $\mathcal{L}$  (which includes  $\text{Tr}(F_{\text{SD}}^2)$ ) is obtained by taking the coefficient of  $(\gamma_+)^0(\tilde{\gamma}^-)^4$ :

$$\mathcal{F}_{\mathcal{L}}^{\text{MHV}} = \delta^{(4)}\left(\sum_{i=1}^n \eta_{+,i}\lambda_i\right) \mathcal{F}_{\phi^2}^{\text{MHV}} = \frac{\langle kl \rangle^4}{\langle 12 \rangle \cdots \langle n1 \rangle} \left(\eta_{+,k}^2 \eta_{+,l}^2 \prod_{i \neq k,l}^n (\tilde{\eta}_i^-)^2\right) + \cdots , \quad (3.78)$$

as expected. Finally, in order to obtain the form factor with  $\tilde{\mathcal{L}}$  (which includes  $\text{Tr}(F_{\text{ASD}}^2)$ ), one extracts the coefficient of  $(\gamma_+)^4(\tilde{\gamma}^-)^0$ :

$$\begin{aligned}\mathcal{F}_{\tilde{\mathcal{L}}}^{\text{MHV}} &= \delta^{(4)}\left(\sum_{i=1}^n \tilde{\eta}_i^- \tilde{\lambda}_i\right) \mathcal{F}_{\phi^2}^{\text{MHV}} = \frac{\sum_{i < j} \langle ij \rangle [ij] \sum_{k < l} \langle kl \rangle [kl]}{\langle 12 \rangle \cdots \langle n1 \rangle} \prod_{i=1}^n (\tilde{\eta}_i^-)^2 \\ &= \frac{q^4}{\langle 12 \rangle \cdots \langle n1 \rangle} \prod_{i=1}^n (\tilde{\eta}_i^-)^2 ,\end{aligned}\quad (3.79)$$

which is indeed also correct. Note that the form factor  $\mathcal{F}_{\tilde{\mathcal{L}}}^{\text{MHV}}$  is the parity conjugate of the form factor of the self-dual field strength with only positive-helicity gluons, which is given in equation (3.62), as expected.

### 3.3.5 Supersymmetric methods

Using the supersymmetric form factors derived in the previous section, it is possible to uplift the MHV rules in the component form to supersymmetric MHV rules. To do so,

$$\mathcal{F}^{\text{MHV}}(1, 2, \dots, n; q) = \frac{\delta^{(4)}(q - \sum_i \lambda_i \tilde{\lambda}_i) \delta^{(4)}(\sum_{i=1}^n \lambda_i \eta_{i,-})}{\langle 1 2 \rangle \langle 2 3 \rangle \cdots \langle n 1 \rangle} , \quad (3.80)$$

is continued off shell with the standard prescription (3.5) of [3], and used as a vertex in addition to the standard MHV vertices. Form factors have a single operator insertion, hence only diagrams with a single form factor MHV vertex are drawn.

The simplest example produces by supersymmetric MHV rules is the NMHV tree-level super form factor. It can be computed by summing over all diagrams in Figure 3.6(a), whose expression is

$$\begin{aligned}\mathcal{F}_{\text{NMHV}}^{(0)} &= \sum_{i=1}^n \sum_{j=i+1}^{i+n-2} \int d^4 P_{ij} \int d^4 \eta_P \mathcal{A}_{\text{MHV}}^{(0)}(i, \dots, j, P_{ij}) \frac{1}{P_{ij}^2} \mathcal{F}_{\text{MHV}}^{(0)}(j+1, \dots, i-1, -P_{ij}; q) \\ &= \mathcal{F}_{\text{MHV}}^{(0)} \sum_{i=1}^n \sum_{j=i+1}^{i+n-2} \frac{\langle i-1 \ i \rangle \langle j \ j+1 \rangle}{\langle i-1 \ P_{ij} \rangle \langle P_{ij} \ i \rangle \langle j \ P_{ij} \rangle \langle P_{ij} \ j+1 \rangle} \frac{1}{P_{ij}^2} \delta^{(4)} \left( \sum_{k=i}^j \langle P_{ij} \ k \rangle \eta_k^A \right) \end{aligned} \quad (3.81)$$

It has been also checked that the tree-level  $N^2$ MHV super form factor up to six points, obtained using supersymmetric MHV diagrams is independent of the reference spinor and the relevant components match the split-helicity result presented in Section 3.2.2.1.

As a final remark, it should be possible to prove the MHV vertex expansion at tree level through a procedure along the lines of [100], namely by using a BCFW recursion relation with an all-line shift and showing that this is identical to the MHV diagram expansion.

### 3.3.6 Supersymmetric recursion relations

The BCFW recursion relations [2, 76] of form factors [57] can be supersymmetrised in the spirit of [38, 101]. For supersymmetric recursions of the form factors considered here, it is suitable to work with an  $[i, j]$  shift,  $\tilde{\lambda}_i \rightarrow \tilde{\lambda}_i + z\tilde{\lambda}_j$ ,  $\lambda_j \rightarrow \lambda_j - z\lambda_i$ ,  $\eta_i \rightarrow \eta_i + z\eta_j$ . Factorisation requires that each term in the recursion relation must contain one form factor and one amplitude. Hence, for each kinematic channel it is necessary to sum over two diagrams, with the form factor appearing either on the left-hand or right-hand side, see Figure 3.5. The result one obtains by summing over these two classes of diagrams has the form

$$\begin{aligned}\mathcal{F}(0) &= \sum_{a,b} \int d^4 P d^4 \eta_P \mathcal{F}_L(z=z_{ab}) \frac{1}{P_{ab}^2} \mathcal{A}_R(z=z_{ab}) \\ &+ \sum_{c,d} \int d^4 P d^4 \eta_P \mathcal{A}_L(z=z_{cd}) \frac{1}{P_{cd}^2} \mathcal{F}_R(z=z_{cd}) .\end{aligned} \quad (3.82)$$

One point deserves a special attention, namely the large- $z$  behaviour of the form factor. Recall that in order to have a recursion relation without boundary terms it is necessary to have  $\mathcal{F}(\dots \hat{p}_i, \dots, \hat{p}_j, \dots) \rightarrow 0$  as  $z \rightarrow \infty$ . This important point is discussed in the following Section. In the form factors considered in this thesis there is no boundary contributions to the sum of the residues. However, in [62] it was observed that the

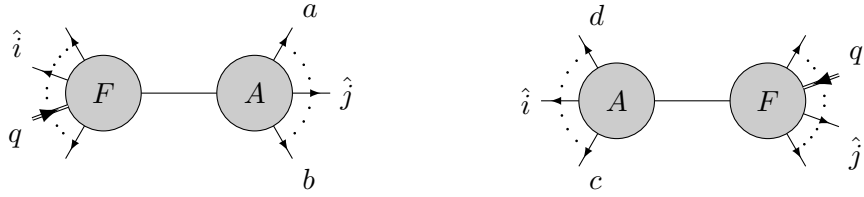


Figure 3.5: The two recursive diagrams discussed in the text.

recursion of form factors of  $\text{Tr}(\phi_{12}^k)$ ,  $k > 2$ , there is indeed a boundary term and it is related to the form factors with a lower  $k$ .

### 3.4 Vanishing of form factors at large $z$

#### 3.4.1 Bosonic form factors

In this Section, a generic non-MHV bosonic form factor of the operator  $\text{Tr}(\phi^2)$  is considered and it is proved that, for a  $[k, l]$  shift

$$\hat{\lambda}_k := \tilde{\lambda}_k + z\tilde{\lambda}_l, \quad \hat{\lambda}_l := \lambda_l - z\lambda_k, \quad (3.83)$$

$F(z)$  vanishes as  $z \rightarrow \infty$  if

$$(h_k, h_l) \text{ is equal to : } (0, +), (+, +), (-, +), (0, 0), (-, 0), (-, -). \quad (3.84)$$

The proof is based on the MHV diagram expansion of form factors, and follows closely that for amplitudes presented in [76].

To begin with, it is immediate to see that an MHV form factor (3.2) with a  $[k, l]$  shift vanishes as  $z \rightarrow \infty$ , with the only exception of the case  $(h_k, h_l) = (+, 0)$ . Consider now a generic non-MHV form factor. Each MHV diagram contributing to its expansion is a product of MHV vertices, times propagators  $1/L^2$ . These propagators will either be independent of  $z$ , or vanish when  $z \rightarrow \infty$ . As in [76], the spinors  $\lambda_L = L|\tilde{\xi}\rangle$  associated to internal legs can also be made  $z$ -independent by choosing the reference spinor  $\tilde{\xi}$  to be equal to  $\tilde{\xi} = \tilde{\lambda}_l$ . Thus, dangerous  $z$ -dependent terms can only arise from terms affected by the shifts in the external legs  $k$  and  $l$ .

For the cases where  $(h_k, h_l)$  is  $(\pm, +)$  or  $(0, +)$ , only the denominators acquire  $z$ -dependence, and hence  $F(z)$  vanishes at large  $z$ . By using anti-MHV diagrams one arrives at the same result for the case where  $(h_k, h_l)$  is equal to either  $(-, -)$  or  $(-, 0)$ .

The case  $(h_k, h_l) = (0, 0)$  needs special attention. The case when  $k$  and  $l$  belong to the same MHV vertex has already been considered, and leads to a falloff of the diagram as  $z \rightarrow \infty$ . When  $k$  and  $l$  belong to different vertices, there will be at least one propagator depending on  $z$ , which will provide a factor of  $1/z$  at large  $z$ . The vertex involving leg  $l$  behaves asymptotically as  $z^2/z^2$  regardless of whether it is an MHV form factor or a conventional MHV vertex, while all other vertices are independent of  $z$ . This proves that each MHV diagram falls off as  $1/z$  at large  $z$ .

The argument described above can also be applied to scattering amplitudes. Shifting two scalars makes the amplitude vanish as  $z \rightarrow \infty$  provided that the scalars take the same  $SU(4)$  indices.

### 3.4.2 Supersymmetric form factors

As it was shown in the previous Section, the bosonic form factor vanishes at infinity for an  $[i, j]$  shift if  $i$  and  $j$  are both scalars. The strategy of this section is to use supersymmetry to relate the large- $z$  behaviour of generic supersymmetric form factors to that of form factors with legs  $i$  and  $j$  being both scalars. This will then prove the validity of the supersymmetric BCFW recursion relation for all supersymmetric form factors in fashion similar to [101].

For supersymmetric non-chiral form factor  $F(\lambda, \tilde{\lambda}, \eta_+, \tilde{\eta}^-)$ , the  $[i, j]$  shift is

$$\begin{aligned} \hat{\tilde{\lambda}}_i(z) &:= \tilde{\lambda}_i + z\tilde{\lambda}_j, & \hat{\lambda}_j &:= \lambda_j - z\lambda_i, \\ \hat{\eta}_{i,+} &:= \eta_{i,+} + z\eta_{j,+}, & \hat{\tilde{\eta}}_j^- &:= \tilde{\eta}_j^- - z\tilde{\eta}_i^-. \end{aligned} \quad (3.85)$$

As in [101], a suitable transformation is where

$$\bar{Q}_{\tilde{\zeta}} = \tilde{\zeta}_{\dot{\alpha}+} \bar{Q}^{\dot{\alpha}+}, \quad Q_{\xi} = \xi_{\alpha-}^- Q_-^{\alpha}, \quad (3.86)$$

where

$$\tilde{\zeta} = \frac{1}{[i \ j]} \left( -\tilde{\lambda}_i \eta_j + \tilde{\lambda}_j \eta_i \right), \quad \xi = \frac{1}{\langle i \ j \rangle} \left( -\lambda_i \tilde{\eta}_j + \lambda_j \tilde{\eta}_i \right). \quad (3.87)$$

One can check that their action on the fermionic coordinates  $\eta_{k,+}, \tilde{\eta}_k^-$  is

$$e^{\bar{Q}_{\tilde{\zeta}}} \eta_{k,+} := \eta'_{k,+} = \eta_{k,+} - \eta_{i,+} \frac{[kj]}{[ij]} + \eta_{j,+} \frac{[ki]}{[ij]}, \quad (3.88)$$

$$e^{Q_{\xi}} \tilde{\eta}_k^- := \tilde{\eta}'_k^- = \tilde{\eta}_k^- - \tilde{\eta}_i^- \frac{\langle kj \rangle}{\langle ij \rangle} + \tilde{\eta}_j^- \frac{\langle ki \rangle}{\langle ij \rangle}, \quad (3.89)$$

and in particular  $e^{\bar{Q}_\zeta} \eta_{i,+} = e^{\bar{Q}_\zeta} \eta_{j,+} = e^{Q_\xi} \tilde{\eta}_i^- = e^{Q_\xi} \tilde{\eta}_j^- = 0$ . Since the form factor is invariant under  $\bar{Q}^+$  and  $Q_-$  transformations, i.e.  $e^{\bar{Q}_\zeta} \mathcal{F} = e^{Q_\xi} \mathcal{F} = \mathcal{F}$  (see (3.73)), one concludes that

$$\begin{aligned} & \mathcal{F}(\lambda_1, \tilde{\lambda}_1, \eta_{1,+}, \tilde{\eta}_1^-; \dots; \lambda_i, \hat{\tilde{\lambda}}_i, \hat{\eta}_{i,+}, \tilde{\eta}_i^-; \dots; \hat{\lambda}_j, \tilde{\lambda}_j, \eta_{j,+}, \hat{\tilde{\eta}}_j^-; \dots; \lambda_n, \tilde{\lambda}_n, \eta_{n,+}, \tilde{\eta}_n^-) \\ = & \mathcal{F}(\lambda_1, \tilde{\lambda}_1, \eta'_{1,+}, \tilde{\eta}'_1^-; \dots; \lambda_i, \hat{\tilde{\lambda}}_i, 0, 0; \dots; \hat{\lambda}_j, \tilde{\lambda}_j, 0, 0; \dots; \lambda_n, \tilde{\lambda}_n, \eta'_{n,+}, \tilde{\eta}'_n^-). \end{aligned} \quad (3.90)$$

Thus, one can always choose a supersymmetry transformation which sets  $i$  and  $j$  to be scalars. It is important to notice that under the  $[i, j]$  shift, the transformed  $\eta'_+$  and  $\tilde{\eta}'_-$  variables are independent of  $z$ . The large- $z$  behaviour of  $\mathcal{F}(z)$  is therefore the same as that of the bosonic form factor with  $i$  and  $j$  being scalars. This case was considered in the previous Section, and shown to fall off as  $1/z$  at large  $z$ . Hence the statement is also true for the shifted supersymmetric form factor  $\mathcal{F}(z)$ . The proof illustrated above concerned the large- $z$  behaviour of the full non-chiral super form factor, but a very similar one applies to the form factor in chiral superspace, since the latter is related to the former by a half-Fourier transform in superspace.

### 3.5 Loop-level

Also at loop level, the form factors of  $\text{Tr } \phi_{12} \phi_{12}$  in MSYM can be computed using very similar bootstrap procedures to those which are used to compute scattering amplitudes, such as unitarity cuts [57] and loop-level MHV diagrams [38]. Unitarity cuts are a particularly efficient method for deriving MHV component form factors with an arbitrary number of particles. Nevertheless, in this Section supersymmetric MHV rules are used to compute a one-loop MHV form factor as a demonstration of the methods developed in the preceding Sections.

Additionaly, one and two-loop results obtained from generalised unitarity [33, 57] are quoted. It has been verified in [33] that the two-loop three-particle form factor presented below exponentiates to a BDS-like form and admits the definition of a remainder function. This remainder has interesting connections to hexagonal Wilson loops in MSYM and Higgs boson amplitudes in QCD, which will be elaborated at the end of this Section.

### 3.5.1 One-loop

General one-loop form factors of the stress-tensor multiplet can be written as a super sum constructed from MHV vertices. As an example, consider the one-loop MHV super form factor. Following [102], this can be computed by summing over all diagrams in Figure 3.6(b), and is given by

$$\begin{aligned} \mathcal{F}_{\text{MHV}}^{(1)} &= \sum_{i=1}^n \sum_{j=i}^{i+n-1} \int \frac{d^D L_1}{L_1^2 + i\varepsilon} \frac{d^D L_2}{L_2^2 + i\varepsilon} \int d^4 \eta_{L_1} \int d^4 \eta_{L_2} \\ &\quad \mathcal{A}_{\text{MHV}}^{(0)}(i \dots, j, L_1, L_2) \mathcal{F}_{\text{MHV}}^{(0)}(-L_2, -L_1, j+1, \dots, i-1; q) . \end{aligned} \quad (3.91)$$

A simple yet illustrative application, in which the relation (3.91) can be used, is the Sudakov form factor of the operator  $\text{Tr}(\phi^{++}\phi^{++})$ . The emergence of the result obtained in [57], which involves only a scalar triangle integral can be presented very explicitly.



Figure 3.6: (a) *MHV diagram for a tree-level NMHV form factor.* (b) *MHV diagram for a one-loop MHV form factor.*

For this form factor, one simply has:

$$\mathcal{A}^{(0)}(1, 2, L_1, L_2) = \frac{\delta^{(4)}(p_1 + p_2 - L_1 - L_2) \delta^{(8)}(\lambda_1 \eta_1 + \lambda_2 \eta_2 + \lambda_{L_1} \eta_{L_1} + \lambda_{L_2} \eta_{L_2})}{\langle 12 \rangle \langle 2L_1 \rangle \langle L_1 L_2 \rangle \langle L_2 1 \rangle} \quad (3.92)$$

and

$$\mathcal{F}^{(0)}(L_1, L_2) = \frac{\delta^{(4)}(q + L_1 + L_2) \delta^{(4)}(\gamma^+ - \lambda_1 \eta_1^+ - \lambda_2 \eta_2^+)}{-\langle L_1 L_2 \rangle^2}, \quad (3.93)$$

where  $\gamma^+$  is the supermomentum carried by the operator of the form factor. To perform the integration over the fermionic coordinates

$$\int d^4 \eta_{L_1} d^4 \eta_{L_2} \delta^{(4)}(\gamma^+ - \lambda_{L_1} \eta_{L_1}^+ - \lambda_{L_2} \eta_{L_2}^+) \delta^{(8)}(\lambda_1 \eta_1 + \lambda_2 \eta_2 + \lambda_{L_1} \eta_{L_1} + \lambda_{L_2} \eta_{L_2}) \quad (3.94)$$

it is useful to change variables to the harmonic projections and write:

$$d^4 \eta_{L_1} d^4 \eta_{L_2} = d^2 \eta_{L_1}^+ d^2 \eta_{L_1}^- d^2 \eta_{L_2}^+ d^2 \eta_{L_2}^- \quad (3.95)$$

and

$$\begin{aligned} & \delta^{(8)}(\lambda_1\eta_1 + \lambda_2\eta_2 + \lambda_{L_1}\eta_{L_1} + \lambda_{L_2}\eta_{L_2}) \\ &= \delta^{(4)}\left(\lambda_1\eta_1^+ + \lambda_2\eta_2^+ + \lambda_{L_1}\eta_{L_1}^+ + \lambda_{L_2}\eta_{L_2}^+\right) \delta^{(4)}\left(\lambda_1\eta_1^- + \lambda_2\eta_2^- + \lambda_{L_1}\eta_{L_1}^- + \lambda_{L_2}\eta_{L_2}^-\right). \end{aligned} \quad (3.96)$$

Moreover, if one is interested with the form factor of  $\text{Tr}(\phi^{++}\phi^{++})$ , one has to pick out the  $\gamma^+$  component of the super form factor, which can also be obtained by setting  $\gamma^+ = 0$ . This simplifies the first delta function to  $\delta^{(4)}(\lambda_1\eta_1^+ - \lambda_2)$ . Then, under the support of this delta function it is possible to simplify the integral (3.94) to:

$$\begin{aligned} & \int d^4\eta_{L_1} d^4\eta_{L_2} \delta^{(4)}\left(\lambda_{L_1}\eta_{L_1}^+ - \lambda_{L_2}\eta_{L_2}^+\right) \\ & \quad \delta^{(4)}\left(\lambda_1\eta_1^+ + \lambda_2\eta_2^+\right) \delta^{(4)}\left(\lambda_1\eta_1^- + \lambda_2\eta_2^- + \lambda_{L_1}\eta_{L_1}^- + \lambda_{L_2}\eta_{L_2}^-\right) \end{aligned} \quad (3.97)$$

The  $\eta_{L_{1,2}}^-$  integrals pick the top component in the delta function containing these variables, with a Jacobian factor of  $\langle L_1 L_2 \rangle^2$ . The  $\eta_{L_{1,2}}^+$  integrals can also be performed in terms of a Jacobian to obtain:

$$\langle L_1 L_2 \rangle^2 \langle 12 \rangle^2 (\eta_1^+)^2 (\eta_2^+)^2, \quad (3.98)$$

which is the only non-vanishing component of  $\delta^{(4)}(\lambda_1\eta_1^+ + \lambda_2\eta_2^+)$ . This is compatible with the fact that one has to saturate the two scalars in the operator with at least two scalars in the multi-particle state to get a non-zero Sudakov form factor at tree level.

Plugging the result (3.98) of the fermionic integration (3.94) into the expression (3.91), one obtains the following integrand <sup>3</sup>:

$$2 \int \frac{d^D L_1}{L_1^2 + i\varepsilon} \frac{d^D L_2}{L_2^2 + i\varepsilon} \frac{\langle L_1 L_2 \rangle \langle 12 \rangle}{\langle 2L_1 \rangle \langle L_2 1 \rangle} \delta^{(4)}(L_1 + L_2 + p_1 + p_2), \quad (3.99)$$

where

$$|L_i\rangle = \frac{L_i|\tilde{\eta}\rangle}{[\tilde{L}_i\tilde{\eta}]}, \quad (3.100)$$

for an arbitrarily chosen reference spinor  $|\tilde{\eta}\rangle$  according to the CSW prescription [3]. The precise value of the spinor  $|\tilde{L}_i\rangle$  is irrelevant as the expressions obtained are neutral with respect to the rescalings of the spinor  $|L_i\rangle$  and the spinor product  $[\tilde{L}_i\tilde{\eta}]$  can be set to 1.

<sup>3</sup>the factor of 2 has been inserted manually like in [57] to match the definition of the 't Hooft coupling in the literature [39].

Setting  $|\tilde{\eta}| = |1|$ , using momentum conservation and integrating over  $L_1$  trivially due to the momentum-conserving delta function one obtains:

$$F^{(1)}(1_{\phi^{++}}, 2_{\phi^{++}}) = 2 \int d^D L_2 \frac{q^2}{L_2^2 (L_2 - p_1 - p_2)^2 (L_2 - p_1)^2}, \quad (3.101)$$

$$= 2 \quad \text{---} \diagup \diagdown \text{---}$$

where  $[1|L_2|1]$  was written as  $(L_2 - p_1)^2$  and the  $i\epsilon$  prescription of the propagators is assumed. This is precisely a one-mass triangle integral and reproduces the well-known result [58], which can also be obtained from unitarity cuts [57].

The form factor or the one-mass triangle integral depends only on a single scale,  $q^2$ , where  $q$  is the momentum of the leg shown with a double line. It is IR divergent with a  $1/\epsilon^2$  pole in dimensional regularisation and captures the IR divergences of one-loop amplitudes (box functions) in MSYM.

Higher-point one-loop MHV form factors are given as a combination of triangles and two-mass-easy box functions:

$$F^{(1)}(1, \dots, n; q) = F^{(0)}(1, \dots, n; q) \left[ - \sum_{l=1}^n \frac{(-s_{ll+1})^\epsilon}{\epsilon^2} + \sum_{a,b} \text{Fin}^{2\text{me}}(p_a, p_b, P, Q) \right], \quad (3.102)$$

where  $F^{(1)}$  is the tree-level MHV form factor and  $\text{Fin}^{2\text{me}}$  is the finite part of the two-mass-easy box functions<sup>4</sup>, which is what remains after the cancellations between the triangles and boxes. The sum over  $a, b$  represents all the ordered partitions of the momenta of the particles, which put  $p_a$  and  $p_b$  on the massless corners of the box function and  $P, Q$  are the sums of the momenta in between these. The IR divergences arise only from neighbouring momenta, as expected.

Supersymmetric generalised unitarity, as well as supersymmetric MHV rules, are easily applied to form factors. Consider for example a two-particle cut, depicted in Figure 3.7. On one side of the cut there is a tree-level form factor, on the other a tree scattering amplitude. For the case of a one-loop supersymmetric MHV form factor, the

<sup>4</sup>See for example [36] for their explicit form.

two-particle cut is equal to

$$\mathcal{F}_{\text{MHV}}^{(1)} \Big|_{s_{a+1,b-1}-\text{cut}} = \int d\text{LIPS}(l_1, l_2; P) \int d^4\eta_{l_1} \int d^4\eta_{l_2} \mathcal{F}_{\text{MHV}}^{(0)}(-l_2, -l_1, b, \dots, a; q) \mathcal{A}_{\text{MHV}}^{(0)}(l_1, l_2, (a+1) \dots, (b-1)) , \quad (3.103)$$

where the Lorentz-invariant phase-space measure is

$$d\text{LIPS}(l_1, l_2; P) := d^D l_1 d^D l_2 \delta^+(l_1^2) \delta^+(l_2^2) \delta^D(l_1 + l_2 + P) . \quad (3.104)$$

The sum over all possible states which can propagate in the loop is automatically

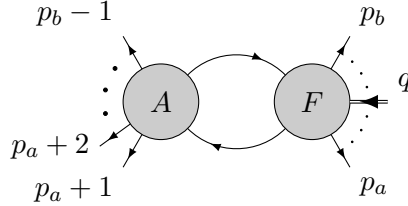


Figure 3.7: A two-particle cut diagram for a one-loop form factor.

performed by the fermionic integration. A simple calculation gives

$$\mathcal{F}_{\text{MHV}}^{(1)} \Big|_{s_{a+1,b-1}-\text{cut}} = \mathcal{F}_{\text{MHV}}^{(0)} \int d\text{LIPS}(l_1, l_2; P_{a+1,b-1}) \frac{\langle a a+1 \rangle \langle l_2 l_1 \rangle}{\langle a l_2 \rangle \langle l_2 a+1 \rangle} \frac{\langle b-1 b \rangle \langle l_1 l_2 \rangle}{\langle b-1 l_1 \rangle \langle l_1 b \rangle} , \quad (3.105)$$

which reproduces the result derived in [57] using component form factors and amplitudes.

### 3.5.2 Two loops

Two-loop form factors can be derived through generalised unitarity methods without major subtleties. Known results include two-loop Sudakov form factor of the half-BPS operator  $\text{Tr}(\phi_{12}\phi_{12})$  and the form factor with an additional gluon. They are given in terms of integrals that planar and non-planar, even in the large- $N_c$  limit. The reason for the non-planar integrals to appear in the leading  $N_c$  term is that the tree-level form factor is proportional to a delta function in colour space. Considering the unitarity cut with a tree-level form factor and a one-loop amplitude, including the sub-leading-in- $N_c$  corrections to the amplitude, it is easy to see that the delta function would form a colour loop with the sub-leading colour structures of the amplitude and enhance their order by  $N_c$ .

The result for the two-loop Sudakov form factor is known for a few decades [58]. It is

given by the combination:

$$F^{(2)}(1_{\phi_{12}}, 2_{\phi_{12}}; q) = 2 \left[ 4 \begin{array}{c} \text{Diagram 1} \\ + \\ \text{Diagram 2} \end{array} \right], \quad (3.106)$$

where the figures represent scalar integrals of the drawn topology. Their values are given below:

$$\begin{array}{c} \text{Diagram 1} \end{array} = (-q^2)^{-2\epsilon} \left[ \frac{1}{4\epsilon} + \frac{5\pi^2}{24\epsilon^2} + \frac{29}{6\epsilon}\zeta_3 + \frac{3}{32}\pi^4 + \mathcal{O}(\epsilon) \right] \quad (3.107)$$

$$\begin{array}{c} \text{Diagram 2} \end{array} = (-q^2)^{-2\epsilon} \left[ \frac{1}{\epsilon^4} - \frac{\pi^2}{\epsilon^2} - \frac{83}{3\epsilon}\zeta_3 - \frac{59}{120}\pi^4 + \mathcal{O}(\epsilon) \right]. \quad (3.108)$$

This result is of uniform transcendentality four and captures correctly the two-loop divergences of amplitudes.

Wheres it is a relatively simple exercise of generalised unitarity to derive the result (3.106), the two-loop form factor with a gluon in addition to the scalars, namely

$$\begin{aligned} g\delta(q - p_1 - p_2 - p_3) F^{(2)}(1_{\phi_{12}}, 2_{\phi_{12}}, 3^+) \\ = \int \frac{d^4x}{(2\pi)^4} e^{iq \cdot x} \langle 0 | \text{Tr}(\phi_{12}\phi_{12})(x) | \phi_{12}(p_1), \phi_{12}(p_2), g^+(p_3) \rangle, \end{aligned} \quad (3.109)$$

is much more involved. One has to consider considerable more unitarity cuts to nail down the integrands contributing to this form factor [33]. The result is given as a linear combination of integrals and evaluates to:

$$F^{(2)}(1_{\phi_{12}}, 2_{\phi_{12}}, 3^+) = F_{\text{BDS}}^{(2)}(1_{\phi_{12}}, 2_{\phi_{12}}, 3^+) + \mathcal{R}_3^{(2)}, \quad (3.110)$$

where  $F_{\text{BDS}}^{(2)}$  is the part that is predicted by the BDS-like exponentiation of the one-loop form factor and

$$\begin{aligned} \mathcal{R}_3^{(2)} = & -2 \left[ J_4 \left( -\frac{uv}{w} \right) + J_4 \left( -\frac{vw}{u} \right) + J_4 \left( -\frac{wu}{v} \right) \right] - 8 \sum_{i=1}^3 \left[ \text{Li}_4(1 - u_i^{-1}) + \frac{\log^4 u_i}{4!} \right], \\ & - 2 \left[ \sum_{i=1}^3 \text{Li}_2(1 - u_i^{-1}) \right]^2 + \frac{1}{2} \left[ \sum_{i=1}^3 \log^2 u_i \right]^2 - \frac{\log^4(uvw)}{4!} - \frac{23}{2}\zeta_4 \end{aligned} \quad (3.111)$$

with  $u = s_{12}/q^2$ ,  $v = s_{23}^2/q^2$  and  $w = p_{31}^2/q^2 = -s_{12}^2/q^2 - s_{23}^2/q^2$ . The function  $J_4$  is

defined as:

$$J_4(z) := \text{Li}_4(z) - \log(-z) \text{Li}_3(z) + \frac{\log^2(-z)}{2!} \text{Li}_2(z) - \frac{\log^3(-z)}{3!} \text{Li}_1(z) - \frac{\log^4(-z)}{48}. \quad (3.112)$$

The result (3.106), in particular the remainder function (3.111), can be computed analytically, as well as bootstrapped from its symbol by imposing symmetry and kinematical constraints on it. This result has multiple extremely interesting properties.

One of these was already mentioned in the Introduction. The two-loop form factor  $F^{(2)}(1_{\phi_{12}}, 2_{\phi_{12}}, 3^+)$  captures the maximally transcendental part of the QCD amplitude  $H \rightarrow ggg$ . The correspondence between the two quantities can be understood by recalling that the half-BPS operator  $\text{Tr}(\phi_{12}\phi_{12})$  sits in the same supersymmetry multiplet with  $\text{Tr } F^2$  and observing that computing this form factor is equivalent to computing the  $H \rightarrow ggg$  amplitude. Nevertheless, it the matching between the transcendental parts is an extremely intriguing phenomenon, which certainly deserves further attention.

The other curious property of the result (3.106), is that the remainder function  $\mathcal{R}_3^{(2)}$  has the same symbol as the light-like hexagonal Wilson loop remainder function in a particular limit [33]. The hexagon remainder function depends on three dual conformal cross ratios:

$$u_1 = \frac{x_{13}^2 x_{46}^2}{x_{14}^2 x_{36}^2} \quad u_2 = \frac{x_{24}^2 x_{51}^2}{x_{25}^2 x_{41}^2} \quad u_3 = \frac{x_{26}^2 x_{35}^2}{x_{36}^2 x_{25}^2}, \quad (3.113)$$

where  $x_{ij} = x_i - x_j$  and  $x_i$  are the coordinates of the vertices of the Wilson loop. Imposing the constraint  $u_3 = 1 - u_1 - u_2$  on the remainder function of this Wilson loop and identifying

$$u_1 \leftrightarrow u, \quad u_2 \leftrightarrow v, \quad u_3 \leftrightarrow w$$

yields the remainder function of the form factor  $F^{(2)}(1_{\phi_{12}}, 2_{\phi_{12}}, 3^+)$ .

This is a very non-trivial result since the normalised Mandelstam invariants of the form factor have nothing to do with the conformal cross ratios parameterising the Wilson loop remainder function. It would be very interesting to look for similar correspondences at higher loops and with a greater number of particles and investigate the underlying principles of this phenomenon.

# 4 Form factors in three dimensions

In this Chapter, the Sudakov form factor in ABJM theory is computed up to two loops. The form factor considered is constructed with a simple, biscalar BPS operator. This quantity has no UV divergences as the operator is protected, but it is IR divergent.

At one loop, the Sudakov form factor in ABJM is  $\mathcal{O}(\epsilon)$  in dimensional regularisation, compatible with the fact that the one-loop amplitudes are either  $\mathcal{O}(\epsilon)$  (for four particles) or finite (for more particles).

At two loops, the form factor is expressed in terms of a single *non-planar* integral. It has a  $1/\epsilon^2$  pole in dimensional regularisation, as expected, and the coefficient of this pole matches that of the IR-divergent parts of two-loop amplitudes in ABJM.

In addition, a discussion of pure functions in three dimensions is included. It was observed that upon imposing certain trivalent vertex cut conditions to integrals, such as the ones used in [55] to construct the four-point amplitude, the integrals become maximally transcendental. This observation is verified by considering other integrals, that do not contribute to the form factor. A basis of pure master integrals for this topology is also included in Appendix E.

## 4.1 BPS operators

Before considering their form factors, the simple BPS operators are derived in this Section. Very similar to MSYM, there exist a biscalar BPS operator in ABJM, which has the form

$$\mathcal{O} = \text{Tr}(\phi^I \bar{\phi}_J) \quad \text{with } I \neq J, \quad (4.1)$$

and is annihilated by half of the supersymmetry generators.

To see this, one can consider the SUSY variation of  $\mathcal{O}$ . Setting for example  $I = 1$  and  $J = 4$ , this expands to

$$\delta \text{Tr}(\phi^1 \bar{\phi}_4) = \text{Tr}(\delta \phi^1 \bar{\phi}_4 + \phi^1 \delta \bar{\phi}_4). \quad (4.2)$$

Following [103], one uses the transformations:

$$\delta\phi^I = i\omega^{IJ}\psi_J, \quad (4.3)$$

$$\delta\bar{\phi}_I = i\bar{\psi}^J\omega_{IJ}. \quad (4.4)$$

The  $\omega_{IJ}$ 's are given in terms of the  $(2+1)$ -dimensional Majorana spinors,  $\epsilon_i$  ( $i = 1, \dots, 6$ ) which are the supersymmetry generators:

$$\omega_{IJ} = \epsilon_i(\Gamma^i)_{IJ}, \quad (4.5)$$

$$\omega^{IJ} = \epsilon_i((\Gamma^i)^*)^{IJ}, \quad (4.6)$$

that are anti-symmetric in  $I, J$ . The  $4 \times 4$  matrices  $\Gamma^i$  are given by:

$$\Gamma^1 = \sigma_2 \otimes 1_2, \quad \Gamma^4 = -\sigma_1 \otimes \sigma_2, \quad (4.7)$$

$$\Gamma^2 = -i\sigma_2 \otimes \sigma_3, \quad \Gamma^5 = \sigma_3 \otimes \sigma_2, \quad (4.8)$$

$$\Gamma^3 = i\sigma_2 \otimes \sigma_1, \quad \Gamma^6 = -i1_2 \otimes \sigma_2, \quad (4.9)$$

and satisfy the following relations,

$$\left\{ \Gamma^i, \Gamma^{j\dagger} \right\} = 2\delta_{ij}, \quad (\Gamma^i)_{IJ} = -(\Gamma^i)_{IJ}, \quad (4.10)$$

$$\frac{1}{2}\epsilon^{IJKL}\Gamma^i_{KL} = -(\Gamma^{j\dagger})^{IJ} = ((\Gamma^i)^*)^{IJ}, \quad (4.11)$$

leading to

$$(\omega^{IJ})_\alpha = ((\omega_{IJ})^*)_\alpha, \quad \omega^{IJ} = \frac{1}{2}\epsilon^{IJKL}\omega_{KL}. \quad (4.12)$$

Explicitly,  $\omega_{IJ}$  is given by the following matrix:

$$\omega_{IJ} = \begin{pmatrix} 0 & -i\epsilon_5 - \epsilon_6 & -i\epsilon_1 - \epsilon_2 & \epsilon_3 + i\epsilon_4 \\ i\epsilon_5 + \epsilon_6 & 0 & \epsilon_3 - i\epsilon_4 & -i\epsilon_1 + \epsilon_2 \\ i\epsilon_1 + \epsilon_2 & -\epsilon_3 + i\epsilon_4 & 0 & i\epsilon_5 - \epsilon_6 \\ -\epsilon_3 - i\epsilon_4 & i\epsilon_1 - \epsilon_2 & -i\epsilon_5 + \epsilon_6 & 0 \end{pmatrix}. \quad (4.13)$$

The term  $\phi^1\delta\bar{\phi}_4$  yields

$$\phi^1\delta\bar{\phi}_4 = \phi^1 [-\bar{\psi}^1(\epsilon_3 + i\epsilon_4) + i\bar{\psi}^2(\epsilon_1 + i\epsilon_2) - i\bar{\psi}^3(\epsilon_5 + i\epsilon_6) + 0]. \quad (4.14)$$

Therefore, requiring  $\phi^1 \delta \bar{\phi}_4 = 0$  the conditions are:

$$\begin{aligned}\epsilon_1 + i\epsilon_2 &= 0, \\ \epsilon_3 + i\epsilon_4 &= 0, \\ \epsilon_5 + i\epsilon_6 &= 0,\end{aligned}\tag{4.15}$$

which relate half of the generators with the other half by constraining the components  $\omega_{4J} = 0$ .

Note that because of the relations (4.12) which set components of the form  $\omega_{4L}$  to zero, the entries  $\omega^{IJ}$  with  $I, J \in (1, 2, 3)$  automatically vanish implying that  $\delta\phi^I = 0 \iff I \in (1, 2, 3)$ . This procedure may be iterated to show that generally the operators  $\text{Tr}(\bar{\phi}_I \phi^J)$  for  $I \neq J$  are indeed half-BPS. In the present work the operators under consideration are of the type

$$\mathcal{O} = \text{Tr}(\phi^A \bar{\phi}_4),\tag{4.16}$$

where  $A \neq 4$ .

## 4.2 Sudakov form factor at loop level

In this section the Sudakov form factor of BPS operators presented in the previous Section is derived at one loop and at two loops. Similar to the Sudakov form factor in MSYM which is reviewed in Section 3.5, the object considered here capture the IR divergences of scattering amplitudes in ABJM theory. Moreover, since they are constructed with a half-BPS operator, they are free of UV divergences.

More precisely the objects of interest are the colour-ordered functions  $F(q^2)$ , defined in the following way.

$$\langle (\bar{\phi}_A)_{i_1}^{\bar{i}_1}(p_1) (\phi^4)_{i_2}^{i_2}(p_2) | \text{Tr}(\bar{\phi}_A \phi^4)(0) | 0 \rangle := [1, 2] F(q^2),\tag{4.17}$$

The colour-ordered form factors are normalised to unity at tree level:

$$F^{(0)}(q^2) = 1.\tag{4.18}$$

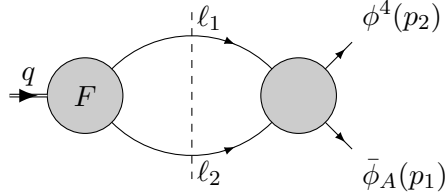


Figure 4.1: The  $q^2$  cut of the Sudakov form factor. Note that the amplitude on the right-hand side of the cut is summed over all possible colour orderings.

### 4.2.1 One-loop Sudakov form factor in ABJM

At one loop it is possible to determine the integrand of the form factor from a single unitarity cut in the  $q^2$  channel. As shown in Figure 4.1, on one side of the cut there is the Sudakov form factor and on the other side the complete four-point amplitude, both at tree level. The colour-ordered tree amplitude is given in (2.72). Let us work out the colour factor first. It is given by

$$\delta_{i_{\ell_1}}^{\bar{i}_{\ell_2}} \delta_{i_{\ell_2}}^{\bar{i}_{\ell_1}} (\delta_{i_2}^{\bar{i}_1} \delta_{i_{\ell_1}}^{i_2} \delta_{i_{\ell_2}}^{\bar{i}_{\ell_1}} \delta_{i_1}^{i_{\ell_2}} - \delta_{i_{\ell_2}}^{\bar{i}_1} \delta_{i_1}^{i_2} \delta_{i_2}^{\bar{i}_{\ell_1}} \delta_{i_{\ell_1}}^{i_{\ell_2}}) = (N' - N) \delta_{i_2}^{\bar{i}_1} \delta_{i_1}^{i_2}. \quad (4.19)$$

Obviously, the one-loop form factor vanishes identically in ABJM theory, because in this case  $N' = N$ .

We now consider the kinematic part. Since the operator is built solely out of scalars, only the four-point scalar amplitude can appear in the cut. To match the particles of the tree amplitude in Figure 4.1, we pick the  $(\eta_1)^1 (\eta_{\ell_1})^3 (\eta_{\ell_2})^2 (\eta_2)^0$  component from the  $\delta^6(Q)$  to write the  $q^2$  cut of the one-loop form factor as:

$$\frac{\delta^{(6)}(Q)|_{(\eta_1)^1 (\eta_{\ell_1})^3 (\eta_{\ell_2})^2 (\eta_2)^0}}{\langle 1 2 \rangle \langle 2 \ell_1 \rangle} = \frac{\langle \ell_1 \ell_2 \rangle^2 \langle 1 \ell_1 \rangle}{\langle 1 2 \rangle \langle 2 \ell_1 \rangle} = \frac{\langle 1 2 \rangle \langle 1 \ell_1 \rangle}{\langle 2 \ell_1 \rangle} = -\frac{\text{Tr}(\ell_1 p_1 p_2)}{2(\ell_1 \cdot p_2)}, \quad (4.20)$$

which can be immediately lifted to a full integral as it is the only possible cut of the form factor. Thus we get,

$$F^{(1)}(q^2) = (N' - N) \int \frac{d^D \ell_1}{i\pi^{D/2}} \frac{\text{Tr}(\ell_1 p_1 p_2)}{\ell_1^2 (\ell_1 - p_2)^2 (\ell_1 - p_1 - p_2)^2}. \quad (4.21)$$

The integral in (4.21) is a linear triangle and is of  $\mathcal{O}(\epsilon)$ . Hence, we conclude that the one-loop Sudakov form factor in ABJ theory vanishes in strictly three dimensions. Moreover, the three-dimensional integrand vanishes in ABJM theory but is non-vanishing for  $N \neq N'$  and can (and does) participate in unitarity cuts at two loops in ABJ theory. Note, that the vanishing of the one-loop form factors in ABJ(M) is consistent with the

infrared finiteness of one-loop amplitudes in ABJ(M).

### 4.2.2 Two-loop Sudakov form factor in ABJM

Next, we come to the computation of the two-loop Sudakov form factor. In order to construct an ansatz for its integrand we will make use of two-particle cuts, and fix potential remaining ambiguities with various three-particle cuts described in detail in Sections 4.2.2.2 and 4.2.2.3.

Three-particle cuts are very useful because they receive contributions from planar as well as non-planar integral functions at the same time, and thus are particularly constraining. A special feature of ABJM theory is that all amplitudes with an odd number of external particles vanish and, as a consequence, all cuts involving such amplitudes are identically zero [55]. In our case this observation will be important for triple cuts, where three- and five-particle amplitudes would appear.

A particular type of such cuts, first considered in [55] in the context of loop amplitudes in ABJM, involves three adjacent cut loop momenta meeting at a three-point vertex. The vanishing of these cuts imposes strong constraints on the form of the loop integrands. We will discuss and exploit this later in this section, where we will also make the intriguing observation that integral functions with numerators satisfying such constraints are transcendental and free of certain unwanted infrared divergences.

#### 4.2.2.1 Two-particle cuts

We begin by considering the cut shown in Figure 4.2, which contains a tree-level Sudakov form factor merged with the integrand of the complete one-loop, four-point amplitude. The internal particle assignment is fixed and is determined by the particular operator we consider. The integrand of this cut is schematically given by

$$F^{(0)}(\bar{\ell}_2, \ell_1)[\ell_2, \ell_1] \tilde{\mathcal{A}}^{(1)}(\bar{\phi}_A(p_1), \phi^4(p_2), \bar{\phi}_4(-\ell_1), \phi^A(-\ell_2)) , \quad (4.22)$$

where we picked the relevant component amplitude of the complete one-loop amplitude  $\tilde{\mathcal{A}}^{(1)}$ , given in (2.86), and we recall that the colour factor  $[a, b]$  is defined in (2.89).

We begin by working out the colour structures that will appear in the result. Firstly we consider the planar amplitude (2.87) and combine it with the part of the non-planar amplitude (2.88) containing  $I(1, 2, -\ell_1, -\ell_2)$ . Intriguingly, by contracting this with the

tree-level form factor (given in (4.17) and (4.18)) we obtain a vanishing result:

$$\left( N([1, 2, \ell_1, \ell_2] + [1, \ell_2, \ell_1, 2]) - 2[1, 2][\ell_1, \ell_2] \right) [\ell_2, \ell_1] = 0. \quad (4.23)$$

We now consider the remaining contributions arising from the non-planar one-loop amplitude (2.88). There are two possible colour contractions to consider,

$$c_{\text{NP}}^{(1)} := 2[1, 2][\ell_1, \ell_2][\ell_2, \ell_1] = 2N^2[1, 2], \quad (4.24)$$

and

$$c_{\text{NP}}^{(2)} := 2[\ell_1, 2][1, \ell_2][\ell_2, \ell_1] = 2[1, 2]. \quad (4.25)$$

Note that (4.25) is sub-leading in the large  $N$  limit, and can be discarded in the large- $N$  limit. Moreover, the corresponding coefficient actually vanishes which implies that the two-loop form factor does not have non-planar corrections.

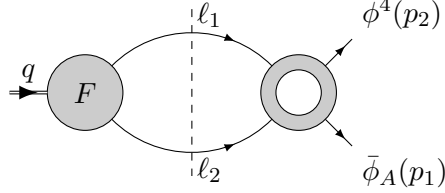


Figure 4.2: *Tree-level form factor glued to the complete one-loop amplitude.*

We now need to determine the coefficient of  $c_{\text{NP}}^{(1)}$ . On the two-particle cut  $\ell_1^2 = \ell_2^2 = 0$  its integrand is given by the appropriate component tree-level amplitude (4.20) times a particular box integral (2.88):

$$\mathcal{C}_1^{(\text{NP})}|_{s-\text{cut}} := \frac{1}{2} \frac{\langle 12 \rangle \langle 1\ell_1 \rangle}{\langle 2\ell_1 \rangle} I(-\ell_2, 2, -\ell_1, 1) + \ell_1 \leftrightarrow \ell_2. \quad (4.26)$$

Recall that we have to symmetrise in order to include all particle species in the sum over intermediate on-shell states. Since  $I(-\ell_2, 2, -\ell_1, 1)$  is anti-symmetric under  $\ell_1 \leftrightarrow \ell_2$  the complete cut-integrand can be written as<sup>1</sup>

$$\begin{aligned} \mathcal{C}_1^{(\text{NP})}|_{s-\text{cut}} &:= \frac{1}{2} \left( \frac{\langle 12 \rangle \langle 1\ell_1 \rangle}{\langle 2\ell_1 \rangle} - \frac{\langle 12 \rangle \langle 1\ell_2 \rangle}{\langle 2\ell_2 \rangle} \right) I(-\ell_2, 2, -\ell_1, 1) \\ &= -\frac{1}{2} \int \frac{d^D \ell_3}{i\pi^{D/2}} \frac{q^2 [\text{Tr}(p_1 p_2 \ell_1 \ell_3) - q^2 \ell_3^2]}{\ell_3^2 (\ell_1 - \ell_3)^2 (p_1 - \ell_3)^2 (\ell_3 - \ell_1 + p_2)^2}. \end{aligned} \quad (4.27)$$

<sup>1</sup>Similarly as done earlier for the complete one-loop amplitude, we include a factor of 1/2 in the symmetrisation.

Summarising, the two-particle cut indicates that the two-loop form factor is expressed in terms of a single crossed triangle with a particular numerator, represented in Figure 4.3,

$$\mathbf{XT}(q^2) = \int \frac{d^D \ell_1 d^D \ell_3}{(i\pi^{D/2})^2} \frac{q^2 [\text{Tr}(p_1 p_2 \ell_1 \ell_3) - q^2 \ell_3^2]}{\ell_1^2 \ell_2^2 \ell_3^2 (\ell_1 - \ell_3)^2 (p_1 - \ell_3)^2 (\ell_3 - \ell_1 + p_2)^2}, \quad (4.28)$$

so that

$$\mathcal{C}_1^{(\text{NP})} = -\frac{1}{2} \mathbf{XT}(q^2). \quad (4.29)$$

For future convenience we will define

$$\mathbf{xt} := \frac{q^2 [\text{Tr}(p_1 p_2 \ell_1 \ell_3) - q^2 \ell_3^2]}{\ell_1^2 \ell_2^2 \ell_3^2 (\ell_1 - \ell_3)^2 (p_1 - \ell_3)^2 (\ell_3 - \ell_1 + p_2)^2}. \quad (4.30)$$

The result of the evaluation of  $\mathbf{XT}(q^2)$  is quoted in (4.39) and shows that this quantity has maximal degree of transcendentality. Before evaluating  $\mathbf{XT}(q^2)$ , we use triple cuts in order to confirm the correctness of the ansatz obtained from two-particle cuts.

#### 4.2.2.2 Three-vertex cuts

To confirm the uplift of the two-particle cut to the integral (4.28), we will study additional cuts. We begin by considering three-point vertex cuts involving three adjacent legs meeting at a three-point vertex. These cuts were first examined in [55], where it was observed that they must vanish since there are no three-particle amplitudes in ABJM theory. Calling  $k_1$ ,  $k_2$  and  $k_3$  the momenta meeting at the vertex, we have

$$k_1 + k_2 + k_3 = 0, \quad k_1^2 = k_2^2 = k_3^2 = 0. \quad (4.31)$$

The conditions (4.31) imply that all spinors associated to these momenta are proportional, thus

$$\langle k_1 k_2 \rangle = \langle k_2 k_3 \rangle = \langle k_3 k_1 \rangle = 0. \quad (4.32)$$

As an example consider the three-point vertex cut of  $\mathbf{XT}(q^2)$  with momenta  $\ell_2$ ,  $\ell_4$  and  $\ell_6 := \ell_2 - \ell_4$  (see Figure 4.3 for the labelling of the momenta). Importantly, the form factor is expected to vanish as the three momenta belonging to a three-point vertex become null. By rewriting the numerator of (4.28) using only cut momenta, it is immediately seen that it vanishes, since

$$\begin{aligned} \text{Tr}[p_1 p_2 (p_1 - \ell_2)(p_1 - \ell_6)] - q^2 (p_1 - \ell_6)^2 &= -\text{Tr}[p_1 p_2 (p_1 - \ell_2) \ell_6] - q^2 (p_1 - \ell_6)^2 \\ &= -\text{Tr}(p_1 p_2 p_1 \ell_6) + 4(p_1 \cdot p_2)(p_1 \cdot \ell_6) = 0, \end{aligned} \quad (4.33)$$

where we have used  $\langle \ell_2 \ell_6 \rangle = 0$  to set  $\text{Tr}(p_1 p_2 \ell_2 \ell_6) = 0$ . It is easy to see that all other three-vertex cuts of the integral (4.28) vanish in a similar fashion because of the particular form of its numerator.

Important consequences of these specific properties of the numerator of the integral function (4.28) are that the result is transcendental as we will show below and is free of unphysical infrared divergences related to internal three-point vertices. These divergences appear generically in three-dimensional two-loop integrals with internal three-vertices even if the external kinematics is massive (unlike in four dimensions) and it appears that master integrals with appropriate numerators to cancel these peculiar infrared divergences are a preferred basis for amplitudes and form factors in ABJM. Related discussions in the context of ABJM amplitudes have appeared in [55, 104]. Note that for form factors we do not have dual conformal symmetry, which gives further constraints on the structure of the numerators of integral functions appearing in amplitudes.

#### 4.2.2.3 Three-particle cuts

The remaining cut we will study is a triple cut of the type illustrated in Figure 4.4. These cuts may potentially detect additional integral functions which have no two-particle cuts at all, and are thus very important. Moreover, such cuts are sensitive to both planar and non-planar topologies. In this triple cut, a tree-level amplitude is connected to a tree-level form factor by three cut propagators. Due to the vanishing of amplitudes with an odd number of external legs in the ABJM theory, the triple cut in question vanishes. We will now check that the triple cut of the two-loop crossed triangle **XT** of (4.28), which we have detected using two-particle cuts, is indeed equal to zero.

To this end, we note that there are two possible ways to perform a triple-cut on **XT**, shown in Figures 4.5a and 4.5b. The cut loop momenta are called  $\ell_2$ ,  $\ell_5$  and  $\ell_3$  and satisfy

$$\ell_2 + \ell_5 + \ell_3 = p_1 + p_2, \quad \ell_2^2 = \ell_5^2 = \ell_3^2 = 0. \quad (4.34)$$

We observe that these two cuts cannot be converted into one another by a simple relabelling of the cut momenta because of the non-trivial numerators. The A-cut depicted in Figure 4.5a of the non-planar integrand is:

$$\mathbf{XT}|_{3\text{-p cut A}} = -q^2 \frac{\langle 1 2 \rangle}{\langle \ell_3 \ell_5 \rangle \langle \ell_5 2 \rangle \langle 1 \ell_3 \rangle}. \quad (4.35)$$

After a similar calculation, the  $B$ -cut of this integral, depicted in Figure 4.5b, turns out to be identical to the  $A$ -cut:

$$\mathbf{XT}|_{3\text{-p cut } B} = \mathbf{XT}|_{3\text{-p cut } A} = -q^2 \frac{\langle 1 2 \rangle}{\langle \ell_3 \ell_5 \rangle \langle \ell_5 2 \rangle \langle 1 \ell_3 \rangle} . \quad (4.36)$$

A quick way to establish the vanishing of the triple cuts consists in symmetrising in the particle momenta  $p_1$  and  $p_2$ , which is allowed since the Sudakov form factor is a function of  $q^2$ . This symmetrisation gives

$$- \frac{q^2 \langle 1 2 \rangle}{\langle \ell_3 \ell_5 \rangle} \left[ \frac{1}{\langle \ell_5 2 \rangle \langle 1 \ell_3 \rangle} - \frac{1}{\langle \ell_5 1 \rangle \langle 2 \ell_3 \rangle} \right] = - \frac{q^4}{\langle 1 | \ell_5 | 2 \rangle \langle 1 | \ell_3 | 2 \rangle} . \quad (4.37)$$

This expression is symmetric in  $\ell_5$  and  $\ell_3$ . In evaluating the triple cut one has to introduce a Jacobian proportional to  $\epsilon(\ell_2, \ell_3, \ell_5)$  [55] which effectively makes this triple cut vanish upon integration. This implies that the complete answer for the two-loop form factor in ABJM is proportional  $\mathbf{XT}(q^2)$  and no additional integral functions have to be introduced.

#### 4.2.2.4 Results and comparison to the two-loop amplitudes

Combining the information from the unitarity cuts discussed above, we conclude that the two-loop Sudakov form factor in ABJM is given by a single non-planar integral

$$F_{\text{ABJM}}(q^2) = -2 \left( \frac{N}{k} \right)^2 \left( -\frac{1}{2} \right) \mathbf{XT}(q^2) , \quad (4.38)$$

where  $\mathbf{XT}(q^2)$  is defined in (4.28) and we have reintroduced the dependence on the Chern-Simons level  $k$ . The integral  $\mathbf{XT}(q^2)$  can be computed by reduction to master integrals using integration by parts identities. The details of the reductions are provided in Appendix E. The expansion of the result in the dimensional regularisation parameter  $\epsilon$  can then be found using the expressions for the the master integrals (E.18)–(E.21). Plugging these masters into the reduction (E.15), we arrive at

$$\mathbf{XT}(q^2) = \left( \frac{-q^2 e^{\gamma_E}}{\mu^2} \right)^{-2\epsilon} \left[ \frac{\pi}{\epsilon^2} + \frac{2\pi \log 2}{\epsilon} - 4\pi \log^2 2 - \frac{2\pi^3}{3} + \mathcal{O}(\epsilon) \right] , \quad (4.39)$$

where  $\gamma_E$  is the Euler-Mascheroni constant. One comment is in order here. We have derived (4.39) in a normalisation where the the loop integration measure is written as  $d^D \ell (i\pi^{D/2})$ . This should be converted to the standard one  $d^D \ell (2\pi)^D$ . At two loops, this implies that (4.39) has to be multiplied by a factor of  $-1/(4\pi)^D$ . The result in the

standard normalisation is then

$$\mathcal{F}_{\text{ABJM}}(q^2) = -\frac{1}{(4\pi)^3} \left(\frac{N}{k}\right)^2 \left(\frac{-q^2 e^{\gamma_E}}{4\pi\mu^2}\right)^{-2\epsilon} \left[ \frac{\pi}{\epsilon^2} + \frac{2\pi \log 2}{\epsilon} - 4\pi \log^2 2 - \frac{2\pi^3}{3} + \mathcal{O}(\epsilon) \right]. \quad (4.40)$$

We note that  $\mathcal{F}(q^2)$  can be expressed more compactly by introducing a new scale

$$\mu'^2 := 8\pi e^{-\gamma_E} \mu^2, \quad (4.41)$$

in terms of which we get

$$\mathcal{F}_{\text{ABJM}}(q^2) = \frac{1}{64\pi^2} \left(\frac{N}{k}\right)^2 \left(\frac{-q^2}{\mu'^2}\right)^{-2\epsilon} \left[ -\frac{1}{\epsilon^2} + 6\log^2 2 + \frac{2\pi^2}{3} + \mathcal{O}(\epsilon) \right], \quad (4.42)$$

which is our final result.

We now discuss two consistency checks that confirm the correctness of (4.42). Firstly, we recall that the Sudakov form factor captures the infrared divergences of scattering amplitudes. We now check that (4.42) matches the infrared poles of the four-point amplitude evaluated in [87, 105]. Here we quote its expression as given in [105]:

$$\mathcal{A}_4^{(2)} = -\frac{1}{16\pi^2} \mathcal{A}_4^{(0)} \left[ \frac{(-s/\mu'^2)^{-2\epsilon}}{4\epsilon^2} + \frac{(-t/\mu'^2)^{-2\epsilon}}{4\epsilon^2} - \frac{1}{2} \log^2 \left(\frac{-s}{-t}\right) - 4\zeta_2 - 3\log^2 2 \right], \quad (4.43)$$

where  $\mu'$  is related to  $\mu$  in the same way as in (4.41). Hence, the Sudakov form factor (4.42) is in perfect agreement with the form of the infrared divergences of (4.43). Secondly, we have also checked that the expansion of our result in terms of master integrals (i.e. the expansion of the two-loop non-planar triangle **XT** defined in (4.28)) is identical to that obtained from the Feynman diagram based result of [106]. This implies that the cut-based calculation of this paper and the Feynman diagram calculation of [106] agree to all orders in  $\epsilon$  – even though we have been using cuts in strictly three dimensions.

### 4.3 Pure functions in three dimensions

As discussed in Section 4.2.2.2, the integrand **xt** that appears in the Sudakov form factor in ABJM has a particular numerator such that all the cuts which isolate a three-point vertex vanish. We have observed in this example that this property ensures that the integral **XT** has a uniform (and maximal) degree of transcendentality – failure to obey the triple-cut condition, for instance by altering the form of the numerator, would

result in the appearance of new terms with lower degree of transcendentality. In this section we present further integrals that vanish in these three-particle cuts and have maximal degree of transcendentality. These integrals are expected to appear in the form factor of ABJ theory where cancellations between colour factors such as that in (4.23), do not occur.

We begin by considering the following planar integral function:

$$\begin{aligned} \text{LT}(q^2) &= \int \frac{d^D \ell_1 d^D \ell_3}{(i\pi^{D/2})^2} \frac{-q^2 [\text{Tr}(p_1 \ell_3 p_2 \ell_1) - (\ell_1 - p_1)^2 (\ell_3 - p_2)^2]}{\ell_1^2 (p_1 + p_2 - \ell_1)^2 \ell_3^2 (p_1 + p_2 - \ell_3)^2 (\ell_1 - \ell_3)^2 (\ell_3 - p_2)^2} \quad (4.44) \\ &= \left( \frac{-q^2 e^{\gamma_E}}{\mu^2} \right)^{-2\epsilon} \left[ -\frac{\pi}{4\epsilon^2} - \frac{\pi \log 2}{\epsilon} + 2\pi \log^2 2 - \frac{5\pi^3}{8} + \mathcal{O}(\epsilon) \right], \end{aligned}$$

which is shown in Figure 4.6a. It is easy to see that the three vertex cut  $\{\ell_1, \ell_3, \ell_5\}$  vanishes, since on this cut the numerator can be placed in the form

$$\langle \ell_1 1 \rangle \langle \ell_3 2 \rangle \langle 1 2 \rangle \langle \ell_3 \ell_1 \rangle, \quad (4.45)$$

after using a Schouten identity. (4.45) vanishes because  $\langle \ell_3 \ell_1 \rangle = 0$  on this cut.

A further property of (4.44) emerges when we consider particular triple cuts involving two adjacent massless legs, which in three dimensions are associated with soft gluon exchange [55]. With reference to Figure 4.6a, we cut the three momenta  $\ell_3$ ,  $\ell_6$  and  $\ell_4$ . The cut conditions  $\ell_3^2 = \ell_6^2 = \ell_4^2 = 0$  together with the masslessness of  $p_1$  and  $p_2$  can only be satisfied if  $\ell_6$  becomes soft, that is

$$\ell_6 \rightarrow 0, \quad \ell_4 \rightarrow p_1, \quad \ell_3 \rightarrow p_2. \quad (4.46)$$

In this limit, the second term of (4.44) vanishes since  $\ell_3 - p_2 = \ell_6 \rightarrow 0$ . The first term becomes

$$-q^2 \frac{\text{Tr}(p_1 \ell_3 p_2 \ell_1)}{8\epsilon(\ell_3, p_1, p_2)} \rightarrow -q^2 \frac{\langle 2 | \ell_1 | 1 \rangle}{4\langle 12 \rangle}, \quad (4.47)$$

where  $8\epsilon(\ell_3, p_1, p_2)$  is the Jacobian.<sup>2</sup> After restoring the remaining propagators we are left with

$$\frac{2\epsilon(\ell_1, p_1, p_2)}{\ell_1^2 (\ell_1 - p_2)^2 (q - \ell_1)^2}, \quad (4.48)$$

which reproduces the one-loop integrand of the one-loop form factor, given earlier in

---

<sup>2</sup>This Jacobian arises from re-writing the  $\delta$ -functions of the cut momenta,  $\ell_3^2 = \ell_4^2 = \ell_6^2 = 0$ , in terms of  $p_1, p_2$  and  $\ell_6$ .

(4.21).

Other examples of integrals with different topologies that satisfy the three-particle cut condition are depicted in Figures 4.6b and 4.6c. The definitions of the integrals as well as their values are listed below:

$$\begin{aligned} \mathbf{CT}(q^2) &= \int \frac{d^D \ell_1 d^D \ell_3}{(i\pi^{D/2})^2} \frac{\text{Tr}(p_1, p_2, \ell_3, \ell_1)}{\ell_1^2 (p_1 + p_2 - \ell_1)^2 \ell_3^2 (\ell_1 - \ell_3)^2 (\ell_3 - p_2)^2} \quad (4.49) \\ &= \left( \frac{-q^2 e^{\gamma_E}}{\mu^2} \right)^{-2\epsilon} \left[ -\frac{\pi}{4\epsilon^2} + \frac{7\pi^3}{24} + \mathcal{O}(\epsilon) \right], \end{aligned}$$

$$\begin{aligned} \mathbf{FAN}(q^2) &= \int \frac{d^D \ell_1 d^D \ell_3}{(i\pi^{D/2})^2} \frac{\text{Tr}(p_1, p_2, \ell_3, \ell_1)}{\ell_1^2 \ell_3^2 (p_1 + p_2 - \ell_1 - \ell_3)^2 (\ell_1 - p_1)^2 (\ell_3 - p_2)^2} \quad (4.50) \\ &= \left( \frac{-q^2 e^{\gamma_E}}{\mu^2} \right)^{-2\epsilon} \left[ -\frac{\pi}{4\epsilon^2} + \frac{7\pi^3}{24} + \mathcal{O}(\epsilon) \right]. \end{aligned}$$

Note that the  $\epsilon$  expansion of (4.49) and (4.50) agree up to  $\mathcal{O}(1)$ . It is simple to show that these integrals satisfy the properties discussed earlier, for example by setting  $\{\ell_1, \ell_3, \ell_5\}$  on shell in **CT** and  $\{\ell_1, p_1, \ell_5\}$  in **FAN** and similarly for all other possible three-vertex cuts.

The reductions of the integrals considered in this section in terms of scalar master integrals through IBP identities can be found in Appendix E.

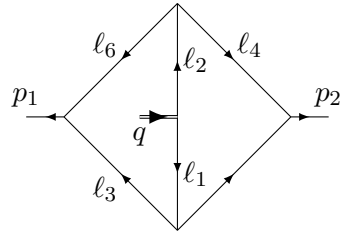


Figure 4.3: The crossed triangle integral arising from gluing a tree form factor with the complete one-loop four-point amplitude. The arrow in the middle denotes the location where the momentum  $q = p_1 + p_2$  is injected. We call these integrals ‘‘crossed triangles’’ because they have the topology of the master integral (E.21). Note however that the latter integral is non-transcendental, while the particular numerator in (4.28) makes this integral transcendental.

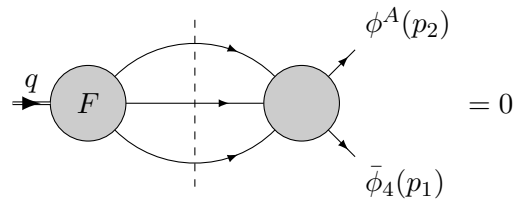


Figure 4.4: The (vanishing) three-particle cut of the two-loop Sudakov form factor.

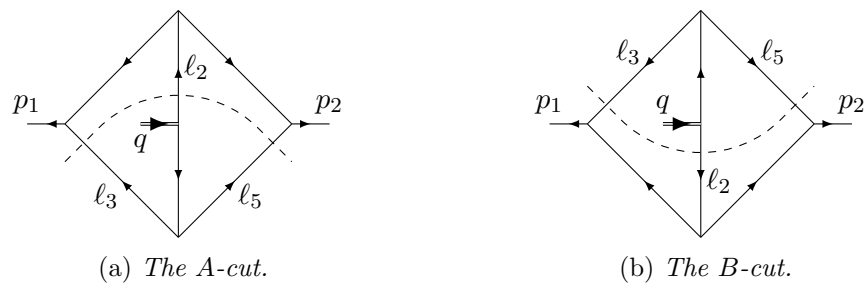


Figure 4.5: The two triple cuts of the crossed triangle, with  $\ell_2 + \ell_3 + \ell_5 = q$ . In the second figure we have relabelled the loop momenta in order to merge the two contributions.

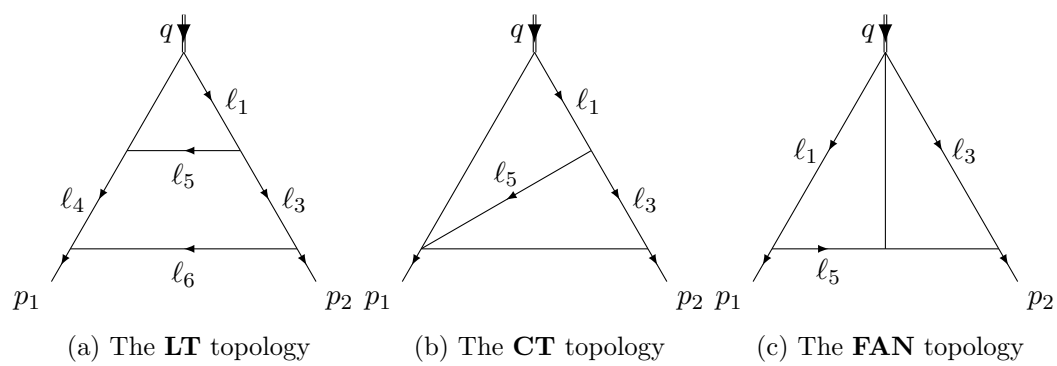


Figure 4.6: *The three maximally transcendental integrals considered in (4.44), (4.49) and (4.50).*

# 5 Conclusion

In this work, the tree and loop-level form factors in MSYM and ABJM theories using bootstrap methods have been presented. In particular, recursion relations have been applied to construct all split-helicity form factors of the protected bi-scalar operator  $\text{Tr } \phi_{12}\phi_{12}$  in MSYM. It has been demonstrated with examples how form factors can be computed as an MHV-diagram expansion. Furthermore, supermultiplets of form factors have been constructed which involve the supersymmetrisation of the operator  $\text{Tr } \phi_{12}\phi_{12}$  as well as the supersymmetrisation of external multi-particle state. In ABJM theory, the two-loop Sudakov form factor of the bi-scalar operator has been computed analytically. As an ingredient of this computation, the sub-leading colour dependence of one-loop four-particle superamplitudes has been derived.

Thanks to the factorisation properties of form factors, the bootstrap methods work the same way as they do for scattering amplitudes. The main theme in adopting these methods to form factors is to augment the set of elementary vertices to include an elementary form factor vertex. In the MHV diagrams technique, this is done by including all tree-level MHV form factors in the recursion. For BCFW-type recursion, the higher-point form factors factorise into a simple form factor and a scattering amplitude.

The construction of all-loop integrands using on-shell diagrams such as in [29] rely only on the factorisation properties of scattering amplitudes. Considering that the form factors have the same properties, it would be very interesting to see if the addition of a simple trivalent vertex to the on-shell diagrams of [29] could generate all-loop form factors or the integrands thereof from an integral over a Grassmannian.

On the other hand, there are essential differences between form factors and scattering amplitudes. The most important of these is the apparent absence of dual conformal symmetry. Therefore, the advantages that the dual conformal symmetry brings to the computation of scattering amplitudes in MSYM are not there for form factors. In particular, when applying generalised unitarity, non-dual-conformal-invariant integrals have to be considered. This can be seen from the triangle and non-planar integrals contributing to the loop-level form factors included in Section 3.5.

The results presented in this thesis can be carried further on to several natural directions. Form factors with more particles, higher MHV degree and more loops are very interesting challenges. In particular, it would be very nice to extend the two loop result for form factor of the half-BPS operator to three and perhaps to four loops due to a very curious observation about the two-loop form factor of  $\text{Tr } \phi_{12}\phi_{12}$  with two scalars and a gluon in MSYM. This form factor depends on the following variables, namely  $u = s_{12}/q^2$ ,  $v = s_{23}/q^2$  and  $w = s_{31}/q^2$ , where  $s_{ij} = (p_i + p_j)^2$  and  $q$  is the momentum carried by the operator, as usual. Obviously momentum conservation relates the three to each other:  $u + v + w = 1$ .

It turns out that the remainder function of the two-loop correction to the light-like hexagonal Wilson loop expectation value [47] matches this form factor, when the the variables  $u_{1,2,3}$  that parameterise the Wilson loop are taken such that they satisfy  $u_1 + u_2 + u_3 = 1$ . This is a highly surprising phenomenon as the variables  $u_{1,2,3}$  are the dual conformal cross ratios and have no relation to the Mandelstam invariants of the form factor. This hints a non-trivial principle that constrains the seemingly unrelated quantities in this theory. It would be very interesting to see whether such a relationship exists between other form factors and higher-point Wilson loops in MSYM.

With the higher-loop results for the form factor, it would be possible to check whether this relation extends to higher loops. In the case where a match is observed, an very interesting problem would be to investigate the underlying principles of this phenomenon.

In MSYM, integrability is being exploited in an increasingly powerful way. It has been possible to compute tree-level scattering amplitudes through mapping the problem to spin chain. These constructions rely on the Yangian symmetry, which includes dual conformal symmetry - a feature the form factors are lacking. Nevertheless it needs to be understood how powerful the predictions can be made form factors through integrability.

There are some open questions left from the analysis of the integrals that contribute to the Sudakov form factor ABJM, considered in Chapter 4 and Appendix E. It is known that pure integrals such as the ones considered here satisfy simplified differential equations [107]. It unclear how the analysis made here through trivalent unitarity cuts relates to the differential equations satisfied by pure integrals. Moreover, it could be interesting to construct bases of pure master integrals for more complicated topologies and attempt to relate these constructions to higher (four) dimensional master integrals.

To conclude, form factors in superconformal gauge theories in three and four dimensions, in particular MSYM and ABJM are special objects, as the scattering amplitudes

in these theories. They share many properties such as the existence of simple MHV form factors, maximal transcendentality principle to name a couple. Modern methods such as recursion relation and MHV diagrams can be used to compute them very efficiently. Although the computations in this thesis and relevant work [33, 57, 59–62, 106, 108–110] have verified much of this, there is a large room for further explorations of similarities and differences between form factors and scattering amplitudes.

# A Spinor/helicity in four dimensions

Lorentz vectors, which transform under the fundamental representation of the  $SO(3,1)$  Lorentz transformations, can be written as  $SL(2, \mathbb{C})$  matrices through the group homomorphism<sup>1</sup>:

$$SO(3,1) \rightarrow SL(2, \mathbb{C}). \quad (A.1)$$

The map between the linear spaces on which the groups act is done by the  $\sigma$ -matrices:

$$x^\mu \mapsto x_{\alpha\dot{\alpha}} = \sigma_{\mu, \alpha\dot{\alpha}} x_\mu, \quad \sigma^\mu = \left\{ \begin{pmatrix} 1 & 0 \\ 0 & 1 \end{pmatrix}, \begin{pmatrix} 0 & 1 \\ 1 & 0 \end{pmatrix}, \begin{pmatrix} 0 & -i \\ i & 0 \end{pmatrix}, \begin{pmatrix} 1 & 0 \\ 0 & -1 \end{pmatrix} \right\} \quad (A.2)$$

$x_{\alpha\dot{\alpha}}$  transforms in the  $(\frac{1}{2}, \frac{1}{2})$  representation of  $SL(2, \mathbb{C})$ ,

$$x^\mu \mapsto \Lambda^\mu_\nu x^\nu \quad \Leftrightarrow \quad x_{\alpha\dot{\alpha}} \mapsto N(\Lambda)_\alpha^\beta x_{\beta\dot{\beta}} N(\Lambda)^{* \dot{\beta}} \quad (A.3)$$

therefore it carries indices  $\alpha = 1, 2$  and  $\dot{\alpha} = 1, 2$ . The norm of a Lorentz vector is given by the determinant which is preserved by  $SL(2, \mathbb{C})$  transformations.

For massless vectors the determinant of  $x_{\alpha\dot{\alpha}}$  is zero. That is  $x_{\alpha\dot{\alpha}}$  has rank at most one and it can be written in the following form:

$$x_{\alpha\dot{\alpha}} = \lambda_\alpha \tilde{\lambda}_{\dot{\alpha}}, \quad \lambda, \tilde{\lambda} \in \mathbb{C}^2 \quad (A.4)$$

$\lambda_\alpha$  transform under the fundamental  $(\frac{1}{2}, 0)$  while  $\tilde{\lambda}_{\dot{\alpha}}$  transform under the anti-fundamental  $(0, \frac{1}{2})$  representations of  $SL(2, \mathbb{C})$ . The former are called left handed Weyl spinors and the latter are called right handed spinors. The fundamental and anti-fundamental representations are complex conjugates of each other. This restricts  $\lambda$  and  $\tilde{\lambda}$  in (A.4) so that they are the complex conjugates of each other. Therefore the only freedom in the decomposition (A.4) is the unitary re-scaling:

$$\lambda \rightarrow e^{i\theta} \lambda, \quad \tilde{\lambda} \rightarrow e^{-i\theta} \tilde{\lambda} \quad (A.5)$$

---

<sup>1</sup>The isomorphism is:  $SO(3,1) \cong SL(2, \mathbb{C})/\mathbb{Z}_2$

For the complex Minkowski space-time the homomorphism (A.1) takes the following form:

$$\mathrm{SO}(3, 1; \mathbb{C}) \rightarrow \mathrm{SL}(2, \mathbb{C}) \times \mathrm{SL}(2, \mathbb{C}). \quad (\mathrm{A}.6)$$

Therefore a  $2 \times 2$  complex matrix corresponding to complex Lorentz vector transforms by the left and right actions of two *independent* linear matrices.

$$x^\mu \mapsto \Lambda^\mu{}_\nu x^\nu, \quad \Lambda \in \mathrm{SO}(3, 1; \mathbb{C}) \quad \Leftrightarrow \quad x_{\alpha\dot{\alpha}} \mapsto N(\Lambda)_{\alpha}{}^{\beta} x_{\beta\dot{\alpha}} M(\Lambda)^{*}{}^{\dot{\beta}}{}_{\dot{\alpha}}, \quad (\mathrm{A}.7)$$

where  $(N, M) \in \mathrm{SL}(2, \mathbb{C}) \times \mathrm{SL}(2, \mathbb{C})$ . As a result, the spinors that correspond to massless complex Lorentz vectors are independent whereas they are the complex conjugates of each other in the real case.

The decomposition (A.4) is valid also for null complex vectors with the only difference being that  $\lambda$  and  $\tilde{\lambda}$  are independent of each other. For complex vectors, there is more freedom in the definition of the corresponding vectors. Namely, one is allowed to do the following re scaling of the spinors

$$\lambda \rightarrow t\lambda \quad \tilde{\lambda} \rightarrow \frac{1}{t}\tilde{\lambda} \quad (\mathrm{A}.8)$$

which leave the momentum  $p^\mu = \sigma_{\mu, \alpha\dot{\alpha}}$  invariant.

By Lorentz symmetry the scattering amplitudes have to be functions of the following spinor products:

$$\langle ij \rangle = \epsilon^{\alpha\beta} \lambda_{i, \alpha} \lambda_{j, \beta} \quad [ij] = \epsilon^{\dot{\alpha}\dot{\beta}} \tilde{\lambda}_{i, \dot{\alpha}} \tilde{\lambda}_{j, \dot{\beta}} \quad (\mathrm{A}.9)$$

where  $\lambda_i$  and  $\tilde{\lambda}_i$  are the spinors associated with the momentum of the particle labelled with  $i$ ,  $p_i$ . The brackets are co-bvariant under the transformations (A.8) and so is the amplitude. In essence, the weight  $h_i$  of the particle  $i$  under these transformation, which is given by

$$\hat{h} = \frac{1}{2} \left( \tilde{\lambda}_{i\dot{\alpha}} \frac{\partial}{\partial \tilde{\lambda}_{i\dot{\alpha}}} - \lambda_i^\alpha \frac{\partial}{\partial \lambda_i^\alpha} \right) \quad (\mathrm{A}.10)$$

is the helicity of the particle  $i$ . This way of writing scattering amplitudes, and other quantities that depend on the helicity of the particles, avoids polarisation vectors and thus eliminates the redundancy in the definition thereof.

There are various identities that are useful for computations in the spinor helicity formalism. One raises and lowers the spinor indices with the anti-symmetric tensor:

$$\lambda^\alpha = \epsilon^{\alpha\beta} \lambda_\beta, \quad \tilde{\lambda}^{\dot{\alpha}} = \epsilon^{\dot{\alpha}\dot{\beta}} \tilde{\lambda}_{\dot{\beta}} \quad (\mathrm{A}.11)$$

The  $\sigma$ -matrices with upper spinor indices are defined as:

$$\bar{\sigma}_\mu^{\dot{\alpha}\alpha} = \epsilon^{\alpha\beta} \epsilon^{\dot{\alpha}\dot{\beta}} \sigma_{\mu,\beta\dot{\beta}}. \quad (\text{A.12})$$

The Clifford algebra of the  $\gamma$ -matrices is realised at the level of Weyl spinors with  $\sigma$  and  $\bar{\sigma}$  matrices:

$$\{\sigma_{\alpha\dot{\alpha}}^\mu, \bar{\sigma}^{\nu,\dot{\alpha}\beta}\} = 2\delta_\alpha^\beta \eta^{\mu\nu} \quad \{\bar{\sigma}^{\mu,\dot{\alpha}\alpha}, \sigma_{,\alpha\dot{\beta}}^\nu\} = 2\delta_{\dot{\alpha}}^{\dot{\beta}} \eta^{\mu\nu} \quad (\text{A.13})$$

Lorentz vectors are converted to bi-spinors via equation (A.2) and bi-spinors are converted into Lorentz vectors by:

$$p^\mu = \frac{1}{2} \text{Tr} \left( p_{\alpha\dot{\alpha}} \bar{\sigma}^{\mu\dot{\alpha}\beta} \right). \quad (\text{A.14})$$

The dot product of two massless Lorentz vectors can be written in terms of spinor brackets:

$$2p_i \cdot p_j = \langle ij \rangle [ji]. \quad (\text{A.15})$$

Moreover, an important identity that is satisfied by the spinor brackets is the Schouten identity:

$$\langle ij \rangle \lambda_k + \langle ki \rangle \lambda_j + \langle jk \rangle \lambda_i = 0 \quad \text{or} \quad [ij]\tilde{\lambda}_k + [ki]\tilde{\lambda}_j + [jk]\tilde{\lambda}_i = 0, \quad (\text{A.16})$$

which is a consequence of the fact that spinors live in  $\mathbb{C}^2$  and every third spinor is a linear combination of two linearly independent vectors.

# B Spinor/helicity in three dimensions

The spinor-helicity formalism in three dimensions is similar to four dimensions. As the homomorphism between the vector and spinor representations of the three-dimensional spacetime is just

$$\mathrm{SO}(2, 1) \rightarrow \mathrm{SL}(2; \mathbb{C}), \quad (\mathrm{B}.1)$$

there is only one type of spinors to encode the kinematical data of on-shell processes in 2+1 dimensions. To map the vectors in the  $(+, -, -)$  signature, which has been used throughout this thesis, to the elements of the corresponding Clifford algebra, one can use the following set of real matrices:

$$\sigma_{\alpha\beta}^\mu = \begin{pmatrix} 1 & 0 \\ 0 & 1 \end{pmatrix}, \quad \begin{pmatrix} 0 & 1 \\ 1 & 0 \end{pmatrix}, \quad \begin{pmatrix} 1 & 0 \\ 0 & -1 \end{pmatrix}. \quad (\mathrm{B}.2)$$

In this basis a vector  $p^\mu(p^0, p^1, p^2)$  is mapped to the matrix

$$p_{\alpha\beta} = \sigma_{\alpha\beta}^\mu p_\mu = \begin{pmatrix} p^0 - p^2 & -p^1 \\ p^1 & p^0 + p^2 \end{pmatrix}. \quad (\mathrm{B}.3)$$

The determinant of such a matrix is equal to the norm of the vector, and similar to the case in four dimensions, the constraint  $p^2 = 0$  can be solved by writing  $p_{\alpha\beta}$  as a bi-spinor:

$$p_{\alpha\beta} = \lambda_\alpha \lambda_\beta, \quad (\mathrm{B}.4)$$

where  $\lambda_\alpha$  is a two-component complex vector. The spinor  $\lambda_\alpha$  corresponding to a null vector  $p^\mu$  is not unique and the spinor  $-\lambda_{\alpha\beta}$  would describe the same vector.

It can be seen that spinors with real components correspond to positive energy vectors, whereas purely imaginary spinors correspond to negative energy ones. In the “all-outgoing” convention for scattering processes, the former would correspond to physically outgoing particles whereas the latter would correspond to incoming particles.

The Lorentz invariant quantities can be constructed by contracting the spinors with the 2 dimensional Levi-Civita symbol  $\epsilon^{\alpha\beta}$ , where the convention  $\epsilon_{12} = 1$  has been used. The most basic quantity is the spinor bracket  $\langle ij \rangle$  made out of two spinors  $\lambda_i$  and  $\lambda_j$ ,

and it is defined as

$$\langle ij \rangle = \epsilon_{\alpha\beta} \lambda^\alpha \lambda^\beta. \quad (\text{B.5})$$

Other invariants constructed from on-shell momenta can be written in terms of the spinor bracket. For instance the Mandelstam invariant of two particles in a scattering process is simply

$$(p_i + p_j)^2 = \langle ij \rangle^2. \quad (\text{B.6})$$

Another invariant that can be constructed in three dimensions is the contraction of the three-dimensional Levi-Civita symbol with three vectors. This can be written as:

$$\epsilon_{\mu\nu\rho} p_i^\mu p_j^\nu p_k^\rho = \frac{1}{2} \text{Tr}(\sigma_\mu \sigma_\nu \sigma_\rho) p_i^\mu p_j^\nu p_k^\rho. \quad (\text{B.7})$$

It appears often in the integrands of one-loop amplitudes and form factors and in this thesis it is commonly abbreviated as  $\epsilon(i, j, k)$ . If the vectors are null, then the invariant factorises as:

$$\epsilon(i, j, k) = \frac{1}{2} \langle ij \rangle \langle jk \rangle \langle ki \rangle. \quad (\text{B.8})$$

. Because the spinors of odd-dimensional spaces have no chirality, the concept of MHV degree does not exist in the ABJ(M) theories. In fact, all the amplitudes in ABJM theory come with particle anti-particle pairs of matter and they have the simplicity of a helicity *non-violating* amplitude, where there are equal numbers of particles of either helicity.

# C Symmetry generators in MSYM

For completeness, the representation of generators of the superconformal algebra and the dual superconformal algebra in which they act on on-shell quantities such as scattering amplitudes, are quoted in this Appendix.

In a notation very close to the one used in [37], where the dual symmetry generators first have been written down, the realisation of the superconformal algebra  $\mathfrak{psu}(2, 2|4)$  as superspace transformations is as follows:

Translations:

$$p_{\alpha\dot{\alpha}} = \sum_i \lambda_i{}_\alpha \tilde{\lambda}_i{}^{\dot{\alpha}} \quad (\text{C.1a})$$

Lorentz transformations:

$$m_{\alpha\beta} = \sum_i \lambda_i{}_{(\alpha} \frac{\partial}{\partial \lambda_i{}^{\beta)}}, \quad (\text{C.1b})$$

$$m_{\dot{\alpha}\dot{\beta}} = \sum_i \tilde{\lambda}_i{}_{(\dot{\alpha}} \frac{\partial}{\partial \tilde{\lambda}_i{}^{\dot{\beta)}} \quad (\text{C.1c})$$

Special conformal transformations:

$$k_{\alpha\dot{\alpha}} = \sum_i \frac{\partial}{\partial \lambda_i^\alpha} \frac{\partial}{\partial \tilde{\lambda}_i^{\dot{\alpha}}} \quad (\text{C.1d})$$

Dilatations:

$$d = \sum_i \left[ \frac{1}{2} \lambda_i^\alpha \frac{\partial}{\partial \lambda_i^\alpha} - \frac{1}{2} \tilde{\lambda}_i{}_{\dot{\alpha}} \frac{\partial}{\partial \tilde{\lambda}_i{}^{\dot{\alpha}}} + 2 \right] \quad (\text{C.1e})$$

Superconformal boosts:

$$s_A^\alpha = \sum_i \frac{\partial}{\partial \lambda_{i\alpha}} \frac{\partial}{\partial \eta_i^A} \quad (\text{C.1f})$$

$$\bar{s}_{\dot{\alpha}}^A = \sum_i \eta^{iA} \frac{\partial}{\partial \tilde{\lambda}_{i\dot{\alpha}}} \quad (\text{C.1g})$$

Supersymmetry:

$$q_\alpha^A = \sum_i \lambda_{i\alpha} \eta_i^A \quad (\text{C.1h})$$

$$\bar{q}_{A\dot{\alpha}} = \sum_i \tilde{\lambda}_{i\dot{\alpha}} \frac{\partial}{\partial \eta_i^A} \quad (\text{C.1i})$$

R symmetry:

$$r_B^A = \sum_i \left[ \eta_i^A \frac{\partial}{\partial \eta_i^B} - \frac{1}{4} \eta_i^C \frac{\partial}{\partial \eta_i^C} \right] \quad (\text{C.1j})$$

In addition to these, there is a set of “dual” generators that realise another, independent representation of  $\mathcal{N} = 4$  superconformal algebra. They are the superconformal algebra acting on the variables  $x_i$  and  $\theta_i$ , in addition to the ordinary on shell space made out of  $\lambda, \tilde{\lambda}, \eta$ . The superamplitudes are supported on the hyperspace defined by [37]:

$$\lambda_i \tilde{\lambda}_i = x_i - x_{i+1}, \quad \lambda_i^\alpha \eta_i^A = \theta_i^{A\alpha} - \theta_{i+1}^{A\alpha} \quad (\text{C.2})$$

Again, in a notation closely following that of [37] the dual superconformal generators are:

Dual supersymmetry:

$$Q_{\alpha A} = \sum_i \frac{\partial}{\partial \theta_{i\alpha}^A} \quad (\text{C.3a})$$

$$\bar{Q}_\alpha^A = \sum_i \left( \theta_i^{\alpha A} \frac{\partial}{\partial x^{i\dot{\alpha}\alpha}} + \eta_i^A \frac{\partial}{\partial \tilde{\lambda}^{i\dot{\alpha}}} \right) \quad (\text{C.3b})$$

Dual Lorentz transformations:

$$M_{\alpha\beta} = \sum_i \left( x_{i(\alpha\dot{\alpha}} \frac{\partial}{\partial x_{i\dot{\alpha}}^{\beta)}} + \theta_{i\alpha}^A \frac{\partial}{\partial \theta_i^{\beta A}} + \lambda_i^{(\alpha} \frac{\partial}{\partial \lambda_i^{\beta)}} \right) \quad (\text{C.3c})$$

$$\bar{M}_{\dot{\alpha}\dot{\beta}} = \sum_i \left( x_{i,(\dot{\alpha}}^\alpha \frac{\partial}{\partial x_i^{\dot{\beta}\alpha)} + \tilde{\lambda}_{i,(\dot{\alpha}} \frac{\partial}{\partial \tilde{\lambda}_i^{\dot{\beta})}} \right) \quad (\text{C.3d})$$

Dual R-transformations:

$$R^A_B = \sum_i \left( \theta_i^{\alpha A} \frac{\partial}{\partial \theta^{\alpha B}} + \eta_i^A \frac{\partial}{\partial \eta^i B} - \frac{1}{4} \delta_B^A \theta_i^{\alpha C} \frac{\partial}{\partial \theta^i \alpha C} - \frac{1}{4} \eta_i^C \frac{\partial}{\partial \eta^i C} \right) \quad (\text{C.3e})$$

Dual dilatations:

$$D = \sum_i \left( x_i^{\alpha\dot{\alpha}} \frac{\partial}{\partial x_i^{\alpha\dot{\alpha}}} + \frac{1}{2} \theta_i^{\alpha A} \frac{\partial}{\partial \theta_i^{\alpha A}} + \frac{1}{2} \lambda_i^\alpha \frac{\partial}{\partial \lambda_i^\alpha} + \frac{1}{2} \tilde{\lambda}_i^{\dot{\alpha}} \frac{\partial}{\partial \tilde{\lambda}_i^{\dot{\alpha}}} \right) \quad (\text{C.3f})$$

Central charge / Helicity:

$$C = \sum_i \frac{1}{2} \left( \lambda_i^\alpha \frac{\partial}{\partial \lambda_i^\alpha} - \tilde{\lambda}_i^{\dot{\alpha}} \frac{\partial}{\partial \tilde{\lambda}_i^{\dot{\alpha}}} - \eta_i^A \frac{\partial}{\partial \eta_i^A} \right) \quad (\text{C.3g})$$

Dual superconformal transformations:

$$S_\alpha^A = \sum_i \left( \theta_{i\alpha}^B \theta_i^{\beta A} \frac{\partial}{\partial \theta_i^{\beta B}} - x_{i\alpha}^{\dot{\beta}} \theta_i^{\beta A} \frac{\partial}{\partial x_i^{\beta\dot{\beta}}} - \lambda_{i\alpha} \theta_i^{\gamma A} \frac{\partial}{\partial \lambda_i^\gamma} - x_{i+1,\alpha}^{\dot{\beta}} \eta_i^A \frac{\partial}{\partial \tilde{\lambda}_i^{\dot{\beta}}} + \theta_{i+1,\alpha}^B \eta_i^A \frac{\partial}{\partial \eta_i^B} \right) \quad (\text{C.3h})$$

$$\bar{S}_{\dot{\alpha} A} = \sum_i \left( x_{i\dot{\alpha}}^\beta \frac{\partial}{\partial \theta_i^{\beta A}} + \tilde{\lambda}_{i\dot{\alpha}} \frac{\partial}{\partial \eta_i^A} \right) \quad (\text{C.3i})$$

Dual conformal boosts:

$$K_{\alpha\dot{\alpha}} = \sum_i \left( x_{i\alpha}^{\dot{\beta}} x_{i\dot{\alpha}}^\beta \frac{\partial}{\partial x_i^{\beta\dot{\beta}}} + x_{i\dot{\alpha}}^\beta \theta_{i\alpha}^B \frac{\partial}{\partial \theta_i^{\beta B}} + x_{i+1,\alpha}^{\dot{\beta}} x_{i\dot{\alpha}}^\beta \frac{\partial}{\partial x_i^{\beta\dot{\beta}}} + \tilde{\lambda}_{i\dot{\alpha}} \theta_{i+1,\alpha}^B \frac{\partial}{\partial \eta_i^B} \right) \quad (\text{C.3j})$$

The ordinary superconformal generators together with the dual superconformal generators give rise to the Yangian of the superconformal algebra [48], which is an infinite-dimensional algebra. The generators of this algebra are labelled with “levels”, where the ordinary superconformal generators belong to level 0 and dual superconformal generators belong to level 1.

# D Non-MHV form factors

In this Appendix some results from the MHV diagram expansion of form factors are included for comparison with the results of split-helicity recursion relations and the supersymmetric methods of Chapter 3. In particular, the explicit and rather long expressions for the  $N^2$ MHV bosonic form factors with five and six particles are presented.

As the MHV-diagram method requires, their expressions apparently depend on an auxiliary spinor,  $|\xi]$ . However it has numerically been checked that the  $|\xi]$  dependence cancels in the entire expression.

The first example is the NMHV form factor with three gluons  $F(1_{\phi_{12}}, 2_{\phi_{12}}, 3^-, 4^+, 5^+)$ . The sum of all MHV diagrams contributing to this form factor is equal to:

$$\begin{aligned}
F(1_{\phi_{12}}, 2_{\phi_{12}}, 3^-, 4^+, 5^+) = & - \frac{\langle 1|4\rangle^2 \langle 2|3\rangle \langle 3|2|\xi] (\langle 4|1|\xi] + \langle 4|5|\xi])}{s_{23} s_{45} \langle 1|5\rangle \langle 4|5\rangle (\langle 1|4|\xi] + \langle 1|5|\xi]) \langle 2|3|\xi]} \\
& - \frac{\langle 1|3\rangle^2 (\langle 3|1|\xi] + \langle 3|4|\xi] + \langle 3|5|\xi]) \langle 4|5|\xi]^3}{s_{45} s_{345} \langle 4|5\rangle (\langle 1|4|\xi] + \langle 1|5|\xi]) (\langle 1|3|\xi] + \langle 1|4|\xi] + \langle 1|5|\xi]) (\langle 3|4|\xi] + \langle 3|5|\xi]) \langle 5|4|\xi]} \\
& - \frac{\langle 3|4\rangle^3 (\langle 1|2|\xi] + \langle 1|3|\xi] + \langle 1|4|\xi]) (-[\xi|3|2|\xi] - [\xi|4|2|\xi])}{s_{34} s_{234} \langle 1|5\rangle \langle 3|4|\xi] \langle 4|3|\xi] (\langle 5|2|\xi] + \langle 5|3|\xi] + \langle 5|4|\xi])} \\
& + \frac{\langle 2|3\rangle (\langle 1|2|\xi] + \langle 1|3|\xi] + \langle 1|4|\xi]) \langle 3|2|\xi] (\langle 4|2|\xi] + \langle 4|3|\xi])^2}{s_{23} s_{234} \langle 1|5\rangle \langle 2|3|\xi] (\langle 5|2|\xi] + \langle 5|3|\xi] + \langle 5|4|\xi]) ([\xi|4|2|\xi] + [\xi|4|3|\xi])} \\
& - \frac{\langle 3|4\rangle^3 (-[\xi|3|1|\xi] - [\xi|4|1|\xi] - [\xi|5|1|\xi])}{s_{345} s_{345} \langle 4|5\rangle (\langle 3|4|\xi] + \langle 3|5|\xi]) (\langle 5|3|\xi] + \langle 5|4|\xi])} \\
& + \frac{\langle 3|4\rangle^3 (-[\xi|3|2|\xi] - [\xi|4|2|\xi] - [\xi|5|2|\xi])}{s_{345} s_{2345} \langle 4|5\rangle (\langle 3|4|\xi] + \langle 3|5|\xi]) (\langle 5|3|\xi] + \langle 5|4|\xi])} \\
& + \frac{\langle 1|2\rangle (\langle 3|4|\xi] + \langle 3|5|\xi])^2 \langle 4|5|\xi]^3}{s_{45} s_{345} \langle 4|5\rangle (\langle 1|3|\xi] + \langle 1|4|\xi] + \langle 1|5|\xi]) (\langle 2|3|\xi] + \langle 2|4|\xi] + \langle 2|5|\xi]) \langle 5|4|\xi] (-[\xi|4|3|\xi] - [\xi|5|3|\xi])} \\
& - \frac{\langle 1|4\rangle^2 (\langle 3|1|\xi] + \langle 3|4|\xi] + \langle 3|5|\xi])^2 (\langle 4|1|\xi] + \langle 4|5|\xi])}{s_{45} s_{345} \langle 1|5\rangle \langle 4|5\rangle (\langle 1|4|\xi] + \langle 1|5|\xi]) ([\xi|3|1|\xi] - [\xi|4|3|\xi] - [\xi|5|3|\xi])}
\end{aligned}$$

$$\begin{aligned}
& + \frac{(\langle 2|3\rangle (\langle 3|2|\xi\rangle + \langle 3|4|\xi\rangle + \langle 3|5|\xi\rangle)^2 \langle 4|5|\xi\rangle^3)}{(s_{45} s_{2345} \langle 4|5\rangle (\langle 2|3|\xi\rangle + \langle 2|4|\xi\rangle + \langle 2|5|\xi\rangle) (\langle 3|4|\xi\rangle + \langle 3|5|\xi\rangle))} \\
& + \frac{\langle 2|3\rangle (\langle 1|2|\xi\rangle + \langle 1|3|\xi\rangle) \langle 3|2|\xi\rangle \langle 4|5|\xi\rangle^3}{s_{23} s_{45} \langle 4|5\rangle (\langle 1|4|\xi\rangle + \langle 1|5|\xi\rangle) \langle 2|3|\xi\rangle \langle 5|4|\xi\rangle ([\xi|4|2|\xi] + [\xi|4|3|\xi] + [\xi|5|2|\xi] + [\xi|5|3|\xi])} \\
& - \frac{\langle 2|3\rangle \langle 3|2|\xi\rangle (\langle 4|2|\xi\rangle + \langle 4|3|\xi\rangle) (\langle 4|2|\xi\rangle + \langle 4|3|\xi\rangle + \langle 4|5|\xi\rangle)^2}{s_{23} s_{2345} \langle 4|5\rangle \langle 2|3|\xi\rangle (\langle 5|2|\xi\rangle + \langle 5|3|\xi\rangle + \langle 5|4|\xi\rangle) ([\xi|4|2|\xi] + [\xi|4|3|\xi] + [\xi|5|2|\xi] + [\xi|5|3|\xi])} \\
& - \frac{\langle 1|2\rangle \langle 3|4\rangle^3 ([\xi|5|3|\xi] + [\xi|5|4|\xi])^3}{s_{34} s_{345} (\langle 1|3|\xi\rangle + \langle 1|4|\xi\rangle + \langle 1|5|\xi\rangle) (\langle 2|3|\xi\rangle + \langle 2|4|\xi\rangle + \langle 2|5|\xi\rangle) \langle 3|4|\xi\rangle \langle 4|3|\xi\rangle (\langle 5|3|\xi\rangle + \langle 5|4|\xi\rangle)^2} \\
& + \frac{\langle 3|4\rangle^3 (\langle 1|3|\xi\rangle + \langle 1|4|\xi\rangle)^2 (-[\xi|3|1|\xi] - [\xi|4|1|\xi] + [\xi|5|3|\xi] + [\xi|5|4|\xi])}{s_{34} s_{345} \langle 1|5\rangle (\langle 1|3|\xi\rangle + \langle 1|4|\xi\rangle + \langle 1|5|\xi\rangle) \langle 3|4|\xi\rangle \langle 4|3|\xi\rangle (\langle 5|3|\xi\rangle + \langle 5|4|\xi\rangle)} \\
& - \frac{\langle 3|4\rangle^3 (\langle 2|3|\xi\rangle + \langle 2|4|\xi\rangle) (-[\xi|3|2|\xi] - [\xi|4|2|\xi] + [\xi|5|3|\xi] + [\xi|5|4|\xi])^2}{s_{34} s_{2345} (\langle 2|3|\xi\rangle + \langle 2|4|\xi\rangle + \langle 2|5|\xi\rangle) \langle 3|4|\xi\rangle \langle 4|3|\xi\rangle (\langle 5|3|\xi\rangle + \langle 5|4|\xi\rangle) (\langle 5|2|\xi\rangle + \langle 5|3|\xi\rangle + \langle 5|4|\xi\rangle)}
\end{aligned}$$

As the next example, the result for the  $N^2$ MHV form factor with five particles is reported. Due to the increased MHV degree and the nature of the MHV diagram method, the expression is considerably larger.

This is a form factor with a split-helicity configuration and the result below should be compared with the compact result from of the diagrammatic method obtained in Section 3.2.2.1.

$$\begin{aligned}
F(1_{\phi_{12}}, 2_{\phi_{12}}, 3^-, 4^-, 5^+, 6^+) = & - \frac{\langle 14\rangle^2 \langle 23\rangle \langle 3|2|\xi\rangle (\langle 4|1|\xi\rangle + \langle 4|5|\xi\rangle + \langle 4|6|\xi\rangle)}{s_{23} s_{456} \langle 16\rangle \langle 45\rangle \langle 56\rangle (\langle 1|4|\xi\rangle + \langle 1|5|\xi\rangle + \langle 1|6|\xi\rangle) \langle 2|3|\xi\rangle} \\
& - \frac{(\langle 13\rangle^2 (\langle 3|1|\xi\rangle + \langle 3|4|\xi\rangle + \langle 3|5|\xi\rangle + \langle 3|6|\xi\rangle) (\langle 4|5|\xi\rangle + \langle 4|6|\xi\rangle)^3)}{(s_{456} s_{3456} \langle 45\rangle \langle 56\rangle (\langle 1|4|\xi\rangle + \langle 1|5|\xi\rangle + \langle 1|6|\xi\rangle) (\langle 1|3|\xi\rangle + \langle 1|4|\xi\rangle + \langle 1|5|\xi\rangle + \langle 1|6|\xi\rangle) (\langle 3|4|\xi\rangle + \langle 3|5|\xi\rangle + \langle 3|6|\xi\rangle) (\langle 6|4|\xi\rangle + \langle 6|5|\xi\rangle))} \\
& + \frac{\langle 13\rangle^2 (\langle 3|1|\xi\rangle + \langle 3|4|\xi\rangle + \langle 3|5|\xi\rangle + \langle 3|6|\xi\rangle) \langle 4|5|\xi\rangle^3}{s_{45} s_{3456} \langle 16\rangle \langle 45\rangle (\langle 1|3|\xi\rangle + \langle 1|4|\xi\rangle + \langle 1|5|\xi\rangle + \langle 1|6|\xi\rangle) (\langle 3|4|\xi\rangle + \langle 3|5|\xi\rangle) \langle 5|4|\xi\rangle (\langle 6|4|\xi\rangle + \langle 6|5|\xi\rangle)} \\
& - \frac{(\langle 12\rangle (\langle 3|4|\xi\rangle + \langle 3|5|\xi\rangle + \langle 3|6|\xi\rangle)^3 \langle 4|5|\xi\rangle^3)}{(s_{45} s_{3456} \langle 45\rangle (\langle 1|3|\xi\rangle + \langle 1|4|\xi\rangle + \langle 1|5|\xi\rangle + \langle 1|6|\xi\rangle) (\langle 2|3|\xi\rangle + \langle 2|4|\xi\rangle + \langle 2|5|\xi\rangle + \langle 2|6|\xi\rangle) (\langle 3|4|\xi\rangle + \langle 3|5|\xi\rangle) \langle 5|4|\xi\rangle (\langle 6|4|\xi\rangle + \langle 6|5|\xi\rangle) (\langle 6|3|\xi\rangle + \langle 6|4|\xi\rangle + \langle 6|5|\xi\rangle))}
\end{aligned}$$

$$\begin{aligned}
& - \frac{(\langle 23 \rangle (\langle 3|2|\xi] + \langle 3|4|\xi] + \langle 3|5|\xi] + \langle 3|6|\xi])^2 \langle 4|5|\xi]^3}{(s_{45} s_{23456} \langle 45 \rangle (\langle 2|3|\xi] + \langle 2|4|\xi] + \langle 2|5|\xi] + \langle 2|6|\xi]) (\langle 3|4|\xi] + \langle 3|5|\xi])} \\
& - \frac{\langle 34 \rangle^3 (\langle 1|2|\xi] + \langle 1|3|\xi] + \langle 1|4|\xi]) (-[\xi|3|2|\xi] - [\xi|4|2|\xi])}{s_{34} s_{234} \langle 16 \rangle \langle 56 \rangle \langle 3|4|\xi] \langle 4|3|\xi] (\langle 5|2|\xi] + \langle 5|3|\xi] + \langle 5|4|\xi])} \\
& + \frac{\langle 23 \rangle (\langle 1|2|\xi] + \langle 1|3|\xi] + \langle 1|4|\xi]) \langle 3|2|\xi] (\langle 4|2|\xi] + \langle 4|3|\xi])^2}{s_{23} s_{234} \langle 16 \rangle \langle 56 \rangle \langle 2|3|\xi] (\langle 5|2|\xi] + \langle 5|3|\xi] + \langle 5|4|\xi]) ([\xi|4|2|\xi] + [\xi|4|3|\xi])} \\
& - \frac{\langle 34 \rangle^3 (\langle 1|2|\xi] + \langle 1|3|\xi] + \langle 1|4|\xi] + \langle 1|5|\xi]) (-[\xi|3|2|\xi] - [\xi|4|2|\xi] - [\xi|5|2|\xi])}{s_{345} s_{2345} \langle 16 \rangle \langle 45 \rangle (\langle 3|4|\xi] + \langle 3|5|\xi]) (\langle 5|3|\xi] + \langle 5|4|\xi]) (\langle 6|2|\xi] + \langle 6|3|\xi] + \langle 6|4|\xi] + \langle 6|5|\xi])} \\
& - \frac{(\langle 12 \rangle (\langle 3|4|\xi] + \langle 3|5|\xi])^2 \langle 4|5|\xi]^3)}{(s_{45} s_{345} \langle 16 \rangle \langle 45 \rangle (\langle 2|3|\xi] + \langle 2|4|\xi] + \langle 2|5|\xi])} \\
& \quad \langle 5|4|\xi] (\langle 6|3|\xi] + \langle 6|4|\xi] + \langle 6|5|\xi]) (-[\xi|4|3|\xi] - [\xi|5|3|\xi]))} \\
& - \frac{(\langle 23 \rangle (\langle 1|2|\xi] + \langle 1|3|\xi] + \langle 1|4|\xi] + \langle 1|5|\xi]) (\langle 3|2|\xi] + \langle 3|4|\xi] + \langle 3|5|\xi])^2 \langle 4|5|\xi]^3)}{(s_{45} s_{2345} \langle 16 \rangle \langle 45 \rangle (\langle 2|3|\xi] + \langle 2|4|\xi] + \langle 2|5|\xi]) (\langle 3|4|\xi] + \langle 3|5|\xi]) \langle 5|4|\xi] \\
& \quad (\langle 6|2|\xi] + \langle 6|3|\xi] + \langle 6|4|\xi] + \langle 6|5|\xi]) (-[\xi|4|2|\xi] - [\xi|4|3|\xi] - [\xi|5|2|\xi] - [\xi|5|3|\xi]))} \\
& - \frac{\langle 23 \rangle (\langle 1|2|\xi] + \langle 1|3|\xi]) \langle 3|2|\xi] \langle 4|5|\xi]^3}{s_{23} s_{45} \langle 16 \rangle \langle 45 \rangle \langle 2|3|\xi] \langle 5|4|\xi] (\langle 6|4|\xi] + \langle 6|5|\xi]) ([\xi|4|2|\xi] + [\xi|4|3|\xi] + [\xi|5|2|\xi] + [\xi|5|3|\xi])} \\
& + \frac{(\langle 23 \rangle (\langle 1|2|\xi] + \langle 1|3|\xi] + \langle 1|4|\xi] + \langle 1|5|\xi]) \langle 3|2|\xi] (\langle 4|2|\xi] + \langle 4|3|\xi]) (\langle 4|2|\xi] + \langle 4|3|\xi] + \langle 4|5|\xi])^2}{(s_{23} s_{2345} \langle 16 \rangle \langle 45 \rangle \langle 2|3|\xi] (\langle 5|2|\xi] + \langle 5|3|\xi] + \langle 5|4|\xi])} \\
& \quad (\langle 6|2|\xi] + \langle 6|3|\xi] + \langle 6|4|\xi] + \langle 6|5|\xi]) ([\xi|4|2|\xi] + [\xi|4|3|\xi] + [\xi|5|2|\xi] + [\xi|5|3|\xi]))} \\
& + \frac{\langle 12 \rangle \langle 34 \rangle^3 ([\xi|5|3|\xi] + [\xi|5|4|\xi])^3}{s_{34} s_{345} \langle 16 \rangle (\langle 2|3|\xi] + \langle 2|4|\xi] + \langle 2|5|\xi]) \langle 3|4|\xi] \langle 4|3|\xi] (\langle 5|3|\xi] + \langle 5|4|\xi])^2 (\langle 6|3|\xi] + \langle 6|4|\xi] + \langle 6|5|\xi])} \\
& + \frac{\langle 34 \rangle^3 (\langle 1|2|\xi] + \langle 1|3|\xi] + \langle 1|4|\xi] + \langle 1|5|\xi]) (\langle 2|3|\xi] + \langle 2|4|\xi])}{(s_{34} s_{2345} \langle 16 \rangle (\langle 2|3|\xi] + \langle 2|4|\xi] + \langle 2|5|\xi]) \langle 3|4|\xi] \langle 4|3|\xi] (\langle 5|3|\xi] + \langle 5|4|\xi])^2} \\
& \quad (-[\xi|3|2|\xi] - [\xi|4|2|\xi] + [\xi|5|3|\xi] + [\xi|5|4|\xi])^2 \\
& - \frac{\langle 34 \rangle^3 (-[\xi|3|1|\xi] - [\xi|4|1|\xi] - [\xi|5|1|\xi] - [\xi|6|1|\xi])}{s_{3456} s_{3456} \langle 45 \rangle \langle 56 \rangle (\langle 3|4|\xi] + \langle 3|5|\xi] + \langle 3|6|\xi]) (\langle 6|3|\xi] + \langle 6|4|\xi] + \langle 6|5|\xi])} \\
& + \frac{\langle 34 \rangle^3 (-[\xi|3|2|\xi] - [\xi|4|2|\xi] - [\xi|5|2|\xi] - [\xi|6|2|\xi])}{s_{3456} s_{23456} \langle 45 \rangle \langle 56 \rangle (\langle 3|4|\xi] + \langle 3|5|\xi] + \langle 3|6|\xi]) (\langle 6|3|\xi] + \langle 6|4|\xi] + \langle 6|5|\xi])}
\end{aligned}$$

$$\begin{aligned}
& + \frac{(\langle 12 \rangle (\langle 3|4|\xi \rangle + \langle 3|5|\xi \rangle + \langle 3|6|\xi \rangle)^2 (\langle 4|5|\xi \rangle + \langle 4|6|\xi \rangle)^3)}{(s_{456} s_{3456} \langle 45 \rangle \langle 56 \rangle (\langle 1|3|\xi \rangle + \langle 1|4|\xi \rangle + \langle 1|5|\xi \rangle + \langle 1|6|\xi \rangle) (\langle 2|3|\xi \rangle + \langle 2|4|\xi \rangle + \langle 2|5|\xi \rangle + \langle 2|6|\xi \rangle) \\
& \quad (\langle 6|4|\xi \rangle + \langle 6|5|\xi \rangle) (-[\xi|4|3|\xi] - [\xi|5|3|\xi] - [\xi|6|3|\xi]))} \\
& - \frac{(\langle 14 \rangle^2 (\langle 3|1|\xi \rangle + \langle 3|4|\xi \rangle + \langle 3|5|\xi \rangle + \langle 3|6|\xi \rangle)^2 (\langle 4|1|\xi \rangle + \langle 4|5|\xi \rangle + \langle 4|6|\xi \rangle))}{(s_{456} s_{3456} \langle 16 \rangle \langle 45 \rangle \langle 56 \rangle (\langle 1|4|\xi \rangle + \langle 1|5|\xi \rangle + \langle 1|6|\xi \rangle) ([\xi|3|1|\xi] - [\xi|4|3|\xi] - [\xi|5|3|\xi] - [\xi|6|3|\xi]))} \\
& + \frac{(\langle 23 \rangle (\langle 3|2|\xi \rangle + \langle 3|4|\xi \rangle + \langle 3|5|\xi \rangle + \langle 3|6|\xi \rangle)^2 (\langle 4|5|\xi \rangle + \langle 4|6|\xi \rangle)^3)}{(s_{456} s_{23456} \langle 45 \rangle \langle 56 \rangle (\langle 2|3|\xi \rangle + \langle 2|4|\xi \rangle + \langle 2|5|\xi \rangle + \langle 2|6|\xi \rangle) (\langle 3|4|\xi \rangle + \langle 3|5|\xi \rangle + \langle 3|6|\xi \rangle) \\
& \quad (\langle 6|4|\xi \rangle + \langle 6|5|\xi \rangle) (-[\xi|4|2|\xi] - [\xi|4|3|\xi] - [\xi|5|2|\xi] - [\xi|5|3|\xi] - [\xi|6|2|\xi] - [\xi|6|3|\xi]))} \\
& + \frac{(\langle 23 \rangle (\langle 1|2|\xi \rangle + \langle 1|3|\xi \rangle) \langle 3|2|\xi \rangle (\langle 4|5|\xi \rangle + \langle 4|6|\xi \rangle)^3)}{(s_{23} s_{456} \langle 45 \rangle \langle 56 \rangle (\langle 1|4|\xi \rangle + \langle 1|5|\xi \rangle + \langle 1|6|\xi \rangle) \langle 2|3|\xi \rangle (\langle 6|4|\xi \rangle + \langle 6|5|\xi \rangle) \\
& \quad ([\xi|4|2|\xi] + [\xi|4|3|\xi] + [\xi|5|2|\xi] + [\xi|5|3|\xi] + [\xi|6|2|\xi] + [\xi|6|3|\xi]))} \\
& - \frac{(\langle 23 \rangle \langle 3|2|\xi \rangle (\langle 4|2|\xi \rangle + \langle 4|3|\xi \rangle) (\langle 4|2|\xi \rangle + \langle 4|3|\xi \rangle + \langle 4|5|\xi \rangle + \langle 4|6|\xi \rangle)^2)}{(s_{23} s_{23456} \langle 45 \rangle \langle 56 \rangle \langle 2|3|\xi \rangle (\langle 6|2|\xi \rangle + \langle 6|3|\xi \rangle + \langle 6|4|\xi \rangle + \langle 6|5|\xi \rangle) \\
& \quad ([\xi|4|2|\xi] + [\xi|4|3|\xi] + [\xi|5|2|\xi] + [\xi|5|3|\xi] + [\xi|6|2|\xi] + [\xi|6|3|\xi]))} \\
& - \frac{(\langle 12 \rangle \langle 34 \rangle^3 ([\xi|5|3|\xi] + [\xi|5|4|\xi] + [\xi|6|3|\xi] + [\xi|6|4|\xi])^3)}{(s_{34} s_{3456} \langle 56 \rangle (\langle 1|3|\xi \rangle + \langle 1|4|\xi \rangle + \langle 1|5|\xi \rangle + \langle 1|6|\xi \rangle) (\langle 2|3|\xi \rangle + \langle 2|4|\xi \rangle + \langle 2|5|\xi \rangle + \langle 2|6|\xi \rangle) \\
& \quad \langle 3|4|\xi \rangle \langle 4|3|\xi \rangle (\langle 5|3|\xi \rangle + \langle 5|4|\xi \rangle) (\langle 6|3|\xi \rangle + \langle 6|4|\xi \rangle + \langle 6|5|\xi \rangle))} \\
& + \frac{\langle 34 \rangle^3 (\langle 1|3|\xi \rangle + \langle 1|4|\xi \rangle)^2 (-[\xi|3|1|\xi] - [\xi|4|1|\xi] + [\xi|5|3|\xi] + [\xi|5|4|\xi] + [\xi|6|3|\xi] + [\xi|6|4|\xi])}{s_{34} s_{3456} \langle 16 \rangle \langle 56 \rangle (\langle 1|3|\xi \rangle + \langle 1|4|\xi \rangle + \langle 1|5|\xi \rangle + \langle 1|6|\xi \rangle) \langle 3|4|\xi \rangle \langle 4|3|\xi \rangle (\langle 5|3|\xi \rangle + \langle 5|4|\xi \rangle)} \\
& - \frac{(\langle 34 \rangle^3 (\langle 2|3|\xi \rangle + \langle 2|4|\xi \rangle) (-[\xi|3|2|\xi] - [\xi|4|2|\xi] + [\xi|5|3|\xi] + [\xi|5|4|\xi] + [\xi|6|3|\xi] + [\xi|6|4|\xi])^2)}{(s_{34} s_{23456} \langle 56 \rangle (\langle 2|3|\xi \rangle + \langle 2|4|\xi \rangle + \langle 2|5|\xi \rangle + \langle 2|6|\xi \rangle) \langle 3|4|\xi \rangle \langle 4|3|\xi \rangle (\langle 5|3|\xi \rangle + \langle 5|4|\xi \rangle) \\
& \quad (\langle 6|2|\xi \rangle + \langle 6|3|\xi \rangle + \langle 6|4|\xi \rangle + \langle 6|5|\xi \rangle))} \\
& - \frac{\langle 12 \rangle \langle 34 \rangle^3 ([\xi|6|3|\xi] + [\xi|6|4|\xi] + [\xi|6|5|\xi])^3}{(s_{345} s_{3456} \langle 45 \rangle (\langle 1|3|\xi \rangle + \langle 1|4|\xi \rangle + \langle 1|5|\xi \rangle + \langle 1|6|\xi \rangle) (\langle 2|3|\xi \rangle + \langle 2|4|\xi \rangle + \langle 2|5|\xi \rangle + \langle 2|6|\xi \rangle) \\
& \quad (\langle 3|4|\xi \rangle + \langle 3|5|\xi \rangle) (\langle 5|3|\xi \rangle + \langle 5|4|\xi \rangle) (\langle 6|3|\xi \rangle + \langle 6|4|\xi \rangle + \langle 6|5|\xi \rangle)^2)} \\
& + \frac{\langle 34 \rangle^3 (\langle 1|3|\xi \rangle + \langle 1|4|\xi \rangle + \langle 1|5|\xi \rangle)^2 (-[\xi|3|1|\xi] - [\xi|4|1|\xi] - [\xi|5|1|\xi] + [\xi|6|3|\xi] + [\xi|6|4|\xi] + [\xi|6|5|\xi])}{(s_{345} s_{3456} \langle 16 \rangle \langle 45 \rangle (\langle 1|3|\xi \rangle + \langle 1|4|\xi \rangle + \langle 1|5|\xi \rangle + \langle 1|6|\xi \rangle) \\
& \quad (\langle 3|4|\xi \rangle + \langle 3|5|\xi \rangle) (\langle 5|3|\xi \rangle + \langle 5|4|\xi \rangle) (\langle 6|3|\xi \rangle + \langle 6|4|\xi \rangle + \langle 6|5|\xi \rangle))} \\
& - \frac{\langle 34 \rangle^3 (\langle 2|3|\xi \rangle + \langle 2|4|\xi \rangle + \langle 2|5|\xi \rangle)}{(s_{345} s_{23456} \langle 45 \rangle (\langle 2|3|\xi \rangle + \langle 2|4|\xi \rangle + \langle 2|5|\xi \rangle + \langle 2|6|\xi \rangle) (\langle 3|4|\xi \rangle + \langle 3|5|\xi \rangle) (\langle 5|3|\xi \rangle + \langle 5|4|\xi \rangle) \\
& \quad (\langle 6|3|\xi \rangle + \langle 6|4|\xi \rangle + \langle 6|5|\xi \rangle) (\langle 6|2|\xi \rangle + \langle 6|3|\xi \rangle + \langle 6|4|\xi \rangle + \langle 6|5|\xi \rangle))} \\
\end{aligned}$$

This rather lengthy result has been numerically checked and not only it does not depend on the reference spinor  $|\xi\rangle$  but also it is equal to the much more compact expression obtained using the zig-zag diagrams.

# E Feynman integrals

The appendix chapter includes the details of the evaluation of the Feynman integrals that are relevant to the two-loop Sudakov form factor in ABJM theory presented in Chapter 4. These integrals include the **XT** integral, which is the only integral that is needed for the Sudakov form factor, as well as other maximally transcendental integrals in three dimensions **LT**, **CT**, **FAN**. These are defined as:

$$\mathbf{XT}(q^2) = \int \frac{d^D \ell_1 d^D \ell_3}{(i\pi^{D/2})^2} \frac{q^2 [\text{Tr}(p_1 p_2 \ell_1 \ell_3) - q^2 \ell_3^2]}{\ell_1^2 \ell_2^2 \ell_3^2 (\ell_1 - \ell_3)^2 (p_1 - \ell_3)^2 (\ell_3 - \ell_1 + p_2)^2}, \quad (\text{E.1})$$

$$\mathbf{LT}(q^2) = \int \frac{d^D \ell_1 d^D \ell_3}{(i\pi^{D/2})^2} \frac{-q^2 [\text{Tr}(p_1 \ell_3 p_2 \ell_1) - (\ell_1 - p_1)^2 (\ell_3 - p_2)^2]}{\ell_1^2 (p_1 + p_2 - \ell_1)^2 \ell_3^2 (p_1 + p_2 - \ell_3)^2 (\ell_1 - \ell_3)^2 (\ell_3 - p_2)^2} \quad (\text{E.2})$$

$$\mathbf{CT}(q^2) = \int \frac{d^D \ell_1 d^D \ell_3}{(i\pi^{D/2})^2} \frac{\text{Tr}(p_1, p_2, \ell_3, \ell_1)}{\ell_1^2 (p_1 + p_2 - \ell_1)^2 \ell_3^2 (\ell_1 - \ell_3)^2 (\ell_3 - p_2)^2} \quad (\text{E.3})$$

$$\mathbf{FAN}(q^2) = \int \frac{d^D \ell_1 d^D \ell_3}{(i\pi^{D/2})^2} \frac{\text{Tr}(p_1, p_2, \ell_3, \ell_1)}{\ell_1^2 \ell_3^2 (p_1 + p_2 - \ell_1 - \ell_3)^2 (\ell_1 - p_1)^2 (\ell_3 - p_2)^2} \quad (\text{E.4})$$

All the scalar integrals corresponding to the topologies of **XT**, **LT**, **CT**, **FAN** are known to all orders in  $\epsilon$  in dimensional regularisation. However these integrals have complicated numerators - typical for maximally transcendental integrals in three dimensions. These integrals can be related to the well-known scalar integrals through IBP identities of Feynman integrals.

The IBP identities for Feynman integrals can be easily derived by multiplying a scalar integrand by either one of the external momenta or one of the loop momenta and computing the derivative with respect to one of the loop momenta. This is a total differential and clearly integrates to zero,

$$0 = \int d^L \ell \frac{\partial}{\partial \ell_i^\mu} \left[ k_j^\mu \mathcal{I}(p, \ell) \right], \quad 0 = \int d^L \ell \frac{\partial}{\partial \ell_i^\mu} \left[ p_j^\mu \mathcal{I}(p, \ell) \right], \quad (\text{E.5})$$

assuming the integrand vanishes sufficiently fast at the integration boundaries. Considering the first of the two equations (E.5), when the derivative acts on the momentum factor inside the brackets, it reproduces the original integrand  $\mathcal{I}$ . However when it acts on the integrand, it increases the index of one of the 1propagators of it.

The bubble integral with generic propagator powers (or indices) is a simple but illustrative example. The integral is defined as:

$$\mathbf{BUB}(a_1, a_2; q^2) = \int d^L \ell \frac{1}{[\ell^2]^{a_1} [(\ell - q)^2]^{a_2}}. \quad (\text{E.6})$$

The IBP identity obtained by multiplying the integrand by  $\ell$  implies a relation between **BUB** integrals with different indices

$$0 = \mathbf{BUB}(a_1, a_2; q^2) + \frac{d - 2a_1 - a_2 + 1}{(a_2 - 1)q^2} \mathbf{BUB}(a_1, a_2 - 1; q^2) + \frac{1}{q^2} \mathbf{BUB}(a_1 - 1, a_2; q^2) \quad (\text{E.7})$$

Complicated scalar numerators that appear in Feynman integrals can be written as a linear combination of inverse propagators. In other words, Feynman integrals with complicated numerators can be written as a linear combination of other Feynman integrals with a unit numerator and some of the indices taking smaller values than those of the original Feynman integrals.

The integrals with unit numerator in turn can be related to “simpler” integrals using the IBP identities. The Laporta algorithm defines a sense of simplicity among Feynman integrals with different indices and uses the IBP identities to rewrite any integral in terms of *master integrals* which have the “simplest” indices.

A comment on the simplicity of master integrals is appropriate. Traditionally, master integrals are chosen such that they have the simplest topology which makes them easiest to evaluate via well-established methods. However, in [107] it was shown that it is possible to find a basis of master integrals which have indices such that they are all pure functions i.e., the coefficients of their Laurent expansion in the dimensional regularisation parameter have transcendentality weight  $2L + n$  for the  $\mathcal{O}(\epsilon^n)$  term, where  $L$  is the number of loops. Pure master integrals satisfy a simple differential equation

$$\partial_{x_i} f = \epsilon A_i f, \quad (\text{E.8})$$

where  $f$  is a column matrix collecting all the pure master integrals,  $x_i$  are the kinematical invariant that the integrals  $f$  depend on and  $A$  is a matrix which is independent of  $\epsilon$  and has rational entries as functions of the kinematical invariants  $x_i$ . Using this differential equation it has been possible to compute pure master integrals for several

multi-loop processes [111–114].

Nevertheless, the master integrals relevant to the form factors considered in this thesis are already known all orders in  $\epsilon$  and it is not necessary to find integrals that satisfy (E.8). After rewriting any of the integrals (E.1) in terms of integrals with unit numerators but various different indices, one can run any implementation of the Laporta algorithm and obtain expressions for the original integrals in terms of four masters integrals.

As an instructive example, the procedure of obtaining the reduction of the integral **CT** to master integrals using **FIRE**, which is an implementation of the Laporta algorithm in **Mathematica**, is presented in what follows.

One begins by writing the integral **CT** in the following form:

$$\mathbf{CT}(q^2) = \int \frac{d^D \ell_1 d^D \ell_3}{(i\pi^{D/2})^2} \frac{\mathcal{N}_{\mathbf{CT}}}{D_1 D_2 D_3 D_4 D_5 D_6 D_7}, \quad (\text{E.9})$$

where

$$D_1 = \ell_1^2 \quad (\text{E.10a})$$

$$D_2 = (\ell_1 - p_1 - p_2)^2 \quad (\text{E.10b})$$

$$D_3 = \ell_3^2 \quad (\text{E.10c})$$

$$D_4 = (\ell_3 - p_1 - p_2)^2 \quad (\text{E.10d})$$

$$D_5 = (\ell_1 - \ell_3)^2 \quad (\text{E.10e})$$

$$D_6 = (\ell_3 - p_2)^2 \quad (\text{E.10f})$$

$$D_7 = (\ell_1 - p_1)^2 \quad (\text{E.10g})$$

and

$$\begin{aligned} \mathcal{N}_{\mathbf{CT}} &= -\text{Tr}(12\ell_3\ell_1) \\ &= 2p_1 \cdot p_2 \ell_3 \cdot \ell_1 - 2p_1 \cdot \ell_3 p_2 \ell_1 + 2p_1 \cdot \ell_1 p_2 \cdot \ell_3. \end{aligned} \quad (\text{E.11})$$

The numerator  $\mathcal{N}_{\mathbf{CT}}$  can be written in terms of the denominators  $D_i$ :

$$\begin{aligned} \mathcal{N}_{\mathbf{CT}} &= \frac{1}{2} D_1 D_3 + D_2 D_4 + D_1 D_6 - D_2 D_6 + D_3 D_7 - D_4 D_7 - D_1 q^2 \\ &\quad - D_2 q^2 - D_3 q^2 - D_4 q^2 + D_5 q^2 + D_6 q^2 + D_7 q^2 + (q^2)^2 \end{aligned} \quad (\text{E.12})$$

Substituting (E.12) into (E.5), one can write the original integral in terms of scalar

integrals with modified powers of denominators:

$$\begin{aligned}
 \mathbf{CT}(q^2) = & \mathbf{CT}(0, 1, 0, 0, 1, 1, 0; q^2) + \mathbf{CT}(1, 0, 0, -1, 1, 1, 0; q^2) \\
 & + \mathbf{CT}(0, 1, 1, 0, 1, 1, 0; q^2) - \mathbf{CT}(1, 0, 1, 0, 1, 0, 0; q^2) \\
 & + \mathbf{CT}(1, 1, 0, 0, 1, 1, -1; q^2) - \mathbf{CT}(1, 1, 1, -1, 1, 1, -1; q^2) \\
 & - q^2 \mathbf{CT}(0, 1, 1, 0, 1, 1, 0; q^2) - q^2 \mathbf{CT}(1, 0, 1, 0, 1, 1, 0; q^2) \\
 & - q^2 \mathbf{CT}(1, 1, 0, 0, 1, 1, 0; q^2) - q^2 \mathbf{CT}(1, 1, 1, -1, 1, 1, 0; q^2) \\
 & + q^2 \mathbf{CT}(1, 1, 1, 0, 0, 1, 0; q^2) + q^2 \mathbf{CT}(1, 1, 1, 0, 1, 0, 0; q^2) \\
 & + q^2 \mathbf{CT}(1, 1, 1, 0, 1, 1, -1; q^2) + (q^2)^2 \mathbf{CT}(1, 1, 1, 0, 1, 1, 0; q^2),
 \end{aligned} \tag{E.13}$$

where  $\mathbf{CT}(a_1, a_2, a_3, a_4, a_5, a_6, a_7; q^2)$  is a generalisation of  $\mathbf{CT}(q^2)$

$$\mathbf{CT}(a_1, a_2, a_3, a_4, a_5, a_6, a_7; q^2) = \int \frac{d^D \ell_1 d^D \ell_3}{(i\pi^{D/2})^2} \frac{1}{D_1^{a_1} D_2^{a_2} D_3^{a_3} D_4^{a_4} D_5^{a_5} D_6^{a_6} D_7^{a_7}}. \tag{E.14}$$

Each of the terms that make up  $\mathbf{CT}(q^2)$  in equation (E.13) can be fed into the Laporta algorithm and be expressed in one of the master integrals for this topology.

Using the implementation FIRE [115], this is done by preparing the IBP identities according to the manual of the package and running the function `F[]` for each of the integrals in (E.13). For example for  $\mathbf{CT}(0, 1, 0, 0, 1, 1, 0; q^2)$  one calls

`F[0, 1, 0, 0, 1, 1, 0]`

if FIRE is prepared with the definitions of the propagators as in equation (E.10). The output is a linear combination of integrals of the form

`G[{a_1, a_2, a_3, a_4, a_5, a_6, a_7}]`

where  $a_i$  are such that  $G(a_i)$  correspond to a master integral which can be obtained from of equations (E.14) and (E.10) by setting the values of  $a_i$  that appear in the argument of  $G$ . For example  $G(0, 1, 1, 0, 1, 0, 0)$  is equal to the **SUNSET** master integral.

Below is the summary of the results for the reductions of the integrals listed in (E.1):

$$\begin{aligned}
 \mathbf{XT}(q^2) = & \frac{7(D-3)(3D-10)(3D-8)}{2(D-4)^2(2D-7)} \mathbf{SUNSET}(q^2) \\
 & + (-q^2) \frac{5(D-3)(3D-10)}{2(D-4)(2D-7)} \mathbf{TRI}(q^2) + (-q^2)^3 \frac{D-4}{4(2D-7)} \mathbf{TrianX}(q^2)
 \end{aligned} \tag{E.15}$$

and

$$\mathbf{LT}(q^2) = \frac{8-3D}{D-3} \mathbf{SUNSET}(q^2) + q^2 (\mathbf{GLASS}(q^2) - \mathbf{TRI}(q^2)), \quad (\text{E.16})$$

$$\mathbf{CT}(q^2) = \mathbf{FAN}(q^2) = \left( \frac{1}{4\epsilon} - \frac{3}{2} \right) \mathbf{SUNSET}(q^2). \quad (\text{E.17})$$

In  $D = 3 - 2\epsilon$  dimensions, the master integrals **SUNSET**, **TRI**, **TrianX** and **GLASS** have the following values:

$$\mathbf{SUNSET}(q^2) = \text{---} = - \left( \frac{-q^2}{\mu^2} \right)^{-2\epsilon} \frac{\Gamma(\frac{1}{2} - \epsilon)^3 \Gamma(2\epsilon)}{\Gamma(\frac{3}{2} - 3\epsilon)} \quad (\text{E.18})$$

$$\mathbf{TRI}(q^2) = \text{---} = -(-q^2)^{-1} \left( \frac{-q^2}{\mu^2} \right)^{-2\epsilon} \frac{\Gamma(\frac{1}{2} - \epsilon)^2 \Gamma(-2\epsilon) \Gamma(\frac{3}{2} + \epsilon) \Gamma(2 + 2\epsilon)}{\epsilon(1 + 2\epsilon)^2 \Gamma(\frac{1}{2} - 3\epsilon)} \quad (\text{E.19})$$

$$\mathbf{GLASS}(q^2) = \text{---} = (-q^2)^{-1} \left( \frac{-q^2}{\mu^2} \right)^{-2\epsilon} \frac{\Gamma(\frac{1}{2} - \epsilon)^4 \Gamma(\frac{1}{2} + \epsilon)^2}{\Gamma(1 - 2\epsilon)^2} \quad (\text{E.20})$$

$$\begin{aligned} \mathbf{TrianX}(q^2) = & \text{---} = (-q^2)^{-3} \left( \frac{-q^2}{\mu^2} \right)^{-2\epsilon} e^{-2\gamma_E \epsilon} \left[ \frac{4\pi}{\epsilon^2} + \frac{\pi(3 + 8\log 2)}{\epsilon} \right. \\ & - \frac{2\pi}{3} (81 + 4\pi^2 + 6\log 2 (4\log 2 - 9)) + \frac{\pi}{6} \left( -\pi^2 (7 + 40\log 2) \right. \\ & \left. \left. + 8(69 + 6\log 2 + 2\log^2 2(8\log 2 - 27) - 113\zeta_3) \right) \epsilon + \mathcal{O}(\epsilon) \right], \end{aligned} \quad (\text{E.21})$$

where the conventions of [116] for the integration measure have been used. The first three of these integrals are planar and their expressions in all orders in  $\epsilon$  can be easily obtained by first computing their Mellin-Barnes representations most conveniently using the **AMBRE** package [117] and then performing the Mellin-Barnes integrations using the **MB** tools, in particular **MB.m** [116] and **barnesroutines.m** by David Kosower. The expansion around  $\epsilon = 0$  of the **TRI** and **GLASS** topologies has uniform degree of transcendentality, while this is not the case for the **SUNSET** and **TrianX** topologies.

# References

- [1] S. J. Parke and T. Taylor, *An Amplitude for n Gluon Scattering*, *Phys.Rev.Lett.* **56** (1986) 2459.
- [2] R. Britto, F. Cachazo, and B. Feng, *New Recursion Relations for Tree Amplitudes of Gluons*, *Nucl.Phys.* **B715** (2005) 499–522, [[hep-th/0412308](#)].
- [3] F. Cachazo, P. Svrcek, and E. Witten, *MHV vertices and tree amplitudes in gauge theory*, *JHEP* **0409** (2004) 006, [[hep-th/0403047](#)].
- [4] R. Britto, F. Cachazo, and B. Feng, *Generalized Unitarity and One-Loop Amplitudes in  $\mathcal{N} = 4$  super-Yang-Mills*, *Nucl.Phys.* **B725** (2005) 275–305, [[hep-th/0412103](#)].
- [5] R. J. Eden, P. V. Landshoff, D. I. Olive, and J. C. Polkinghorne, *The Analytic S-Matrix*. Cambridge University Press, 1966.
- [6] N. Arkani-Hamed, F. Cachazo, C. Cheung, and J. Kaplan, *The S-Matrix in Twistor Space*, *JHEP* **1003** (2010) 110, [[arXiv:0903.2110](#)].
- [7] A. B. Goncharov, M. Spradlin, C. Vergu, and A. Volovich, *Classical Polylogarithms for Amplitudes and Wilson Loops*, *Phys.Rev.Lett.* **105** (2010) 151605, [[arXiv:1006.5703](#)].
- [8] J. Golden, A. B. Goncharov, M. Spradlin, C. Vergu, and A. Volovich, *Motivic Amplitudes and Cluster Coordinates*, *JHEP* **1401** (2014) 091, [[arXiv:1305.1617](#)].
- [9] C. Berger, Z. Bern, L. Dixon, F. Febres Cordero, D. Forde, et al., *An Automated Implementation of On-Shell Methods for One-Loop Amplitudes*, *Phys.Rev.* **D78** (2008) 036003, [[arXiv:0803.4180](#)].
- [10] L. Brink, J. H. Schwarz, and J. Scherk, *Supersymmetric Yang-Mills Theories*, *Nucl.Phys.* **B121** (1977) 77.
- [11] S. Ferrara and B. Zumino, *Supergauge Invariant Yang-Mills Theories*, *Nucl.Phys.* **B79** (1974) 413.
- [12] L. Avdeev, O. Tarasov, and A. Vladimirov, *Vanishing of the three loop charge renormalization function in a supersymmetric gauge theory*, *Phys.Lett.* **B96** (1980) 94–96.
- [13] D. Jones, *Charge Renormalization in a Supersymmetric Yang-Mills Theory*, *Phys.Lett.* **B72** (1977) 199.
- [14] M. F. Sohnius and P. C. West, *Conformal Invariance in  $N=4$  Supersymmetric Yang-Mills Theory*, *Phys.Lett.* **B100** (1981) 245.
- [15] S. L. Adler, J. C. Collins, and A. Duncan, *Energy-Momentum-Tensor Trace*

*Anomaly in Spin 1/2 Quantum Electrodynamics, Phys.Rev. **D15** (1977) 1712.*

- [16] G. 't Hooft, *A Planar Diagram Theory for Strong Interactions, Nucl.Phys. **B72** (1974) 461.*
- [17] J. M. Maldacena, *The Large  $N$  limit of Superconformal Field Theories and Supergravity, Adv.Theor.Math.Phys. **2** (1998) 231–252, [hep-th/9711200].*
- [18] N. Beisert, C. Ahn, L. F. Alday, Z. Bajnok, J. M. Drummond, et al., *Review of AdS/CFT Integrability: An Overview, Lett.Math.Phys. **99** (2012) 3–32, [arXiv:1012.3982].*
- [19] N. Kanning, T. Lukowski, and M. Staudacher, *A Shortcut to General Tree-level Scattering Amplitudes in  $N=4$  SYM via Integrability, arXiv:1403.3382.*
- [20] R. Frassek, N. Kanning, Y. Ko, and M. Staudacher, *Bethe Ansatz for Yangian Invariants: Towards Super Yang-Mills Scattering Amplitudes, arXiv:1312.1693.*
- [21] J. Broedel, M. de Leeuw, and M. Rosso, *A dictionary between  $R$ -operators, on-shell graphs and Yangian algebras, arXiv:1403.3670.*
- [22] N. Beisert, J. Broedel, and M. Rosso, *On Yangian-invariant regularisation of deformed on-shell diagrams in  $N=4$  super-Yang-Mills theory, arXiv:1401.7274.*
- [23] L. Ferro, T. Lukowski, C. Meneghelli, J. Plefka, and M. Staudacher, *Harmonic  $R$ -matrices for Scattering Amplitudes and Spectral Regularization, Phys.Rev.Lett. **110** (2013), no. 12 121602, [arXiv:1212.0850].*
- [24] L. J. Dixon, J. M. Drummond, C. Duhr, and J. Pennington, *The four-loop remainder function and multi-Regge behavior at NNLLA in planar  $N=4$  super-Yang-Mills theory, arXiv:1402.3300.*
- [25] L. J. Dixon, *Calculating Scattering Amplitudes Efficiently, hep-ph/9601359.*
- [26] E. Witten, *Perturbative Gauge Theory as a String Theory in Twistor Space, Commun.Math.Phys. **252** (2004) 189–258, [hep-th/0312171].*
- [27] A. Sever and P. Vieira, *Symmetries of the  $N=4$  SYM S-matrix, arXiv:0908.2437.*
- [28] S. Bauberger, M. Bohm, G. Weiglein, F. A. Berends, and M. Buza, *Calculation of two loop selfenergies in the electroweak standard model, Nucl.Phys.Proc.Suppl. **37B** (1994) 95–114, [hep-ph/9406404].*
- [29] N. Arkani-Hamed, J. L. Bourjaily, F. Cachazo, A. B. Goncharov, A. Postnikov, et al., *Scattering Amplitudes and the Positive Grassmannian, arXiv:1212.5605.*
- [30] N. Arkani-Hamed and J. Trnka, *The Amplituhedron, arXiv:1312.2007.*
- [31] N. Arkani-Hamed, J. L. Bourjaily, F. Cachazo, S. Caron-Huot, and J. Trnka, *The All-Loop Integrand For Scattering Amplitudes in Planar  $N=4$  SYM, JHEP **1101** (2011) 041, [arXiv:1008.2958].*
- [32] L. Bianchi, V. Forini, and A. V. Kotikov, *On DIS Wilson coefficients in  $N=4$  super Yang-Mills theory, Phys.Lett. **B725** (2013) 394–401, [arXiv:1304.7252].*
- [33] A. Brandhuber, G. Travaglini, and G. Yang, *Analytic two-loop form factors in  $\mathcal{N} = 4$  SYM, JHEP **1205** (2012) 082, [arXiv:1201.4170].*

- [34] L. F. Alday and J. M. Maldacena, *Gluon scattering amplitudes at strong coupling*, *JHEP* **0706** (2007) 064, [[arXiv:0705.0303](#)].
- [35] G. Korchemsky, J. Drummond, and E. Sokatchev, *Conformal properties of four-gluon planar amplitudes and Wilson loops*, *Nucl.Phys.* **B795** (2008) 385–408, [[arXiv:0707.0243](#)].
- [36] A. Brandhuber, P. Heslop, and G. Travaglini, *MHV amplitudes in  $N=4$  super Yang-Mills and Wilson loops*, *Nucl.Phys.* **B794** (2008) 231–243, [[arXiv:0707.1153](#)].
- [37] J. Drummond, J. Henn, G. Korchemsky, and E. Sokatchev, *Dual Superconformal Symmetry of Scattering Amplitudes in  $\mathcal{N} = 4$  super-Yang-Mills Theory*, *Nucl.Phys.* **B828** (2010) 317–374, [[arXiv:0807.1095](#)].
- [38] A. Brandhuber, P. Heslop, and G. Travaglini, *A Note on dual superconformal symmetry of the  $N=4$  super Yang-Mills S-matrix*, *Phys.Rev.* **D78** (2008) 125005, [[arXiv:0807.4097](#)].
- [39] Z. Bern, L. J. Dixon, and V. A. Smirnov, *Iteration of planar amplitudes in maximally supersymmetric Yang-Mills theory at three loops and beyond*, *Phys.Rev.* **D72** (2005) 085001, [[hep-th/0505205](#)].
- [40] J. Drummond, J. Henn, G. Korchemsky, and E. Sokatchev, *Conformal Ward identities for Wilson loops and a test of the duality with gluon amplitudes*, *Nucl.Phys.* **B826** (2010) 337–364, [[arXiv:0712.1223](#)].
- [41] C. Anastasiou, Z. Bern, L. J. Dixon, and D. Kosower, *Planar amplitudes in maximally supersymmetric Yang-Mills theory*, *Phys.Rev.Lett.* **91** (2003) 251602, [[hep-th/0309040](#)].
- [42] J. M. Henn, S. G. Naculich, H. J. Schnitzer, and M. Spradlin, *Higgs-regularized three-loop four-gluon amplitude in  $N=4$  SYM: exponentiation and Regge limits*, *JHEP* **1004** (2010) 038, [[arXiv:1001.1358](#)].
- [43] Z. Bern, J. Carrasco, L. J. Dixon, H. Johansson, and R. Roiban, *The Complete Four-Loop Four-Point Amplitude in  $N=4$  Super-Yang-Mills Theory*, *Phys.Rev.* **D82** (2010) 125040, [[arXiv:1008.3327](#)].
- [44] Z. Bern, J. Carrasco, H. Johansson, and R. Roiban, *The Five-Loop Four-Point Amplitude of  $N=4$  super-Yang-Mills Theory*, *Phys.Rev.Lett.* **109** (2012) 241602, [[arXiv:1207.6666](#)].
- [45] Z. Bern, M. Czakon, D. Kosower, R. Roiban, and V. Smirnov, *Two-loop iteration of five-point  $N=4$  super-Yang-Mills amplitudes*, *Phys.Rev.Lett.* **97** (2006) 181601, [[hep-th/0604074](#)].
- [46] C. Anastasiou, A. Brandhuber, P. Heslop, V. V. Khoze, B. Spence, et al., *Two-Loop Polygon Wilson Loops in  $N=4$  SYM*, *JHEP* **0905** (2009) 115, [[arXiv:0902.2245](#)].
- [47] V. Del Duca, C. Duhr, and V. A. Smirnov, *The Two-Loop Hexagon Wilson Loop in  $N = 4$  SYM*, *JHEP* **1005** (2010) 084, [[arXiv:1003.1702](#)].

[48] J. M. Drummond, J. M. Henn, and J. Plefka, *Yangian symmetry of scattering amplitudes in  $N=4$  super Yang-Mills theory*, *JHEP* **0905** (2009) 046, [[arXiv:0902.2987](#)].

[49] L. Dolan, C. R. Nappi, and E. Witten, *Yangian symmetry in  $D = 4$  superconformal Yang-Mills theory*, [hep-th/0401243](#).

[50] G. Korchemsky and E. Sokatchev, *Symmetries and analytic properties of scattering amplitudes in  $N=4$  SYM theory*, *Nucl.Phys.* **B832** (2010) 1–51, [[arXiv:0906.1737](#)].

[51] O. Aharony, O. Bergman, D. L. Jafferis, and J. Maldacena,  $\mathcal{N} = 6$  superconformal Chern-Simons-matter theories, *M2-branes and their gravity duals*, *JHEP* **0810** (2008) 091, [[arXiv:0806.1218](#)].

[52] J. H. Schwarz, *Superconformal Chern-Simons theories*, *JHEP* **0411** (2004) 078, [[hep-th/0411077](#)].

[53] O. Aharony, O. Bergman, and D. L. Jafferis, *Fractional M2-branes*, *JHEP* **0811** (2008) 043, [[arXiv:0807.4924](#)].

[54] M. Bianchi, M. Leoni, A. Mauri, S. Penati, and A. Santambrogio, *Four-points two-loop scattering amplitude in ABJM theory*, *Fortsch.Phys.* **60** (2012) 921–927.

[55] S. Caron-Huot and Y.-t. Huang, *The two-loop six-point amplitude in ABJM theory*, *JHEP* **1303** (2013) 075, [[arXiv:1210.4226](#)].

[56] O. T. Engelund and R. Roiban, *Correlation functions of local composite operators from generalized unitarity*, *JHEP* **1303** (2013) 172, [[arXiv:1209.0227](#)].

[57] A. Brandhuber, B. Spence, G. Travaglini, and G. Yang, *Form Factors in  $\mathcal{N} = 4$  Super Yang-Mills and Periodic Wilson Loops*, *JHEP* **1101** (2011) 134, [[arXiv:1011.1899](#)].

[58] W. van Neerven, *Infrared Behavior of on-shell Form Factors in  $\mathcal{N} = 4$  Supersymmetric Yang-Mills Field Theory*, *Z.Phys.* **C30** (1986) 595.

[59] L. Bork, D. Kazakov, and G. Vartanov, *On form factors in  $\mathcal{N} = 4$  sym*, *JHEP* **1102** (2011) 063, [[arXiv:1011.2440](#)].

[60] L. Bork, *On NMHV form factors in  $\mathcal{N} = 4$  SYM theory from generalized unitarity*, *JHEP* **1301** (2013) 049, [[arXiv:1203.2596](#)].

[61] T. Gehrmann, J. M. Henn, and T. Huber, *The three-loop form factor in  $\mathcal{N} = 4$  super Yang-Mills*, *JHEP* **1203** (2012) 101, [[arXiv:1112.4524](#)].

[62] B. Penante, B. Spence, G. Travaglini, and C. Wen, *On super form factors of half-BPS operators in  $N=4$  super Yang-Mills*, [arXiv:1402.1300](#).

[63] Z. Bern, L. J. Dixon, and D. A. Kosower, *Progress in one loop QCD computations*, *Ann.Rev.Nucl.Part.Sci.* **46** (1996) 109–148, [[hep-ph/9602280](#)].

[64] H. Johansson, D. A. Kosower, and K. J. Larsen, *An Overview of Maximal Unitarity at Two Loops*, *PoS* **LL2012** (2012) 066, [[arXiv:1212.2132](#)].

[65] L. J. Dixon, *A brief introduction to modern amplitude methods*, [arXiv:1310.5353](https://arxiv.org/abs/1310.5353).

[66] V. Nair, *A Current Algebra for Some Gauge Theory Amplitudes*, *Phys.Lett.* **B214** (1988) 215.

[67] H. Elvang, Y.-t. Huang, and C. Peng, *On-shell superamplitudes in  $N=4$  SYM*, *JHEP* **1109** (2011) 031, [[arXiv:1102.4843](https://arxiv.org/abs/1102.4843)].

[68] M. L. Mangano and S. J. Parke, *Multiparton Amplitudes in Gauge Theories*, *Phys.Rept.* **200** (1991) 301–367, [[hep-th/0509223](https://arxiv.org/abs/hep-th/0509223)].

[69] V. Del Duca, A. Frizzo, and F. Maltoni, *Factorization of tree QCD amplitudes in the high-energy limit and in the collinear limit*, *Nucl.Phys.* **B568** (2000) 211–262, [[hep-ph/9909464](https://arxiv.org/abs/hep-ph/9909464)].

[70] V. Del Duca, L. J. Dixon, and F. Maltoni, *New color decompositions for gauge amplitudes at tree and loop level*, *Nucl.Phys.* **B571** (2000) 51–70, [[hep-ph/9910563](https://arxiv.org/abs/hep-ph/9910563)].

[71] Z. Bern, J. Carrasco, and H. Johansson, *New Relations for Gauge-Theory Amplitudes*, *Phys.Rev.* **D78** (2008) 085011, [[arXiv:0805.3993](https://arxiv.org/abs/0805.3993)].

[72] Z. Bern and D. A. Kosower, *Color decomposition of one loop amplitudes in gauge theories*, *Nucl.Phys.* **B362** (1991) 389–448.

[73] T. Bargheer, F. Loebbert, and C. Meneghelli, *Symmetries of Tree-level Scattering Amplitudes in  $\mathcal{N} = 6$  Superconformal Chern-Simons Theory*, *Phys.Rev.* **D82** (2010) 045016, [[arXiv:1003.6120](https://arxiv.org/abs/1003.6120)].

[74] A. E. Lipstein, *Integrability of  $N = 6$  Chern-Simons Theory*, [arXiv:1105.3231](https://arxiv.org/abs/1105.3231).

[75] T. Bargheer, N. Beisert, F. Loebbert, T. McLoughlin, N. Beisert, et al., *Conformal Anomaly for Amplitudes in  $\mathcal{N} = 6$  Superconformal Chern-Simons Theory*, *J.Phys.* **A45** (2012) 475402, [[arXiv:1204.4406](https://arxiv.org/abs/1204.4406)].

[76] R. Britto, F. Cachazo, B. Feng, and E. Witten, *Direct Proof of Tree-Level Recursion Relation in Yang-Mills Theory*, *Phys.Rev.Lett.* **94** (2005) 181602, [[hep-th/0501052](https://arxiv.org/abs/hep-th/0501052)].

[77] A. Brandhuber, B. Spence, and G. Travaglini, *Tree-Level Formalism*, *J.Phys.* **A44** (2011) 454002, [[arXiv:1103.3477](https://arxiv.org/abs/1103.3477)].

[78] D. Gang, Y.-t. Huang, E. Koh, S. Lee, and A. E. Lipstein, *Tree-level Recursion Relation and Dual Superconformal Symmetry of the ABJM Theory*, *JHEP* **1103** (2011) 116, [[arXiv:1012.5032](https://arxiv.org/abs/1012.5032)].

[79] A. Brandhuber, G. Travaglini, and C. Wen, *A note on amplitudes in  $\mathcal{N} = 6$  superconformal Chern-Simons theory*, *JHEP* **1207** (2012) 160, [[arXiv:1205.6705](https://arxiv.org/abs/1205.6705)].

[80] Y.-t. Huang, C. Wen, and D. Xie, *The Positive orthogonal Grassmannian and loop amplitudes of ABJM*, [arXiv:1402.1479](https://arxiv.org/abs/1402.1479).

[81] Y.-T. Huang and C. Wen, *ABJM amplitudes and the positive orthogonal grassmannian*, *JHEP* **1402** (2014) 104, [[arXiv:1309.3252](https://arxiv.org/abs/1309.3252)].

[82] C. F. Berger, Z. Bern, L. J. Dixon, D. Forde, and D. A. Kosower, *On-shell unitarity bootstrap for QCD amplitudes*, *Nucl.Phys.Proc.Suppl.* **160** (2006) 261–270, [[hep-ph/0610089](#)].

[83] Z. Bern and Y.-t. Huang, *Basics of Generalized Unitarity*, *J.Phys.* **A44** (2011) 454003, [[arXiv:1103.1869](#)].

[84] T. Bargheer, N. Beisert, and F. Loebbert, *Exact Superconformal and Yangian Symmetry of Scattering Amplitudes*, *J.Phys.* **A44** (2011) 454012, [[arXiv:1104.0700](#)].

[85] J. Drummond, J. Henn, G. Korchemsky, and E. Sokatchev, *Generalized Unitarity for  $\mathcal{N} = 4$  super-amplitudes*, *Nucl.Phys.* **B869** (2013) 452–492, [[arXiv:0808.0491](#)].

[86] A. Agarwal, N. Beisert, and T. McLoughlin, *Scattering in Mass-Deformed  $\mathcal{N} = 4$  Chern-Simons Models*, *JHEP* **0906** (2009) 045, [[arXiv:0812.3367](#)].

[87] W.-M. Chen and Y.-t. Huang, *Dualities for Loop Amplitudes of  $\mathcal{N} = 6$  Chern-Simons Matter Theory*, *JHEP* **1111** (2011) 057, [[arXiv:1107.2710](#)].

[88] B. Feng, Y. Jia, and R. Huang, *Relations of loop partial amplitudes in gauge theory by Unitarity cut method*, *Nucl.Phys.* **B854** (2012) 243–275, [[arXiv:1105.0334](#)].

[89] A. Brandhuber, B. Spence, and G. Travaglini, *From trees to loops and back*, *JHEP* **0601** (2006) 142, [[hep-th/0510253](#)].

[90] R. Britto, B. Feng, R. Roiban, M. Spradlin, and A. Volovich, *All split helicity tree-level gluon amplitudes*, *Phys.Rev.* **D71** (2005) 105017, [[hep-th/0503198](#)].

[91] B. Eden, P. Heslop, G. P. Korchemsky, and E. Sokatchev, *The super-correlator/super-amplitude duality: Part I*, *Nucl.Phys.* **B869** (2013) 329–377, [[arXiv:1103.3714](#)].

[92] M. T. Grisaru, H. Pendleton, and P. van Nieuwenhuizen, *Supergravity and the S Matrix*, *Phys.Rev.* **D15** (1977) 996.

[93] M. T. Grisaru and H. Pendleton, *Some Properties of Scattering Amplitudes in Supersymmetric Theories*, *Nucl.Phys.* **B124** (1977) 81.

[94] H. Elvang, D. Z. Freedman, and M. Kiermaier, *SUSY Ward identities, Superamplitudes, and Counterterms*, *J.Phys.* **A44** (2011) 454009, [[arXiv:1012.3401](#)].

[95] K. A. Intriligator, *Bonus symmetries of  $N=4$  superYang-Mills correlation functions via AdS duality*, *Nucl.Phys.* **B551** (1999) 575–600, [[hep-th/9811047](#)].

[96] B. Eden, P. S. Howe, C. Schubert, E. Sokatchev, and P. C. West, *Extremal correlators in four-dimensional SCFT*, *Phys.Lett.* **B472** (2000) 323–331, [[hep-th/9910150](#)].

[97] B. Eden, C. Schubert, and E. Sokatchev, *Three loop four point correlator in  $N=4$  SYM*, *Phys.Lett.* **B482** (2000) 309–314, [[hep-th/0003096](#)].

[98] L. J. Dixon, E. N. Glover, and V. V. Khoze, *MHV rules for Higgs plus*

*multi-gluon amplitudes*, *JHEP* **0412** (2004) 015, [[hep-th/0411092](#)].

- [99] Y.-t. Huang, *Non-Chiral S-Matrix of  $N=4$  Super Yang-Mills*, [arXiv:1104.2021](#).
- [100] H. Elvang, D. Z. Freedman, and M. Kiermaier, *Proof of the MHV vertex expansion for all tree amplitudes in  $N=4$  SYM theory*, *JHEP* **0906** (2009) 068, [[arXiv:0811.3624](#)].
- [101] N. Arkani-Hamed, F. Cachazo, and J. Kaplan, *What is the Simplest Quantum Field Theory?*, *JHEP* **1009** (2010) 016, [[arXiv:0808.1446](#)].
- [102] A. Brandhuber, B. J. Spence, and G. Travaglini, *One-loop gauge theory amplitudes in  $N=4$  super Yang-Mills from MHV vertices*, *Nucl.Phys.* **B706** (2005) 150–180, [[hep-th/0407214](#)].
- [103] S. Terashima, *On  $M5$ -branes in  $\mathcal{N} = 6$  Membrane Action*, *JHEP* **0808** (2008) 080, [[arXiv:0807.0197](#)].
- [104] M. S. Bianchi, M. Leoni, A. Mauri, S. Penati, and A. Santambrogio, *Scattering in ABJ theories*, *JHEP* **1112** (2011) 073, [[arXiv:1110.0738](#)].
- [105] M. S. Bianchi, M. Leoni, A. Mauri, S. Penati, and A. Santambrogio, *Scattering Amplitudes/Wilson Loop Duality In ABJM Theory*, *JHEP* **1201** (2012) 056, [[arXiv:1107.3139](#)].
- [106] D. Young, *Form Factors of Chiral Primary Operators at Two Loops in ABJ( $M$ )*, *JHEP* **1306** (2013) 049, [[arXiv:1305.2422](#)].
- [107] J. M. Henn, *Multiloop integrals in dimensional regularization made simple*, [arXiv:1304.1806](#).
- [108] R. H. Boels, B. A. Kniehl, O. V. Tarasov, and G. Yang, *Color-kinematic Duality for Form Factors*, *JHEP* **1302** (2013) 063, [[arXiv:1211.7028](#)].
- [109] T. Huber, *The Sudakov form factor to three loops in  $N=4$  super Yang-Mills*, *PoS* **LL2012** (2012) 026, [[arXiv:1210.1339](#)].
- [110] J. Maldacena and A. Zhiboedov, *Form factors at strong coupling via a  $Y$ -system*, *JHEP* **1011** (2010) 104, [[arXiv:1009.1139](#)].
- [111] J. M. Henn, K. Melnikov, and V. A. Smirnov, *Two-loop planar master integrals for the production of off-shell vector bosons in hadron collisions*, [arXiv:1402.7078](#).
- [112] J. M. Henn, A. V. Smirnov, and V. A. Smirnov, *Evaluating single-scale and/or non-planar diagrams by differential equations*, [arXiv:1312.2588](#).
- [113] J. M. Henn and V. A. Smirnov, *Analytic results for two-loop master integrals for Bhabha scattering I*, *JHEP* **1311** (2013) 041, [[arXiv:1307.4083](#)].
- [114] J. M. Henn, A. V. Smirnov, and V. A. Smirnov, *Analytic results for planar three-loop four-point integrals from a Knizhnik-Zamolodchikov equation*, *JHEP* **1307** (2013) 128, [[arXiv:1306.2799](#)].
- [115] A. Smirnov, *Algorithm FIRE – Feynman Integral REDuction*, *JHEP* **0810** (2008) 107, [[arXiv:0807.3243](#)].
- [116] M. Czakon, *Automatized analytic continuation of Mellin-Barnes integrals*, *Comput.Phys.Commun.* **175** (2006) 559–571, [[hep-ph/0511200](#)].

[117] J. Gluza, K. Kajda, T. Riemann, and V. Yundin, *Numerical Evaluation of Tensor Feynman Integrals in Euclidean Kinematics*, *Eur.Phys.J.* **C71** (2011) 1516, [[arXiv:1010.1667](https://arxiv.org/abs/1010.1667)].